Identification and characterization of posttranslational modifications on CenH3 in *Saccharomyces cerevisiae*

Inaugural-Dissertation

zur

Erlangung des Doktorgrades

Dr. rer. nat

der Fakultät für

Biologie

an der

Universität Duisburg-Essen

vorgelegt von

Anke Samel

aus Stralsund

Februar 2012

Die der vorliegenden Arbeit zugrunde liegenden Experimente wurden in der Abteilung für Genetik der Universität Duisburg-Essen durchgeführt.

1. Gutachter: Prof. Dr. A. Ehrenhofer-Murray

2. Gutachter: Prof. Dr. H. Meyer

3. Gutachter: Prof. Dr. B. Horsthemke

Vorsitzender des Prüfungsausschusses: PD Dr. J. Thomale

Tag der mündlichen Prüfung: 31.05.2012

Abstract

The centromeric region in all eukaryotes is characterized by the presence of a histone H3 variant that replaces the canonical histone H3 in centromeric nucleosomes. In the budding yeast *Saccharomyces cerevisiae*, the centromeric histone H3 variant, termed Cse4, is present in a single nucleosome that forms the centromeric structure. The centromeric nucleosome serves as a platform for the assembly of the kinetochore, which ensures the faithful transmission of the genetic information to the daughter cell during the cell cycle. In this study, we identified posttranslational modifications on Cse4 and characterized their contribution to centromere function. We could show for the first time that Cse4 is posttranslationally modified by phosphorylation on serine 33, methylation on arginine 37 and acetylation on lysine 49. Methylation on arginine 37 as well as the acetylation on lysine 49 of Cse4 were determined both by mass spectrometry and by modification-specific Cse4 antibodies. A further analysis of mutations of the modified sites in the N-terminus of Cse4 showed no significant effect in the wild-type. Interestingly, the mutation of Cse4 R37 displayed lethality as well as growth defects in combination with mutations of genes encoding several kinetochore components. Furthermore, *cse4-R37A* caused a defect in the G2/ M-phase of the cell cycle in the absence of the Cbf1 kinetochore protein as well as a maintenance defect of plasmids and chromosome fragments lacking the Cbf1 binding sequence, CDEI. These results indicated that the methylation on arginine 37 of Cse4 contributed to the regulation of chromosome segregation. While Cse4 methylation did not affect its deposition at the centromere, the mutation of Cse4 R37 significantly reduced the recruitment of two kinetochore proteins to the centromeric region. Together with the fact that the level of Cse4 R37 methylation was increased in S-phase arrested cells, these results suggest that the methylation on arginine 37 of Cse4 supports the recruitment of kinetochore components to the centromere. Surprisingly, the additional mutation of lysine 49 to arginine led to the suppression of the growth defects of *cse4-R37A* suggesting an antagonistical effect between both modification sites. In summary, our data show that the centromeric histone H3 variant is posttranslationally modified, and that the methylation on arginine 37 of Cse4 contributes to the recruitment of kinetochore proteins to build a functional kinetochore for accurate chromosome segregation.

Zusammenfassung

Die zentromerische Region in der Bäckerhefe *Saccharomyces cerevisiae* zeichnet sich durch ein einzelnes Nukleosom aus, an dem das Kinetochor bindet. Wie in allen Eukaryoten, wird hier das kanonische Histon H3 durch eine zentromerische Histon H3 Variante ersetzt, welche als Cse4 bezeichnet wird. Diese Struktur ermöglicht die Assemblierung des Kinetochors und garantiert die Weitergabe der genetischen Information an die Tochterzellen während der Mitose. In der vorliegenden Arbeit wurden posttranslationale Modifikationen an Cse4 ermittelt und deren Rolle in der Chromosomensegregation untersucht. Dabei konnte zum ersten Mal gezeigt werden, dass Cse4 posttranslational durch Phosphorylierung am Serin 33, Methylierung am Arginin 37 und Acetylierung am Lysin 49 modifiziert wird. Sowohl durch Massenspektrometrie als auch durch modifikationsspezifische Cse4 Antikörper konnten die Methylierung am Arginin 37 und die Acetylierung am Lysin 49 nachgewiesen werden. Weitere Untersuchungen zeigten, dass die Mutation der Modifikationsstellen im Cse4 keinen Phänotyp in Wildtypzellen zeigte. Jedoch führte die Mutation von Arginin 37 in Stämmen, in denen einzelne Kinetochorproteine mutiert wurden, zu Letalität und Wachstumsdefekten. Interessanterweise führte die Mutation von Cse4 R37 zu einem mitotischen Effekt in Abwesenheit des Kinetochorproteins Cbf1 und zu einem erhöhten Plasmid- und Chromosomenverlust von Fragmenten ohne Cbf1 Bindesequenz (CDEI). Diese Ergebnisse zeigten, dass die Methylierung von Arginin 37 eine Rolle während der Chromosomensegregation spielt. Außerdem konnte gezeigt werden, dass die Argininmethylierung keinen Einfluss auf die Lokalisation des Proteins am Zentromer hat, jedoch führte die Mutation von Cse4 R37 zu einer geringeren Assoziation zweier Kinetochorproteine am Zentromer. Zusätzlich dazu wurde eine erhöhte Methylierung am Arginin 37 in S-phase arretierten Zellen beobachtet. Dies deutete darauf hin, dass die Argininmethylierung eine Rolle in der Rekruitierung des Kinetochors zum Zentromer spielt. Überraschenderweise führte die zusätzliche Mutation vom Lysin 49 zu Arginin zu einer Suppression des Wachstumsdefekts von *cse4-R37A*, welches auf einen möglichen antagonistischen Effekt zwischen beiden Modifikationsstellen hindeutet. Zusammenfassend konnte in dieser Arbeit gezeigt werden, dass die zentromerische Histon H3 Variante posttranslational modifiziert wird und die Methylierung am Arginin 37 eine entscheidende Rolle in der Rekruitierung und Formierung des Kinetochors übernimmt um somit eine korrekte Chromosomensegregation zu gewährleisten.

Table of contents

List of tables

List of figures

Abbreviations

Table 1: Abbreviations

5-FOA	5-fluoro-orotic acid
aa	amino acid
ac	acetylated
ACN	acetonitrile
AT-rich	adenine thymine-rich
ATP	adenosine triphosphate
bp	base pair
CATD	CENP-A targeting domain
Cbf1	centromere binding factor 1
CDEI/II/III	centromere DNA element I/II/III
CenH3	centromeric histone H3
CENP-A	centromere protein A
ChIP	chromatin immunoprecipitation
ChIP-seq	chromatin immunoprecipitation sequencing
cnt	non-repetitive core
Co-IP	co-immunoprecipitation
COMA	Ctf19/Okp1/Mcm21/Ame1
Cse4	chromosome segregation 4
DNA	deoxyribonucleic acid
END	essential n-terminal domain
FACS	fluorescence associated cell sorting
GFP	green fluorescence protein
HAT	histone acetyltransferase
HDAC	histone deacetylase
HeLa cells	Henrietta Lacks cells
HJURP	Holliday Junction Recognition Protein
HML	homothallic mating left
HMR	homothallic mating right
HP1	Heterochromatin Protein 1
HPLC	High Performance Liquid Chromatography
imr	innermost repeat
kDa	kilo Dalton
LB	Luria-Bertani
Mbp	mega base pair

me	monomethylated
me2a	asymmetrical dimethylated
me3	trimethylated
MNase	micrococcal nuclease
MS	mass spectrometry
MTF	methyltransferase
NAD^+	nicotinamide adenine dinucleotide
nm	nano metre
OD	optical densitiy
ORF	open reading frame
otr	outer repeats
PCR	polymerase chain reaction
PEV	position effect variegation
pmol	pico mole
PTM	posttranslational modification
PVDF	polyvinylidene fluoride
rDNA	ribosomal DNA
RNA	ribonucleic acid
rpm	rounds per minute
RT	room temperature
SAC	spindle assembly checkpoint
SAM	S-adenosyl-L-methionine
Scm3	suppressor of chromosome missegregation 3
SDS	sodium dodecyl sulfate
SDS-PAGE	sodium dodecyl sulfate polyacrylamide gel electrophoresis
TAP	Tandem-affinity purification
TAU	Triton-Acetic acid-Urea
TFA	trifluoroacetic acid
ts	temperature sensitive
wt	wild-type
YM	yeast minimal medium
YPD	yeast peptone medium

Yeast genes were named according to nomenclature conventions of *Saccharomyces cerevisiae* genome database (SGD).
Amino acids were given in the single-letter code, e.g. K = lysine, R = arginine, S = serine

1. Introduction

1.1 Epigenetics

The science of epigenetics is a fast-developing field, which started with the observation of a wide range of phenomena and has since evolved into a well-established area of research. The term "epigenetics" was coined by Conrad Hal Waddington in 1942 as "the branch of biology which studies the causal interactions between genes and their products, which bring the phenotype into being" (Waddington 1942). In 1957 he described his perception of epigenetics more precisely in an article about the epigenetic landscape (Waddington 1957). Thereby, the cell is represented as a ball surrounded by valleys and hills. The growth and development of an organism is illustrated as a downhill movement through this landscape and thus in this model is specified, but changeable. The hills and valleys are flexible through the impact of external factors. Up to a certain threshold, the factors will be buffered and cannot affect the pathway of the cell. If the pressure of the outer parameter is high enough, the organism shifts its position in this model, which leads to varying outcomes. At the end of this concept, the organism carries the original genotype, but a distinct, modified phenotype (Slack 2002).

Together with the structural discovery of DNA in 1953 by Watson and Crick (Watson and Crick 1953), the field of epigenetics has developed into an area of investigation that deals with the stable and heritable changes in expression and phenotypes without variations in the DNA sequence. Today's epigenetic research is increasingly focused on the influence of covalent and noncovalent modifications on DNA and proteins and their contribution to the structure of chromatin in development and differentation.

1.2 Organization of eukaryotic chromatin

The DNA in the eukaryotic cell is systematically packaged with histone and non-histone proteins into the chromatin structure (Kornberg 1974). This assembly of DNA and proteins builds the fundament that is relevant for elementary processes like DNA replication, transcription and chromosome segregation.

The fundamental unit of the chromatin is the nucleosome. In this structure, 147 bp of DNA is wrapped in a 1.65 left-handed superhelical turn around an octameric structure of histone proteins. Each octamer consists of two copies of H2A, H2B, H3 and H4 (Richmond and

Davey 2003). All of the four different core histones are distinguished by three structural motifs: the histone fold domain, the extra fold structure element and the exclusive N-terminus. The latter differs in length between 13-42 amino acids (Arents and Moudrianakis 1995). The histone fold domains of all core histones display a highly similar structural motif, consisting of three α-helices interrupted by two loops. This motif is responsible for the formation of the H2A-H2B and H3-H4 heterodimers (Luger et al. 1997). Interestingly, the N-terminal region of H4 enables specific contacts and can directly interact with the acid patch interface of the H2A-H2B dimer of an adjacent nucleosome (Luger et al. 1997).

The DNA surrounding a nucleosome is characterized by a resistance against the cleavage of micrococcal nuclease (MNase), while the linker DNA between two nucleosomes does not show an association with the core histones and is therefore prone to cleavage by MNase (Hansen et al. 1989). The linker DNA varies in length depending on the cell-type and organism (Widom 1992; Prunell and Kornberg 1982). The 11 nm DNA fiber is also described as "beads on a string" (Thoma et al. 1979), which is further condensed to the 30 nm fiber representing the second structural level of DNA organization (Figure 1). This condensation is implemented by the linker histone H1. H1 is less conserved than the core histones (Caterino and Hayes 2011). It was proposed that the molar ratio between the core histones H2A/H2B/H3/H4 and the linker histone H1 is 1:1 in most cell-types (Albright et al. 1979). Conversely, it was previously shown that in the budding yeast *Saccharomyces cerevisiae* the linker histone H1 homologue Hho1 is only bound to every 37th nucleosome (Freidkin and Katcoff 2001). The compaction of DNA to this higher-order chromatin by the linker histone H1 (Hizume et al. 2005) and the associated decrease of DNA accessibility has led to the proposal that this contributes to the regulation of biological processes like transcription.

The determination of the nucleosome at high resolution (1.9Å) (Richmond and Davey 2003) has not resolved the internal structure of the 30 nm chromatin fiber, this is still controversial and remains uncharacterized. Electron microscopy and crystal structure studies have led to the proposition of two models. The solenoid model was proposed by Finch and Klug (Finch and Klug 1976) by their observation of the formation of a nucleofilament under low ion conditions. Here, the DNA is wrapped around 6-8 nucleosome cores per turn and forms a solenoid with a diameter of 25-30 nm. The structure is also described as one-start helix. The second model is based on the crystal structure of a compact tetranucleosome (Schalch et al. 2005) and supports a two-start helix. Two stacks of nucleosomes are connected by the linker DNA in a zig-zag arrangement and

rotated by 70° relative to each other in a left-handed manner. Finally, the 30 nm fiber is further condensed with non-histone proteins to form the metaphase chromosomes.

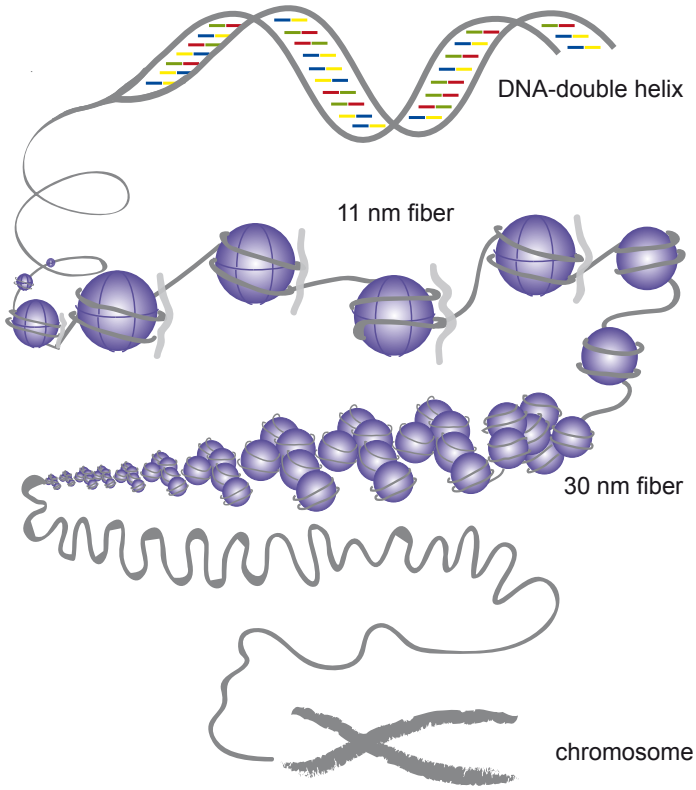

Figure 1: Organization of eukaryotic chromatin.
The picture illustrated the different packaging steps of chromatin from the DNA double helix to the metaphase chromosome. The DNA double helix is bound by histones to form the 11 nm fiber which is more condensed to the 30 nm fiber and subsequently to the metaphase chromosome. (modified from the homepage of the EPIgenetic Treatment Of Neoplastic disease (www.epitron.eu)).

The chromatin state in eukaryotes undergoes different dynamic changes. Emil Heitz observed that the staining of chromosome regions in the same cell-type could differ between individuals. These distinctions are correlated with regions of condensed and decondensed chromatin, also referred to as heterochromatin and euchromatin (Heitz 1928). The euchromatin is characterized by an opened chromatin conformation and is found on active genes. The heterochromatin, which comprises the facultative and the constitutive heterochromatin, is highly ordered in nucleosome arrays and condensed. This represents the inaccessible form of the chromatin. The constitutive heterochromatin is localized to regions of highly repetitive and noncoding sequences, like telomeres and centromeric regions (Grewal and Jia 2007). The transcription rate at these genomic regions is generally rather low in comparison to euchromatic regions (Trojer and Reinberg 2007). The regions

of facultative heterochromatin are transcriptionally silent but can alternate, depending on cellular signal, between heterochromatin and euchromatin, and consequently allow transcription after decondensation. This could be due to changes in the nuclear localization or in response to different developmental and cell cycle states.

The first link between the structural form of chromatin and the influence of the transcription rate of the gene is represented by an observation in *Drosophila melanogaster*. After X-ray irradiation of flies, mutants were observed that showed variegation in the eye color (Muller 1930). This phenomenon, termed position effect variegation (PEV), is explained by the suppression of the gene encoding the red eye pigmentation ($white^{+}$) through translocation to heterochromatic regions.

In *S. cerevisiae,* heterochromatin is found at three genomic regions, the telomeres, the rDNA locus and the silent mating-type loci *HMR* and *HML*. In higher eukaryotes, heterochromatin can also cover an entire chromosome, as is the case in X-chromosome inactivation. One X-chromosome in female mammals is constantly silenced by the activation of the non-coding RNA Xist (Brown et al. 1991). After coating the X-chromosome by Xist, chromosomal changes like hypoacetylation and lysine methylation on the histone occur that result in silency of the whole chromosome (Heard 2005).

The chromatin structure of eukaryotes can be altered by the incorporation or removal of histones by ATP-dependent remodelling complexes, by histone modifications or by the presence of histone variants. The functions and mechanisms of theses will be introduced in the next chapters.

1.3 ATP-dependent remodelling complexes

As such, the chromatin structure can be assumed to be a relatively static material, and the nucleosomes are characterized by high stability and limited mobility. Therefore, it is necessary for the cell to provide factors that give the chromatin structure a dynamic character to ensure access to the DNA for biological processes like transcription, chromosome segregation or DNA repair.

The chromatin remodelers are highly specialized multi-protein complexes that increase the accessibility of the DNA template by changing the structure and position of the nucleosomes. The nucleosomes are consequently spaced and the protein factors, for example those required for transcription and DNA repair, are able to access DNA gaps. In eukaryotes, five families of chromatin remodelers are described: SWI/SNF, ISWI, NURD/MI-2/CHD, INO80 and SWR1 (Saha et al. 2006). The effects on the nucleosome

structure and positioning are remodeler dependent. The ATP-dependent remodelling complexes consist of a catalytic ATP-subunit and belong to the Swi2/Snf2 ATPase superfamiliy. All of them are characterized by using the energy of the hydrolysis of ATP to alter the chromatin structure within the nucleosome.

The best-characterized classes of chromatin remodelers are the SWI/SNF and ISWI families. In spite of the same catalytic domain, the classes execute different tasks *in vivo*. The SWI/SNF class is characterized by an additional bromodomain in the C-terminus, a motif that is highly conserved (Haynes et al. 1992) and facilitates the binding of the complex to acetylated histone tails. In the yeast *S. cerevisiae* it was previously shown that the bromodomains of both the SWI/SNF complex and the SAGA histone acetyltransferase complex are necessary for stable binding to acetylated promoter nucleosomes (Hassan et al. 2002). Other functions of the SWI/SNF complex in budding yeast include an increase in the binding affinity of transcription factors to nucleosomes and the displacement of H2A/H2B dimers (Bruno et al. 2003). About 5 % of the yeast genome is transcriptional regulated by the SWI/SNF complex (Holstege et al. 1998). In comparison to the SWI/SNF family, the ISWI class is characterized by the presence of two characteristic domains in the C-terminus. Both are necessary for the recognition of the histone tail and the linker DNA (Grune et al. 2003). As it was shown in *D. melanogaster*, the ISWI complex contributes to the organization of nucleosome positioning and promotes transcriptional repression *in vivo* (Deuring et al. 2000).

Many studies have provided important insights into the strategies that are used by SWI/SNF and ISWI complexes to slide the nucleosomes along the DNA. It is proposed that the ATP hydrolysis generates a DNA wave that pulls the linker DNA into the nucleosome and propagates it to the distal linker by diffusion (Saha et al. 2006).

1.4 Histone modifications

The modification of amino acid side chains in the histones also contributes to the dynamic regulation of the chromatin structure. One function of such histone modifications is the recruitment or signalling of downstream effectors or the regulation of interaction with other nucleosomes. However, the histone modifications also operate as epigenetic marks that are inherited by the daughter cells to maintain diverse types of information, for instance during replication. In order to maintain the epigenetic information, the old histones are segregated to the daughter cells and in principle can be used as template to copy their epigenetic information to new histones (Martin and Zhang 2007). There exists a

wide range of posttranslational modifications (PTMs) like acetylation, methylation, phosphorylation, ubiquitinylation and farnesylation. Such modifications are added predominantly to the N-terminus of the histone by special histone modifying enzymes (Figure 2). There is also evidence for modifications in the histone fold domain, which are primarily accessible during nucleosome unfolding or assembly (Williams et al. 2008). For example, the methylation on lysine 79 of histone H3 (H3K79me) in *S. cerevisiae* by the histone methyltransferase Dot1 represented the first methylation mark identified in the histone fold domain (van Leeuwen et al. 2002).

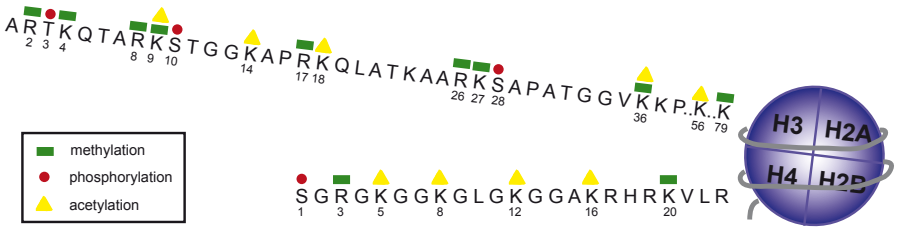

Figure 2: Known histone modifications on the histone H3 and H4 regulate and contribute to the chromatin state.
Methylation on histones is characterized on arginines and lysines (green box), phosphorylation on serine or threonine (red circle) and acetylation occurs on lysine residues (yellow triangle). (modified from Scharf and Imhof 2010).

Genome-wide studies of histone modifications show that the specific state of a gene can be linked to the appearance of histone modifications. Modifications like di- and trimethylation on lysine 4 of histone H3 (H3K4me2,3) and H3K36me2,3 are associated with actively transcribed regions. In contrast, marks like H3K27me3 and H4K20me3 are linked to regions where transcription is repressed. This observation led to the hypothesis of a "histone code" (Strahl and Allis 2000), which suggests that histone modifications determine the activity state of a gene through the regulation of downstream effectors. Some studies extend this view over the chromosome structure and propose the "nucleosome code", which enables different epigenetic states through the local accumulation and combination of modified nucleosomes (Jenuwein and Allis 2001). However, these concepts are highly controversial in the epigenetic field. For instance, it is debated whether these effects on the gene expression are either cumulative or the combination of the histone modifications (Barth and Imhof 2010).

Histone modifications can also influence each other, either on the same histone domain or to another histone in the nucleosome. In *S. cerevisiae,* it was shown that the ubiquitination on lysine 123 of histone H2B mediates the methylation of histone H3 at lysine 4, which

regulates gene silencing (Sun and Allis 2002). This study was the first described "trans-tail" regulation of histone modifications. Furthermore, the histone marks can influence each other on one histone tail. An example for the "binary-switch" model is the phosphorylation on serine 10 and methylation on lysine 9 of histone H3. The methylation on lysine 9 leads to binding of the heterochromatin protein HP1, which causes heterochromatin formation and gene silencing (Li et al. 2003). Once, serine 10 is phosphorylated during mitosis by Aurora B kinase, this decreases the binding of HP1 (Fischle et al. 2005). This model of a binary "methyl/phos switch" is confirmed by the fact that the phosphatase PPI binds to phosphorylated serine 10 after exit from mitosis, thus causing a subsequent increase in binding of HP1 (Hsu et al. 2000).

1.4.1 Histone methylation

The methylation mark can be attached to the amino acids arginine and lysine on the histone. Lysines can be mono-, di- and trimethylated (me1, me2, me3), in contrast to arginine, which can occur in a mono-methyl and asymmetrical or symmetrical di-methyl state (me1, me2a, me2s). Both of these histone marks contribute both to active and repressive effects on chromatin function. The nine members of the PRMT class in mammalian cells catalyse arginine methylation (Di Lorenzo and Bedford 2011). Thereby, they transfer a methyl group from S-adenosyl-L-methionine to the guanidine nitrogen of arginine and are classified from type I to III according to the final methylated arginine. In contrast to human, only three genes for arginine methyltransferases are annotated in *S. cerevisiae* – *HSL7*, *HMT1* and *RMT2*. It has been predicted that around 1 % of the human and yeast genome encode S-adenosyl-L-methionine-dependent methyltransferases (Katz et al. 2003).

Lysine methylation can be catalyzed by a protein family containing the SET (Su(var), Enhancer of Zeste and Trithorax) domain, by yeast Dot1 and its homologues. Instead of the typical SET domain, the Dot enzyme class possesses a class I methyltransferase domain, which is also found in arginine methyltransferases (Dlakic 2001).

The methylation of lysines and arginines does not affect the charge of the amino acid group, which suggests that this modification stores information for chromatin regulation (Lachner et al. 2001) by changes in the interaction with other proteins. The methyltransferases are characterized by either a processive or a distributive methylation mechanism. Some of the enzymes methylate the amino acids in the histone tail in a sequential manner, whereas others can form the methylation state independently of the

presence of a lower methylated form. Arginine methylation in mammals is found on arginine 2, 8, 17 and 26 of histone H3 and arginine 3 of histone H4 (Wysocka et al. 2006). Surprinsingly, the different methylation states for H3R2 have different outcomes for the transcription in *S. cerevisiae*. The monomethylation of H3R2 is linked to activation, while the asymmetrical dimethylation H3R2me2a is associated with repression (Kirmizis et al. 2009).

Methylation on lysine 4, 36 and 79 of histone H3 is linked to active regions of chromatin, in contrast to lysine 9 and 27 of histone H3, which are associated with silenced regions (Klose and Zhang 2007). It was shown that methylation of H3K4 and H3K36 is directly coupled to the transcription process by the association to the RNA-polymerase II during elongation (Krogan et al. 2003). Interestingly, the methylation of H3K9 serves to recruit the heterochromatin protein HP1, both in humans and in *S. pombe*, demonstrating that this event is evolutionarily conserved (Nakayama et al. 2001; Lachner et al. 2001). However, previous data show that H3K9me3 and HP1 are also localized in the coding regions of active genes (Vakoc et al. 2005). The dimethylation of lysine 4 on histone H3 is characterized as a mark of the canonical histone H3 in the centromeric region in human cells and thereby contributes to the centromere specificity (Sullivan and Karpen 2004).

The degree of methylation on the genome is not solely due to the activity of methyltransferases. In addition, demethylases contribute to the methylated state within the cell. So far, three enzyme families are characterized for histone demethylation, PADI, LSD and JMJC (Klose and Zhang 2007). The PADI4 enzyme catalyzes the conversion of arginine to citrulline in histone H3 and H4 by deimination and subsequently prevents further methylation of arginine (Cuthbert et al. 2004). In the budding yeast the JmjC-domain-containing histone demethylase is the only described lysine demethylase, which is able to demethylate H3K36me1,2 (Tsukada et al. 2006). The observation of demethylases demonstrates that methylation is not a static modification, but rather a dynamic histone mark.

1.4.2 Acetylation on lysine residues in histones

The best-characterized histone modification is lysine acetylation. Thereby, an acetyl group from the cofactor acetyl-coenzyme A is transferred to the ε-amino group of the lysine, leading to the neutralization of the basic charge of the amino acid. *In vitro* studies show that the lysine acetylation antagonizes the folding of the chromatin (Annunziato and Hansen 2000) and the formation of the 30 nm fiber, in particular the acetylation on lysine

16 of histone H4 (Shogren-Knaak et al. 2006). Radioactive analysis shows that the turn-over of acetyl groups on all histones is rather high with a half-life time of less than 15 min (Chestier and Yaniv 1979).

Histone acetyltransferases are divided into three different groups: the GNAT (Gcn5-related N-acetyltransferase) family, the MYST (MOZ, Ybf2/Sas3, Sas2, Tip60) family and the CBP (CREB-binding protein)/p300 related family (Bannister and Kouzarides 2011). Members of the GNAT family are involved in the regulation of transcription and DNA repair (Carrozza et al. 2003). The histone acetyltransferase Gcn5 is the first histone-modifying enzyme identified (Brownell et al. 1996) and is part of the SAGA complex that acetylates lysines 9, 14, 18 and 23 of histone H3 *in vivo* (Grant et al. 1999). Free Gcn5 is not able to acetylate nucleosomes, demonstrating that the acetyltransferase activity is dependent on the influence of multisubunit complexes like SAGA and ADA (Grant et al. 1997). Interestingly, it was shown that Gcn5 could acetylate H3K14 more effectively to promote transcription when H3S10 is phosphorylated (Clements et al. 2003).

Besides regulation of transcription, the MYST family is also implicated in transcriptional silencing. The histone acetyltransferase Sas2 in the SAS-I complex catalyzes together with Sas4 and Sas5 the acetylation on H4K16 and thereby defines boundaries between transcriptionally active and silenced regions (Suka et al. 2002). The essential histone acetyltransferase Esa1 is the catalytic subunit of the NuA4 (nucleosomal acetyltransferase of histone H4) complex and important for global acetylation of histone H4 and H2A leading to transcriptional activation. Recently it was shown that the acetylation by NuA4 increases the incorporation of the histone variant H2A.Z at promoters via the SWR1 complex (Altaf et al. 2010), thus linking lysine acetylation to chromatin remodeling.

The deacetylation of lysine residues is characteristic of transcriptional repression and is carried out by histone deacetylases (HDACs). Four classes of HDACs are described dependent on sequence similarities and cofactor usage. Classes I and II are related to the yeast proteins Rpd3 and Hda1, while class III are homologous to yeast Sir2 and are dependent on the cofactor NAD^+. The fourth class is chararcterized by only one enzyme, HDAC11 (Bannister and Kouzarides 2011).

1.4.3 Histone phosphorylation

Phosphorylation is the most frequent posttranslational modification on proteins in the living cell. Kinases catalyze the transfer of γ-phosphate of the ATP molecule to the hydroxyl group of serines, threonines and tyrosines. The phosphorylation on histones

occurs predominantly on the N-terminus, leading to changes in protein-protein interactions by introducing more negative charges on the amino acid. Several cellular processes are affected by this modification, like chromosome segregation, transcriptional activation and DNA repair. The phosphorylation on serine 14 of histone H2B is linked to apoptosis (Cheung et al. 2003), whereas the phosphorylation on serine 36 of histone H2B leads to transcriptional activation (Bungard et al. 2010). The phosphorylation sites in the histone H3 are of great interest, because it was shown that they are linked both to transcription and chromosome segregation. In interphase, histone H3 is phosphorylated on serine 10 for gene activation (Nowak and Corces 2004), while in mitosis the phosphorylation is necessary for chromosome condensation (Crosio et al. 2002). Phosphorylation was also identified on tyrosine 41 of histone H3. It was shown that this phosphorylation decreases the binding of the heterochromatin protein HP1 and subsequently leads to transcriptional activation (Dawson et al. 2009).

Phosphorylation is also found on histone variants. The centromeric histone H3 variant CENP-A is phosphorylated on serine 7, which prevents the formation of misaligned chromosomes (Zeitlin et al. 2001; Kunitoku et al. 2003).

Like acetylation and methylation, phosphorylation is a dynamic event, whereby phosphatases act as antagonists. The most prominent protein phosphatase is PP1. In *S. cerevisiae*, it was shown that the PPI homologue Glc7 antagonizes the Ipl1/Aurora activity by dephosphorylation of its targets (Pinsky et al. 2006; Francisco and Chan 1994) to ensure the fidelity of chromosome segregation. Interestingly, the dephosphorylation on threonine 3 of histone H3 is promoted by a complex containing PP1 and the regulator Repo-man (Qian et al. 2011). In comparison to kinases, the specificity and activity of phosphatases is not yet clearly defined and requires further studies of their targets.

1.5 Histone variants

A way to modulate and regulate the chromatin is by the incorporation of histone variants. In most organisms, the canonical histones are encoded by multiple genes that are highly similar in sequence and are expressed during S-phase. They are incorporated during DNA replication. However, the histone variants, the nonallelic variants of the major histones, are expressed independently of S-phase during the cell cycle and deposited in a DNA synthesis-independent manner (Boyarchuk et al. 2011).

Histone H1 has several variants that differ in their function and distribution. Some H1 variants are linked to transcriptional repression, as it was shown in mouse, chicken and for

the histone H1.1 from *Caenorhabditis elegans*. The absence of H1.1 in worms causes a global increase of H3 lysine 4 methylation and a decrease of H3 lysine 9 methylation, a repressive histone mark (Jedrusik and Schulze 2007).

The canonical histone H2A has the largest number of histone variants among the core histones. The H2A variants like MacroH2A and H2A.Z differ both in length and sequence of the C-terminal tail as well as in their distribution in the genome in comparison to the canonical histone H2A. MacroH2A localizes to the inactive X-chromosome and is thought to have roles in transcriptional repression (Costanzi and Pehrson 1998). It has been proposed that MacroH2A blocks access to transcription factors and coactivators (Perche et al. 2000). In comparison to MacroH2A, the histone variant H2A.Z is linked to both transcriptional repression and activation (Meneghini et al. 2003). Intriguingly, H2A.Z is also present in centromeric chromatin and connects this variant to roles in chromosome segregation. In *S. cerevisiae*, however, H2A.Z is mostly absent from the centromeric region (Albert et al. 2007). In contrast, H2A.Z containing nucleosomes in mammals are present in pericentric and centric chromatin and contribute to the chromatin structure at the centromere (Greaves et al. 2007).

The variants of the canonical histone H3 are well characterized with regard to H3.3 and CenH3. In 2006, Hake and Allis proposed the model “H3 barcode hypothesis”, which suggests that the distribution of H3 variants over the mammalian genome determines specific territories (Hake and Allis 2006). Unlike other histone variants, H3.3 is constitutively expressed during the cell cycle and has high sequence similarity to the canonical histone H3. In *Drosophila melanogaster,* the histone variant shows only four amino acid differences to the canonical histone (Ahmad and Henikoff 2002). This histone variant localizes to genes that are either poised for transcription or actively transcribed. Recently, it was also shown in human cells that H3.3 acts as a placeholder at the centromeres in S-phase and is replaced by the histone variant CenH3 in the G1-phase (Dunleavy et al. 2011). The histone variant CenH3 is highly conserved throughout eukaryotes and is characterized by highly divergent N-terminal tails. One function of CenH3 is the formation of the proteinaceous kinetochore structure, because the depletion of this histone variant leads to altered localization of kinetochore proteins (Howman et al. 2000; Blower and Karpen 2001). Other histone variants do not show as wide a range of distribution as H2A and H3. The histone variant of the canonical histone H2B has a very exclusive function in gametogenesis. For the canonical histone H4, no sequence variants are known so far (Kamakaka and Biggins 2005).

1.6 The centromeric histone H3 variant Cse4

The centromeric regions in eukaryotes are characterized by the exclusive localization of the histone H3 variant CenH3 (Earnshaw and Rothfield 1985; Palmer et al. 1987). A conserved histone fold domain in the C-terminus and a highly variable N-terminus characterizes the centromeric histone H3 variant from yeast, fly, worm and human. In humans, the centromeric region is interspersed by blocks of the histone H3 variant CENP-A with blocks of canonical histone H3 (Blower et al. 2002). The CATD (CENP-A targeting domain), comprising loop 1 and the alpha2 helix in the C-terminus of CENP-A, distinguishes the histone variant from canonical histone H3 and is necessary for the localization of the histone variant on the centromere (Black et al. 2004; Black et al. 2007).

In *S. cerevisiae,* the centromeric histone H3 variant, which is termed Cse4, was found in different screens for mutations defective in chromosome segregation (Smith et al. 1996; Baker et al. 1998). By immunofluorescence and immunoprecipitation, its localization was physically described at the centromeric chromatin (Meluh et al. 1998). Interestingly, it was also shown by chromatin immunoprecipitation sequencing (ChIP-seq) that Cse4 is located at highly transcribed regions at a low level (Lefrancois et al. 2009). Cse4 has a molecular weight of 27 kDa and shows homology within the C-terminus of more than 60 % to the canonical histone H3 (Figure 3). The N-terminus is about 129 amino acids in length and interacts with the Ctf19 kinetochore protein (Chen et al. 2000). In a systematic mutagenesis of the N-terminus of Cse4, the region of amino acids 28 to 60 was described as sufficient for Cse4 function and was named END (essential N-terminal domain) (Keith et al. 1999). It was also shown that a deletion of the human ortholog CENP-A could be rescued by Cse4 (Wieland et al. 2004; Allshire and Karpen 2008). The overexpression of Cse4 does not lead to euchromatic localization and ectopic kinetochore formation, whereas this is the case for the *D. melanogaster* homologue Cid (Heun et al. 2006).

Unlike for the human centromeric histone variant CENP-A, so far no posttranslational modifications like phosphorylation or acetylation are described for Cse4. Only ubiquitin-mediated proteolysis by the E3 ubiquitin ligase Psh1 has been described, which prevents the mislocalization of Cse4 (Ranjitkar et al. 2010; Hewawasam et al. 2010). However, different posttranslational modifications on Cse4 are possible according to a comparison of the centromeric histone H3 variants to histone H3 modifications (Figure 3).

Several studies characterized the function of chromatin remodelling factors at the centromeric region. Snf2 as a subunit of the ATP-dependent chromatin remodelling complex SWI/SNF also has a role in the maintenance of centromeres by removal of

misincorporated Cse4 from ectopic sites. Reduced levels of Cse4 at the centromeres and defects in chromosome segregation are observed upon deletion of *SNF2* (Gkikopoulos et al. 2011). In the last years, several investigations have provided evidence for the contribution of ATP-dependent chromatin remodelers to target the centromeric histone H3 variant to the centromeric region. In HeLa cells, an interaction between CENP-A and the remodelling and spacing factor (RSF) was described. In RSF-deleted cells, a reduction of the CENP-A level at the centromere was observed. In this study it was proposed that RSF contributes to the stability of the predeposited CENP-A-containing nucleosomes at the centromeres (Perpelescu et al. 2009). It was also shown that in *S. pombe* the Chromodomain-helicase-DNA-binding protein 1 (Chd1) homologue Hrp1 is responsible for keeping the Cnp1 level constant (Walfridsson et al. 2005), and a knockdown of Chd1 in HeLa cells leads to defects in the deposition of CENP-A (Okada et al. 2009). However, the ATP dependent chromatin remodelers seem to be involved in the targeting of CENP-A to the centromeric region and in preventing it from being incorporated into non-centromeric loci.

Because of the fact that other histones and variants are deposited into the genome by histone chaperones, it was assumed that CenH3 also has a specific loading complex. *In vitro* studies in *D. melanogaster* lead to the purification of a new CenH3 chaperone, RbAp48, that targets CenH3 to the centromere (Furuyama et al. 2006) and also plays a role in CenH3 incorporation in *S. pombe* and humans (Hayashi et al. 2004). However, a direct association between CenH3 and this chaperone was not observed. It was previously shown that the Scm3 protein binds to CenH3 and is necessary for incorporation into the centromere (Camahort et al. 2007; Mizuguchi et al. 2007; Stoler et al. 2007) in *S. pombe* as well as in *S. cerevisiae*. In human cells, a direct association was described between CENP-A and the Scm3 homologue HJURP (Holliday Junction Recognition Protein) in a prenucleosomal complex (Dunleavy et al. 2009; Foltz et al. 2009), that is ensuring the recruitment of CENP-A in early G1 to the centromeric region (Jansen et al. 2007).

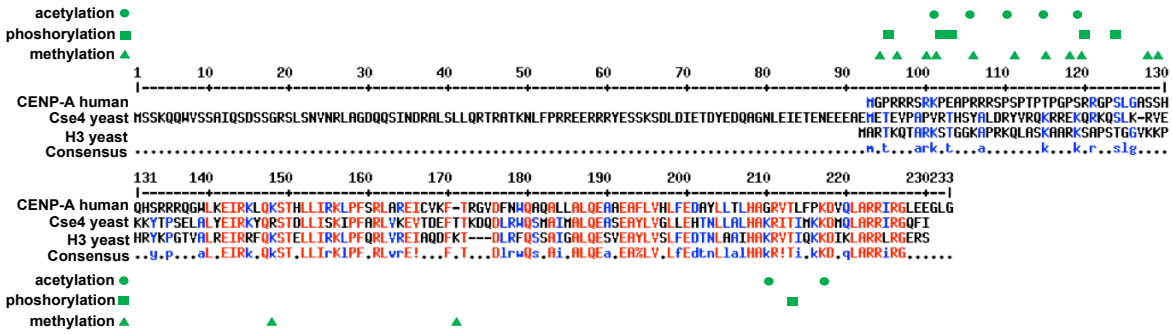

Figure 3: Sequence comparison of CenH3.
Alignment of CENP-A, Cse4 and histone H3 in relation to known modifications on the human canonical histone H3 (indicated as filled circle, square and triangle). Alignments were generated using Multalin (bioinfo.genopole-toulose.prd.fr/multalin).

1.7 Composition of the centromeric nucleosome in *S. cerevisiae*

The organization of the centromeric nucleosome in *S. cereivisae* is controversial and a matter of much debate. So far, three models for the architecture of the composition of the budding yeast centromeric nucleosome exist. The first one describes the nucleosome as an octamer, consisting of two copies of Cse4, H2A, H2B and H4 (Camahort et al. 2009) and is based in general on the sequence homology of the C-terminus of Cse4 with the canonical histone H3 of more than 60 % (Figure 4a). This is consistent with the centromeric nucleosome conformation in human (Tachiwana et al. 2011). The second model is predicted from an observation from interphase *Drosophila* S2 cells (Dalal et al. 2007). A tetrameric complex containing one copy of CenH3, H2A, H2B and H4 was purified by crosslinking of the CENP-A homologue Cid to chromatin (Figure 4b). This so called "hemisome" structure showed a stable association with 120 bp of DNA. Atomic force microscopy confirmed the heterotypic tetramers, because the hemisomes showed half of the height of a canonical octameric nucleosome (Dalal et al. 2007). The third and most recent model suggests a centromeric nucleosome with a newly identified protein, Scm3. Scm3 was identified in a screen for high-copy suppressors of the C-terminus of Cse4 (Chen et al. 2000). Different groups have shown independently by co-immunoprecipitation that Cse4 is associated with Scm3 (Stoler et al. 2007; Camahort et al. 2007; Mizuguchi et al. 2007; Pidoux et al. 2009; Williams et al. 2009). In a Scm3-depleted mutant, the Cse4 localization to the centromere is disturbed, and the cells show a G2/ M arrest (Stoler et al. 2007). It was proposed that Scm3 displaces H2A/H2B dimers in the preassembled Cse4-containing octamer *in vitro* (Mizuguchi et al. 2007) and forms a hexameric centromeric nucleosome (Figure 4c). This model is supported by chromatin immunopreciptiation

experiments that suggest that the histones H2A and H2B are absent at the centromere and that an octameric nucleosome (Cse4/H4/H2A/H2B) reconstitution is not efficient on centromeric DNA *in vitro* (Mizuguchi et al. 2007; Xiao et al. 2011).

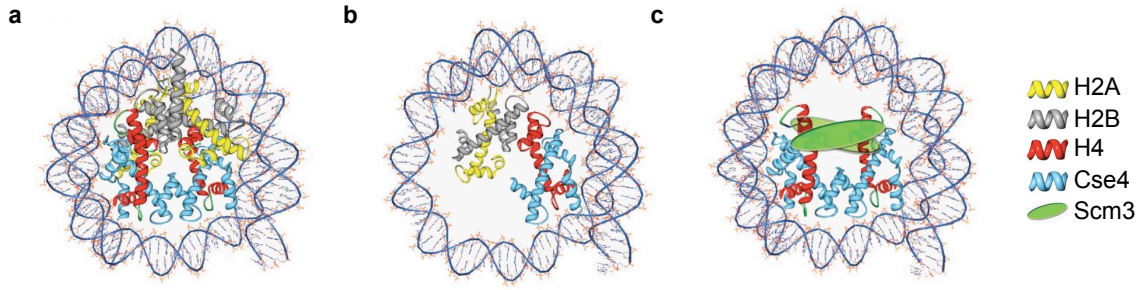

Figure 4: Models of centromeric nucleosome in *S. cerevisiae*.
(a) The centromeric nucleosome as an octamer consisting of two copies Cse4, H4, H2A and H2B. (b) One molecule of CenH3, H4, H2A and H2B forming the tetrameric structure. (c) The H2A/H2B dimer is replaced by Scm3 constituting a hexameric nucleosome. Figure was taken from Camahort et al. 2009.

1.8 Kinetochore-centromere organization in eukaryotes

The kinetochore is a multi-protein complex that links the centromere to the plus end of the spindle microtubules and ensures the transmission of genetic information by coupling the chromosomes during mitosis and meiosis. The microtubules are highly dynamic polymers forming cylindrical tubes by switching between association and disassembly of alpha and beta tubulin (Desai and Mitchison 1997). Their instability plays an important role during the cell cycle to drive chromosome segregation, meaning that sister kinetochores are connected to opposite spindle poles. Even a single unattached kinetochore turns on the spindle assembly checkpoint (SAC) and prevents the onset of anaphase until all kinetochore-microtubule interactions are correctly formed.

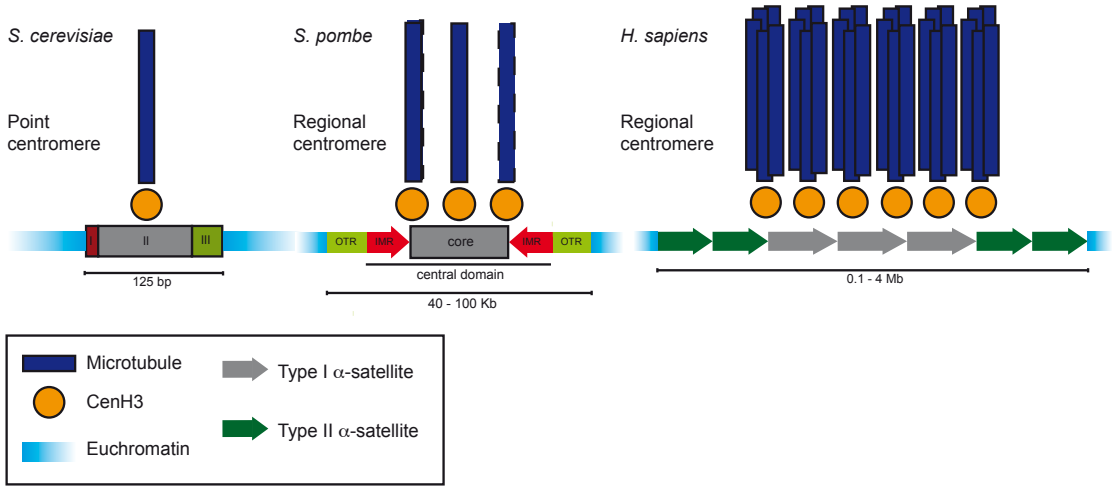

Figure 5: Composition of the centromeric region in eukaryotes.
In the budding yeast *S. cerevisiae* the centromeric region encompasses 125 bp of DNA dividing into CDEI/II/III. The typic point centromere is only attached by a single microtubule. *S. pombe* is characterized by a regional centromere. The centromeric nucleosomes are localized at the core element (gray box), which is bordered by the innermost repeats (red arrow) and the heterochromatic outer repeats (green box). The regional centromere in human is divided into type I α-satellite DNA (gray arrow), which is associated with CENP-A and the type II α-satellite DNA (green arrow). During metaphase, 20-30 microtubules bind to each kinetochore. (modified from Vagnarelli et al. 2008).

The kinetochore-centromere organization differs in the DNA sequence among species, but the presence of the centromeric histone H3 variant at the kinetochore and the segregation machinery are conserved (Figure 5). In S. *cerevisiae,* ~ 125 bp of DNA are wrapped around the centromeric nucleosome that is attached to only one microtubule (Clarke and Carbon 1985; Furuyama and Biggins 2007). All 16 chromosomes in the budding yeast are characterized at the centromeric region by three consensus elements: CDEI, CDEII and CDEIII. CDEI has a length of 8 bp (consensus motif: RTCACRTG) that is directly bound by the kinetochore protein Cbf1 (Cai and Davis 1989; Baker et al. 1989). The CDEIII element is a 25 bp DNA fragment that is the binding site for the CBF3 kinetochore complex. In contrast to CDEI, the CDEIII element is essential for centromeric activity. Both elements flank an AT-rich element of about 78-86 bp, designated CDEII (Clarke and Carbon 1985). Changes in the CDEII composition and length affect the centromere function by causing aberrant segregation (Gaudet and Fitzgerald-Hayes 1987).

In contrast to *S. cerevisiae*, the regional centromere in *S. pombe* has an overall size of 40-110 kbp, depending on the chromosome. The centromeric histone H3 variant Cnp1 localizes to the non-repetitive core (cnt), which is surrounded by the innermost repeat (imr). The outer repeats (otr) are heterochromatic and contain chromatin methylated on H3K9 (Pidoux and Allshire 2004). The core region as well as the innermost repeats are required for the assembly of the kinetochore, where each kinetochore is bound by 2 to 4

microtubules. In comparison to yeast centromeres, the centromeric region in *Homo sapiens* is comprised of much larger DNA arrays, which results in a larger kinetochore interacting with 20-30 microtubules. The DNA sequence generally consists of a 171 bp α-satellite motif repeated in tandem over a region of about 0.1- 4 Mbp (Choo et al. 1991).

1.9 Kinetochore organization in *S. cerevisiae*

In *S. cerevisiae,* more than 60 proteins assemble hierarchically into diverse subcomplexes in order to generate the kinetochore. The kinetochore is stable throughout most of the cell cycle. Only during DNA replication in S-phase, the kinetochore disassembles from the centromeric region, enabling the replication machinery to pass through. Afterwards, the kinetochore quickly reassembles to link the sister chromatids to the microtubules. According to their position and distance from the centromeric DNA, the kinetochore proteins can be categorized into three classes (Figure 6; Westermann et al. 2007). The first class includes the inner kinetochore proteins, which are directly bound to the centromeric DNA and form a platform for the assembly of the other kinetochore components. Secondly, the microtubule-associated proteins contain motor-proteins and other microtubule-binding proteins. The third category comprises the central kinetochore proteins, which connect the outer microtubule-associated proteins with the inner kinetochore elements and act as a linker complex (Westermann et al. 2007). In the further chapters, the different categories are described in more detail with respect to their composition and function.

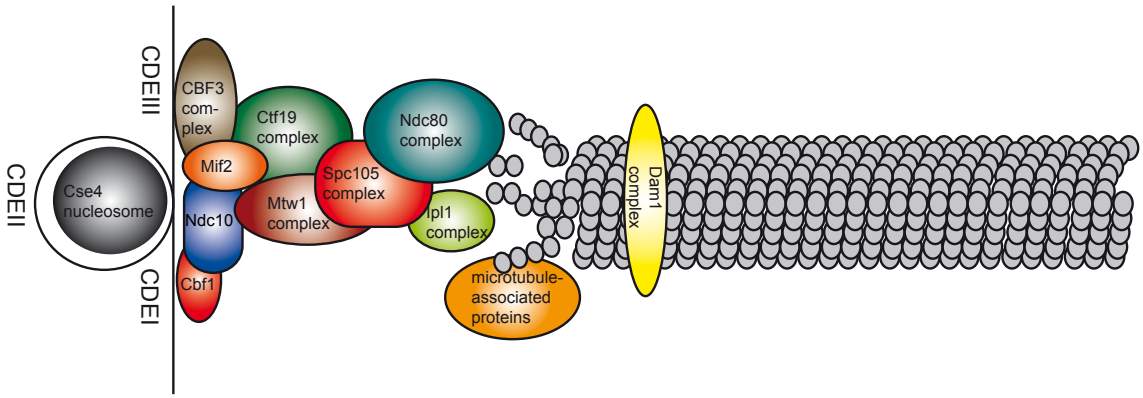

Figure 6: Model of the *S. cerevisiae* kinetochore.
The different subcomplexes are coloured and arranged according to their distance from the centromeric nucleosome and are attached to the microtubules (gray).(based on Westermann et al. 2007, and Santaguida and Musacchio 2009).

1.9.1 The inner kinetochore proteins

A major protein component in the initiation of the yeast kinetochore formation is the four-protein complex CBF3. It consists of the essential proteins Cep3, Ctf13, Skp1 and Ndc10, which bind to the CDEIII element of the centomeric DNA. The DNA binding activity of this complex is provided by the zinc-finger protein Cep3 (Espelin et al. 1997), and the assembly of the complex is regulated by the conserved proteins Sgt1 and HSP90 that activate the phosphorylation of Skp1 and Ctf13 (Kitagawa et al. 1999; Bansal et al. 2004; Stemmann et al. 2002). It was previously shown that the Ndc10 component binds independently of the CBF3 complex to the CDEII DNA element *in vitro* (Espelin et al. 2003).

Other inner kinetochore proteins like Mif2 and Cbf1 are recruited to the centromeric DNA in a CBF3-dependent manner. The first identified kinetochore protein, Cbf1, (Cai and Davis 1989; Baker et al. 1989) binds to the CDEI sequence and is not conserved in higher eukaryotes. Deletion of *CBF1* leads to a decrease in growth rate and an increase in chromosome loss. In a colony colour assay, the minichromosome stability was measured to be 10-fold decreased in the *cbf1*Δ than in wild-type cells (Cai and Davis 1990). However, its role in the kinetochore in budding yeast is still unclear. Beside its localization in the kinetochore, Cbf1 binds also as a transcription factor (Cai and Davis 1990) to the DNA motif CACRTG, which is present at several sites including promoters of methionine-biosynthesis gene.

The essential budding yeast CENP-C homologue Mif2 was shown to copurify with the histones H2A, H2B, H4 and Cse4 by TAP-purification, indicating that the centromeric nucleosome plays a critical role in the recruitment of Mif2 (Westermann et al. 2003). Chromatin immunoprecipitation (ChIP) experiments verifiy that Mif2 is associated with the CDEIII sequence *in vivo* (Cohen et al. 2008). Temperature-sensitive *mif2* alleles isolated by *in vitro* mutagenesis show an increased chromosome loss and aberrant spindles, leading to the hypothesis that Mif2 is responsible for the integrity of the spindle during anaphase spindle elongation (Brown et al. 1993). Phosphorylation of serine 54 and 325 on Mif2 is mediated by the yeast Aurora B kinase homologue Ipl1 (Westermann et al. 2003). However, its precise function in the kinetochore regulation is still unclear.

1.9.2 The central kinetochore proteins

After DNA replication in early S-phase, the kinetochores are reassembled on the sister centromeres by hierarchically recruiting middle and outer kinetochore components. The Ctf19 complex consists of 12 proteins, whose detailed composition was characterized by TAP-purification (Cheeseman et al. 2002). Within this complex, Ctf19, Okp1, Mcm21 and Ame1 act as a four-protein complex, also known as COMA complex. However, only Okp1 and Ame1 are required for cell viability. The COMA complex builds a platform for further assembly of other inner kinetochore components. A direct association between the COMA complex and the Mtw1 components was shown by pull-down experiments of Flag-tagged Ame1 (Hornung et al. 2011). Like the COMA complex, the Mtw1 complex is a four-protein complex whose subunits are essential (Euskirchen 2002). *In vitro* analysis demonstrated that the complex can assemble from two heterodimers consisting of Mtw1-Nnf1 and Nsl1-Dsn1, which directly interact with the microtubule-binding Ndc80 complex (Maskell et al. 2010). Both, COMA and Mtw1 mutants exhibit defects in chromosome segregation, caused for example by unstable spindle and monopolar attachment (Ortiz et al. 1999; Scharfenberger et al. 2003).

The best-characterized linker in the kinetochore is the four-protein Ndc80 complex, which is conserved from yeast to human (Wigge et al. 1998). All four proteins (Ndc80, Nuf2, Spc24 and Spc25) are essential for cell viability and have been named according to their close proximity to the spindle pole bodies. Mutants of the Ndc80 complex, like *ndc80-1* or mutants of *SPC24* or *SPC25*, show a complete detachment of the chromosomes from the mitotic spindle at the restrictive temperature (Wigge et al. 1998; Wigge and Kilmartin 2001). This phenotype illustrates the importance of the Ndc80 complex in the connectivity between the kinetochore and microtubule attachment. The phosphorylation on the N-terminus of Ndc80 by Ipl1 was shown to be not essential, but to participate in the segregation and checkpoint function of Ipl1 (Cheeseman et al. 2006; Akiyoshi et al. 2009).

The fourth protein complex in the linker region in the budding yeast kinetochore is the essential Spc105 complex. Together with Kre28, the heterotrimeric complex bridges the centromeric heterochromatin and the microtubules. Cells lacking Spc105 show an increase of mono-orientated sister chromatids (Pagliuca et al. 2009). Next to the task to ensure the bi-orientation of sister chromatids, Spc105 also maintains the spindle assembly checkpoint to misaligned kinetochores until the sister chromatids are correctly orientated. Furthermore, it was shown that the Spc105 complex interacts with the protein phosphatase

Glc7, leading to the hypothesis that this interaction contributes to the regulation of the phosphorylation and dephosphorylation level in the kinetochore (Rosenberg et al. 2011).

1.9.3 The outer kinetochore proteins

The outer kinetochore proteins form the direct kinetochore-microtubule interface by coordinating the activity of several ATP-dependent microtubule motor proteins and coupling the kinetochore to the plus-end of the microtubule (Westermann et al. 2007). The Dam1 complex is a heterodecamer, which oligomerizes in a 50 nm ring around a microtubule. Several studies have contributed to our understanding of the molecular mechanisms of Dam1 in transforming the depolymerization of the microtubules to poleward movement. A recent study allowed insights into the mechanism of the Dam1-tubulin interaction and the movement on the microtubule lattice (Ramey et al. 2011). Mutations of different subcomponents of the Dam1 complex show high rates of chromosome missegregation (Cheeseman et al. 2001; Westermann et al. 2006; Jones et al. 2001) demonstrating an essential role of Dam1 in the maintenance of the kinetochore-microtubule attachment.

Other components of the outer kinetochore layer are the motorproteins Cin8, Kip1 and Kip3. They act as microtubule-associated kinesins, which contribute to the integrity of the microtubule-kinetochore interaction, for example by cross-linking clustered neighboring nonsister kinetochores (Hoyt et al. 1992).

The Aurora kinase complex Ipl1 is conserved from yeast to human and consists of four components - Ipl1, Sli15, Bir1 and Npl1. The serine-threonine kinase Ipl1 constitutes the enzymatic subunit of this complex. Mutants with defects in Ipl1 activity show high frequencies of chromosome missegregation (Biggins et al. 1999). One function of Ipl1 is to facilitate chromosome biorientation by the turnover of monopolar attachment until tension occurs between kinetochores and the spindle pole bodies (Tanaka et al. 2002).

1.10 Role of posttranslational modifications in the kinetochore-centromere organization

The interaction between the centromere-attached kinetochore and the microtubules ensures the precise segregation of chromosomes in mitosis as well as in meiosis. To regulate the kinetochore activity accurately, a large number of proteins are posttranslationally modified. The most common posttranslational modification in the kinetochore is

phosphorylation. The protein kinase families Polo and Aurora catalyze most of this modification to the target proteins during the cell cycle. The Polo-like kinases (Plk) are highly conserved from yeast to humans and coordinate for example the entry into M-phase by the activation and control of cyclin-dependent kinase 1 (CDK1) (Archambault and Glover 2009).

The Aurora family encompasses Aurora A, B and C, while only Aurora B is present in the budding and fission yeast. It was shown that the phosphorylation of Dam1 by the Aurora B homologue Ipl1 in yeast is essential for proper attachment of the microtubules (Cheeseman et al. 2002), while the phosphorylation on the N-terminus of Ndc80 decreases the affinity to the microtubules (Biggins et al. 1999; Cheeseman et al. 2006).

Beside the modification of certain kinetochore proteins, canonical histones and histone variants are also targets for posttranslational modifications in centromeric chromatin. Phosphorylation on the centromeric histone H3 variant occurs on serine 7 in humans and on serine 50 in maize (Zeitlin et al. 2001; Kunitoku et al. 2003; Zhang et al. 2005). Other posttranslational modifications are also characteristic for the centromeric region, as it was shown for the histone H3 that is dimethylated at lysine 4 at the centromeric chromatin in *D. melanogaster* and human (Sullivan and Karpen 2004), and that is methylated on lysine 9 in the pericentromeric heterochromatin (Pidoux and Allshire 2004). Most of the functions and roles of the posttranslational modifications on the kinetochore as well as on the centromeric histones are not sufficiently characterized and are topics of current research.

1.11 Aim of this thesis

Chromosomes need to be accurately transmitted to the daughter cells during cell division. This process is mediated through the attachment of the microtubules to the kinetochore, which ensures the movement of the sister chromatids to the spindle poles. The kinetochore is associated in all eukaryotes with a defined chromosomal location, the centromere. This centromeric region is characterized by the presence of a histone H3 variant, which replaces the canonical histone H3 in centromeric nucleosomes. In former studies it was shown that posttranslational modification of this histone H3 variant in human cells prevents the formation of misaligned chromosomes during mitosis, and therefore contributes to correct chromosome segregation (Zeitlin et al. 2001; Kunitoku et al. 2003). Posttranslational modifications, like acetylation and methylation of the centromeric histone H3 variant, termed Cse4, have not been described so far in the budding yeast *S. cerevisiae*.

The aim of this study was to identify such posttranslational modifications on Cse4 and to characterize their function during chromosome segregation and their contribution to centromere biology. To this end, a method was evaluated to purify the protein from *S. cerevisiae* cells and the posttranslational modifications were subsequently determined by mass spectrometry. Furthermore, strains encoding the mutation of the modification sites of Cse4 were constructed and analysed for effects on the cell viability. In this content, it was also determined whether the mutation of the modification site influenced plasmid and chromosome stability. In a next approach, it was investigated whether a loss of the modification affected the deposition of Cse4 at the centromeric region or whether it influenced the kinetochore assembly. Moreover, antibodies against these posttranslational modifications of Cse4 were generated and used in Western blotting to answer the question whether the modification of Cse4 was cell-cycle dependent. In this study, different strategies were used to investigate the identity of the enzymes responsible for the modifications of Cse4.

Taken together, this study provided insights into the identification of novel posttranslational modifications of the centromeric histone H3 variant and contributed to the understanding of the function of the centromeric region. Furthermore, the characterization of these modifications highlighted their relevance for the regulation of the kinetochore and their involvement in chromosome segregation.

2. Materials and Methods

2.1 Materials

2.1.1 Bacterial strains

DH5α — F$^-$ Φ80d*lac*ZΔM15 Δ(*lac*ZYA-*arg*F)U169 *rec*A1 *end*A1 *hsd*R17(r_k^-, m_k^+) *pho*A *sup*E44 *thi*-1 *gyr*A96 *rel*A1 λ^- (Invitrogen)

TOP10 — F$^-$ *mcr*A Δ(*mrr-hsd*RMS-*mcr*BC) Φ80*lac*ZΔM15 Δ*lac*X74 *rec*A1 *ara*D139Δ(ara-leu)7697 *gal*U *gal*K *rps*L (Str^R) *end*A1 *nup*G (Invitrogen)

2.1.2 *Escherichia coli* media growth conditions

E. coli strains used for plasmid amplification were cultured according to standard procedures (Sambrook et al. 1989) in LB (Luria-Bertani) medium (5 g/l yeast extract, 10 g/l tryptone, 5 g/l NaCl) supplemented with 100 µg/ml ampicillin at 37°C.

2.1.3 *Sacccharomyces cerevisiae* growth and media conditions

Media were used as described previously (Sherman 1991). Yeast minimal medium (YM: 6.7 g/l yeast nitrogen base w/o amino acids and 2 % glucose or YM (msg): 1.7 g/l yeast nitrogen base w/o amino acids and w/o ammonium sulphate with 1 g/l L-glutamic acid monosodium salt and 2 % glucose) was supplemented with amino acids according to the auxotrophic markers (20 µg/ml adenine, histidine, methionine, tryptophan and uracil or 30 µg/ml leucine and lysine). YPD (10 g/l yeast extract, 20 g/l peptone, 2 g/l glucose) was used as yeast full medium. For the counterseletion against the synthesis of uracil, 5-FOA (5-fluoro-orotic acid; US Biological) was used in YM plates with a concentration of 1 mg/ml with an additional supplementation of 20 µg/ml uracil. Unless indicated otherwise, the yeast strains were grown at 30°C. For synchronization of yeast cells, the strains were grown for three hours at 30°C in full medium supplemented with nocodazole (10 µg/ml) or hydroxyurea (200 mM).

2.1.4 Generation of yeast strains and plasmids

Yeast strains and plasmids used in this study are described in Table 2 and 3. Yeast cells were grown and manipulated according to standard genetic techniques (Sherman 1991). *Cse4*-alleles on plasmids were constructed by using the plasmid gap repair method in yeast. For this purpose, *cse4* fragments containing the respective mutation were amplified by PCR-sewing and introduced by homologous recombination into a linearized plasmid in yeast. DNA was isolated and transferred in *E. coli* for amplification of the plasmid. The point mutations were confirmed by sequence analysis.
For the integration of *cse4-R37A*, the *cse4*-allele was cloned into the *URA3*-marked integrative pRS306 plasmid, and the plasmid was linearized in the *CSE4* ORF with *SphI*. The fragment was transformed into yeast cells (AEY4) and thus integrated into the *CSE4*

ORF. Yeast transformants were plated on 5-FOA (5-fluoro-orotic acid) medium to select against *URA3*. In order to test for the presence of the *cse4-R37A* allele, genomic DNA was isolated and *CSE4* ORF was amplified by PCR for sequence analysis.

Table 2: *S. cerevisiae* strains used in this study

Strain[a]	Genotype	Source[b]
AEY1	*MATα ade2-101 his3-11,15 trp1-1 leu2-3,112 ura3-1* (W303)	J. Rine
AEY2	AEY1, but *MAT***a**	J. Rine
AEY3	AEY1, but *ADE2 lys2*Δ	J. Rine
AEY4	AEY2, but *ADE2 lys2*Δ	J. Rine
AEY7	*MAT***a***/α HMR*a*/ HMR*-ssΔ*I ade2*	
AEY685	*MATα HMR*a*-e** cin8*Δ*::LEU2 ade2 LYS2*	
AEY2781	*MATα cse4*Δ::KanMX *ade2 lys2* + pRS426-3xHA-*CSE4* (pAE977)	
AEY2797	*MAT***a** *cep3-2* (SBY162)	S. Biggins
AEY2799	*MAT***a** *ndc10-1* (SBY164)	S. Biggins
AEY2800	*MAT***a** *ndc10-2* (SBY165)	S. Biggins
AEY2801	*MAT***a** *cep3-1* (SBY168)	S. Biggins
AEY2802*	*MAT***a** *mif2-3 leu2 trp1 ura3 ADE2 LYS2 HIS3*	L. Hartwell
AEY4217	*MAT***a** *his3 200 trp1-901 leu2-3,112 ade2 LYS2::14lexAop-HIS3 URA3::8lexAop-lacZ-GAL4*	
AEY4651	AEY2781 + pRS313-3xHA-*cse4-S33A* (pAE1485)	
AEY4653	AEY2781 + pRS313-3xHA-*cse4-K49R* (pAE1487)	
AEY4655	AEY2781 + pRS313-3xHA-*cse4-S33A-K49R* (pAE1492)	
AEY4657	AEY2781 + pRS313-3xHA-*CSE4* (pAE615)	
AEY4759	AEY2781 + pRS313-3xHA-*cse4-103* (pAE1514)	
AEY4814	AEY2781 *cbf1Δ::*NatMX	
AEY4816	AEY1 *cbf1Δ::*NatMX	
AEY4818	AEY4 *hmt1Δ::*KanMX	
AEY4820	AEY4 *rmt2Δ::*KanMX	
AEY4822	AEY4 *hsl7Δ::*KanMX	
AEY4840	AEY2781 + pRS313-3xHA-*cse4-R37A* (pAE1579)	
AEY4841	AEY2781 + pRS313-3xHA-*cse4-R37A-K49R* (pAE1581)	
AEY4846	AEY4814 + pRS313-3xHA-*CSE4* (pAE615)	
AEY4847	AEY4814 + pRS313-3xHA-*cse4-S33A* (pAE1485)	
AEY4848	AEY4814 + pRS313-3xHA-*cse4-R37A* (pAE1579)	
AEY4849	AEY4814 + pRS313-3xHA-*cse4-K49R* (pAE1487)	
AEY4850	AEY4814 + pRS313-3xHA-*cse4-S33A-K49R* (pAE1492)	
AEY4851	AEY4814 + pRS313-3xHA-*cse4-R37A-K49R* (pAE1581)	
AEY4852	AEY4814 + pRS313-3xHA-*cse4-S33A-R37A* (pAE1594)	
AEY4853	AEY4814 + pRS313-3xHA-*cse4-S33A-R37A-K49R* (pAE1596)	
AEY4854	*MAT***a** *cbf1Δ::*NatMX *hsl7Δ::*KanMX *ade2 LYS2 met*	
AEY4855	*MAT***a** *cbf1Δ::*NatMX *hsl7Δ::*KanMX *ade2 lys2 met*	
AEY4856	*MAT***a** *cbf1Δ::*NatMX *hmt1Δ::*KanMX *ade2 lys2 met*	
AEY4857	*MATα cbf1Δ::*NatMX *hmt1Δ::*KanMX *ade2 LYS2 met*	
AEY4858	*MATα cbf1Δ::*NatMX *rmt2Δ::*KanMX *ade2 LYS2 met*	
AEY4859	*MAT***a** *cbf1Δ::*NatMX *rmt2Δ::*KanMX *ade2 LYS2 met*	
AEY4860	AEY2781 *ctf19Δ::*NatMX	

AEY4874	AEY4858 *hsl7Δ::*HisMX	
AEY4876	AEY 4846 *sas2Δ::TRP1*	
AEY4877	AEY 4848 *sas2Δ::TRP1*	
AEY4878	AEY4849 *sas2Δ::TRP1*	
AEY4879	AEY4851 *sas2Δ::TRP1*	
AEY4880	YJL146 *MAT***a** *ade2-101 trp1-Δ63 leu2-Δ1 ura3-52 his3-Δ200 lys2-801 mcm21Δ::TRP1*	J. Lechner
AEY4881	YJL 158 *MAT***a** *ade2-101 trp1-Δ63 leu2-Δ1 ura3-52 his3-Δ200 lys2-801 okp1-5Δ::TRP1*	J. Lechner
AEY4898	AEY2781 + pRS313-3xHA-*cse4-S33A-R37A* (pAE1594)	
AEY4899	AEY2781 + pRS313-3xHA-*cse4-S33A-R37A-K49R* (pAE1596)	
AEY4917	*MAT***a** *csm3Δ::*KanMX *ade2 LYS2*	A. Marston
AEY4918	*MAT***a** *iml3Δ::*KanMX *ade2 LYS2*	A. Marston
AEY4919	*MAT***a** *chl4Δ::*KanMX *ade2 LYS2*	A. Marston
AEY4920	*MAT***a** *ctf3Δ::*KanMX *ade2 LYS2*	A. Marston
AEY4921	*MAT***a** *mtw1-11 ade2-1 trp1-1 can1-100 leu2-3,112 his3-11,15 ura3 ssd1*	J. Kilmartin
AEY4922	*MAT***a** *ndc80-1 ade2-1 trp1-1 can1-100 leu2-3,112 his3-11,15 ura3 ssd1*	J. Kilmartin
AEY4923	*MAT***a** *spc24-1 ade2-1 trp1-1 can1-100 leu2-3,112 his3-11,15 ura3 ssd1*	J. Kilmartin
AEY4924	*MAT***a** *spc25-1 ade2-1 trp1-1 can1-100 leu2-3,112 his3-11,15 ura3 ssd1*	J. Kilmartin
AEY4925	*MAT***a** *spc105-4 ade2-1 trp1-1 can1-100 leu2-3,112 his3-11,15 ura3 ssd1*	J. Kilmartin
AEY4929	AEY4 *CSE4*-GFP (*TRP1*)	
AEY4931	AEY4874 *hmt1Δ::*URAMX	
AEY4936	AEY4860 + pRS426-3xHA-*CSE4* + pRS313-3xHA-*CSE4* (pAE615)	
AEY4937	AEY4860 + pRS426-3xHA-*CSE4* + pRS313-3xHA-*cse4-S33A* (pAE1485)	
AEY4938	AEY4860 + pRS426-3xHA-*CSE4* + pRS313-3xHA-*cse4-R37A* (pAE1579)	
AEY4939	AEY4860 + pRS426-3xHA-*CSE4* + pRS313-3xHA-*cse4-K49R* (pAE1487)	
AEY4940	AEY4860 + pRS426-3xHA-*CSE4* + pRS313-3xHA-*cse4-S33A-R37A* (pAE1594)	
AEY4941	AEY4860 + pRS426-3xHA-*CSE4* + pRS313-3xHA-*cse4-S33A-K49R* (pAE1492)	
AEY4942	AEY4860 + pRS426-3xHA-*CSE4* + pRS313-3xHA-*cse4-R37A-K49R* (pAE1581)	
AEY4943	AEY4860 + pRS426-3xHA-*CSE4* + pRS313-3xHA-*cse4-S33A-R37A-K49R* (pAE1596)	
AEY4944	AEY4860 + pRS426-3xHA-*CSE4* + pRS313-3xHA-*cse4-103* (pAE1514)	
AEY4945	AEY4860 + pRS426-3xHA-*CSE4* + pRS313 (pAE260)	
AEY4946	*MAT***a** *ame1-4::TRP1 ade2 lys2*	J. Vogel
AEY4965	AEY4 *cse4-R37A* (pAE1636 integrated)	
AEY4974	AEY1 *ctf19Δ::*KanMX	
AEY4981	*MATα cse4-R37A ADE2 lys2*	
AEY4982	*MATα cse4-R37A ade2 LYS2*	

AEY4983	*MATα cse4-R37A ADE2 lys2*
AEY4984	*MAT***a** *cse4-R37A cbf1Δ::*NatMX *ade2 lys2 met*
AEY4985	*MAT***a** *cse4-R37A cbf1Δ::*NatMX *ADE2 LYS2 met*
AEY4986	*MATα cse4-R37A cbf1Δ::*NatMX *ADE2 LYS2 met*
AEY4987	*MATα cse4-R37A cbf1Δ::*NatMX *ADE2 lys2 met*
AEY4990	*MAT***a** *cse4-R37A iml3Δ::*KanMX *ade2 LYS2*
AEY4991	*MATα cse4-R37A iml3Δ::*KanMX *ade2 lys2*
AEY4992	*MATα cse4-R37A chl4Δ::*KanMX *ade2 lys2*
AEY4993	*MAT***a** *cse4-R37A chl4Δ::*KanMX *ade2 LYS2*
AEY4994	*MAT***a** *cse4-R37A LYS2 ade2*
AEY4995	*MATα cse4-R37A ade2 lys2*
AEY4996	*MAT***a** *cse4-R37A csm3Δ::*KanMX *ade2 LYS2*
AEY4997	*MAT***a** *cse4-R37A csm3Δ::*KanMX *ADE2 lys2*
AEY4998	*MATα cse4-R37A ctf3Δ::*KanMX *ADE2 LYS2*
AEY4999	*MAT***a** *cse4-R37A ctf3Δ::*KanMX *ADE2 lys2*
AEY5003	*MATα cse4-R37A okp5-1::TRP1 ade2 lys2*
AEY5005	*MAT***a***/α cse4-R37A/ cse4-R37A ade2 LYS2*
AEY5006	*MAT mcm21Δ:: TRP1 ade2 lys2*
AEY5014	*MATα cse4-R37A ndc80-1 ade2 LYS2*
AEY5015	*MATα cse4-R37A ndc80-1 ADE2 LYS2*
AEY5016	*MAT***a** *cse4-R37A spc25-1 ADE2 LYS2*
AEY5017	*MAT***a** *cse4-R37A spc25-1 ADE2 lys2*
AEY5022	*MAT cse4-R37A spc105-4 ade2 LYS2*
AEY5024	*MATα cse4-R37A ndc10-1 ade2 lys2*
AEY5025	*MAT***a** *cse4-R37A ndc10-1 ade2 LYS2*
AEY5026	*MATα cse4-R37A cep3-1 ADE2 LYS2*
AEY5032	*MAT***a** *cse4-R37A mtw1-11 ADE2 LYS2*
AEY5033	*MAT***a** *cse4-R37A mtw1-11 ade2 LYS2*
AEY5040	AEY2781 + pRS423-3xHA-*cse4-R37A*
AEY5042	AEY2781 + pRS423-3xHA-*cse4-R37A-K49R*
AEY5057	AEY2781 + pRS423-3xHA-*CSE4*
AEY5082	*MATα mif2-3 cse4-R37A ADE2 LYS2*
AEY5083	AEY1 *ctf19Δ::*NatMX
AEY5084	AEY4 *cse4-K49R*
AEY5085	AEY4 *cse4-R37A-K49R*
AEY5086	*MATα cbf1Δ::*NatMX *cse4-R37A-K49R ADE2 lys2 met*
AEY5088	*MATα ctf19Δ::*KanMX *cse4-R37A-K49R ADE2 lys2*
AEY5146	AEY4 Mtw1-9xmyc-KanMX
AEY5147	AEY4 Ame1-9xmyc-KanMX
AEY5165	*MATα cbf1Δ::*NatMX Mtw1-9xmyc-KanMX *cse4-R37A ade2 LYS2*
AEY5166	*MAT***a** *cbf1Δ::*NatMX Mtw1-9xmyc-KanMX *ade2 LYS2*
AEY5173	*MATα cbf1Δ::*NatMX Ame1-9xmyc-KanMX *ADE2 LYS2*
AEY5174	*MAT***a** *cbf1Δ::*NatMX Ame1-9xmyc-KanMX *cse4-R37A ade2 LYS2*
AEY5186	AEY2781 + pRS313-3xHA-*CSE4*
AEY5187	AEY2781 + pRS313
AEY5188	AEY2781 + pRS313-3xHA-*cse4-R37A*
AEY5189	AEY2781 + pRS313-3xHA-*cse4-R37K*
AEY5190	AEY2781 + pRS313-3xHA-*cse4-R37Q*
AEY5191	AEY2781 + pRS313-3xHA-*cse4-R37A-K49R*
AEY5192	AEY2781 + pRS313-3xHA-*cse4-R37A-K49Q*

AEY5193	AEY4814 + pRS313-3xHA-*CSE4*
AEY5194	AEY4814 + pRS313
AEY5195	AEY4814 + pRS313-3xHA-*cse4-R37A*
AEY5196	AEY4814 + pRS313-3xHA-*cse4-R37K*
AEY5197	AEY4814 + pRS313-3xHA-*cse4-R37Q*
AEY5198	AEY4814 + pRS313-3xHA-*cse4-R37A-K49R*
AEY5199	AEY4814 + pRS313-3xHA-*cse4-R37A-K49Q*
AEY5200	AEY4860 + pRS313-3xHA-*CSE4*
AEY5201	AEY4860 + pRS313
AEY5202	AEY4860 + pRS313-3xHA-*cse4-R37A*
AEY5203	AEY4860 + pRS313-3xHA-*cse4-R37K*
AEY5204	AEY4860 + pRS313-3xHA-*cse4-R37Q*
AEY5205	AEY4860 + pRS313-3xHA-*cse4-R37A-K49R*
AEY5206	AEY4860 + pRS313-3xHA-*cse4-R37A-K49Q*
AEY5254	AEY2781 *rmt2Δ::*NatMX
AEY5256	AEY2781 *hmt1Δ::*NatMX
AEY5266	AEY2781 *hsl7Δ::*NatMX

[a] Strains were isogenic to W303 (AEY1-4) except those with an asterisk.
[b] Unless indicated otherwise, the strains were constructed during this study or were taken from the laboratory strain collection.

Table 3: Plasmids used in this study

Plasmid[a]	Description	Source
pAE615	pRS313-3xHA-*CSE4*	
pAE524	pACT2	
pAE940	pRS423-3xHA-*cse4-K49R*	
pAE956	pBTM 117c-*CTF19*	
pAE977	pRS426-3x HA-*CSE4*	
pAE1485	pRS313-3xHA-*cse4-S33A*	
pAE1487	pRS313-3xHA-*cse4-K49R*	
pAE1492	pRS313-3xHA-*cse4-S33A-K49R*	
pAE1510	pRS313 *cse4-103*	
pAE1513	pRS316-3xHA-*CSE4*	
pAE1514	pRS313 3xHA-*cse4-103*	
pAE1579	pRS313-3xHA-*cse4-R37A*	
pAE1581	pRS313-3xHA-*cse4-R37A-K49R*	
pAE1594	pRS313-3xHA-*cse4-S33A-R37A*	
pAE1596	pRS313-3xHA-*cse4-S33A-R37A-K49R*	
pAE1636	pRS306-*cse4-R37A*	
pAE1637	pRS306-*cse4-K49R*	
pAE1638	pRS306-*cse4-R37A-K49R*	
pAE1755	pRS423-3xHA-*cse4-R37A*	
pAE1756	pRS423-3xHA-*cse4-R37A-K49R*	
pAE1768	*URA3*, ARS3, SUP11, TEL, CEN6 CDEIΔ (pYCF5/d66)	P. Hieter
pAE1769	*URA3*, ARS3, SUP11, TEL (pYCF5)	P. Hieter
pAE1771	*TRP1*, ARS1, CEN6-CDEIΔ (d66)	P. Hieter
pAE1810	pACT2-*CSE4*	
pAE1811	pACT2-*cse4-K49R*	
pAE1812	pACT2-*cse4-R37A*	
pAE1822	pRS313-3xHA-*cse4-R37K*	

pAE1840	pRS313-3xHA-*cse4-R37A-K49Q*
pAE1841	pRS313-3xHA-*cse4-R37Q*

[a] Unless indicated otherwise, plasmids were constructed during this study or taken from the laboratory plasmid collection.

The oligonucleotides used in this study were synthesized by Metabion (Martinsried) and dissolved at a concentration of 100 pmol/µl. Genome sequences derived from the *Saccharomyces* Genome database (www.sgd.com) were used to design the primers.

Table 4: Oligonucleotides used in this study

Primer	Primer sequence
Cse4-pRS313 –fw	GCTATGACCATGATTACGCCAAGC
Cse4-pRS313 –rev	CGCCAGGGTTTTCCCAGTCACG
Cse4-S33A-fw	GGAGACCAACAAGCTATTAACGATCGTGCGTTATCGTTAGC
Cse4-S33A-rev	CGATCGTTAATAGCTTGTTGGTCTCCTGCAAGCC
Cse4-R37A-fw	CAATCTATTAACGATGCTGCGTTATCGTTATTGCAGAG
Cse4-R37A-rev	CGATAACGCAGCATCGTTAATAGATTGTTGGTCTCCTGC
Cse4 R37Q fw	CAATCTATTAACGATCAAGCGTTATCGTTATTGCAGAG
Cse4 R37Q rev	CGATAACGCTTGATCGTTAATAGATTGTTGGTCTCCTGC
Cse4 R37K fw	CAATCTATTAACGATAAAGCGTTATCGTTATTGCAGAG
Cse4 R37K rev	CGATAACGCTTTATCGTTAATAGATTGTTGGTCTCCTGC
Cse4-S33A-R37A-fw	CTTGCAGGAGACCAACAAGCTATTAACGATGCTGCGTTATCGTTATTGCAG
Cse4-S33A-R37A-rev	CTGCAATAACGATAACGCAGCATCGTTAATAGCTTGTTGGTCTCCTGCAAG
Cse4-K49R-fw	GCGACAAGGAACCTGTTTCCAAGAAGAGAGGAAAGAAGACG
Cse4-K49R-rev	GGAAACAGGTTCCTTGTCGCTCTTGTTCTCTGCAATAACG
Cse4-K49Q-fw	GCGACACAGAACCTGTTTCCAAGAAGAGAGGAAAGAAGACG
Cse4-K49Q-rev	GGAAACAGGTTCTGTGTCGCTCTTGTTCTCTGCAATAACG
Cse4-R37A-3`-fw	GACCAACAATCTATTAACGATGC
Cse4-K49R-3`fw	GAGAACAAGAGCGACAAG
KanMX K2	GCCCCTGAGCTGCGCACGTC
KanMX K3	CCCAGATGCGAAGTTAAGTGCGC
Cse4-S1-for	GAAGGACTGAATATAGAAAGAATACTAATATAACATAATCATGCGTACGCTGCAGGTCGAC
Cse4-S2	ATAAACCCCGAAAAAGGGAAAAATCGGCTCCAGCCCTGAAGCACAAATATCACTAATCGATGAATTCGAGCTCG
Cse4-S3	TACTATAATGAAGAAAGACATGCAACTAGCAAGAAGAATCAGGGGACAGTTTATTCGTACGCTGCAGGTCGAC
Cse4-S4-rev	CGAATCACTTTGAATAGCAGAACTAACCCATTGTTGTTTACTTGACATCGATGAATTCTCTGTCG
Cse4 A1 fw	GATAATCGTATAGCCGATGTG
Cse4 A4 rev	TTGTAGAAAACATGGTGC
Cse4 rev	CTAAATAAACTGTCCCCTGATTC
pRS313-fw-seq	GCACCCCAGGCTTTACACTTTATGC
pRS313-rev-seq	CGCAACTGTTGGGAAGGGCG
CBF1-S1-for	GTGCTTAAAATATAATACGGTTTTCTACACTTTTATTAACG

	ATGCGTACGCTGCAGGTCGAC
CBF1-S2-rev	CATAGGGAGACTCGAAATACATTTAGCTATCTATTTTTAAC TCTCAATCGATGAATTCGAGCTCG
CBF1-300bp-for	GTACATCGATGTACGTGATC
CBF1-300bp-rev	GAAAACGGAGGTTGTGC
CTF19-S1-for	GCTAGTGTGATCTTGTTGATACTAGGTCGGCAAAGAACGCA AATATGCGTACGCTGCAGGTCGAC
CTF19-S2-rev	CGTTTAAGCAAGCCGTCCAGTTGGCAATGGCAAATGGAAC ATCAATCGATGAATTCGAGCTCG
CTF19-300bp-for	CTGTGTTGTATTAAGCCACGTG
CTF19-300bp-rev	CAAAGGCTCGCATCCCATATC
HMT1-S1-for	CCAAAAAAGAGTTAGAACCGACAAATTCATCCAAAGAAAA TAATGCGTACGCTGCAGGTCGAC
HMT1-S2-rev	GTTTATTTGCTTTTCAAATTTTTTTCTTTCTCCAGCAAACAA AAGTCTTAATCGATGAATTCGAGCTCG
HMT1-300bp-for	GTTAGACTAGCCCCATGAG
HMT1-300bp-rev	CCGACATAGGTTGGAAATTG
HSL7-S1-for	CTTTTATACATATAATTTTTATATATACAAAGGGTTCAGTTT GCATATGCGTACGCTGCAGGTCGAC
HSL7-S2-rev	GGATAGTTATTTGTTGCCGCAGTATATAGTATACAATGCAG AATTCAATCGATGAATTCGAGCTCG
HSL7-300bp-for	CCCTCGTTTTGCACTGAG
HSL7-300bp-rev	GACAAGGCTGAAGGAAAAC
RTM2-S1-for	CAACGGCTAGGTGTTTACACCAAGGACTTTTAATATATTCA AGTATGCGTACGCTGCAGGTCGAC
RMT2-S2-rev	GGAAATCGGCCCCTGCCATTGTGCAATTTACATTATTCTAT AATTAATCGATGAATTCGAGCTCG
RMT2-300bp-for	GTGACATTAGCTGCGAGTAAG
RMT2-300bp-rev	GAGATTTTGAATATTCTTGCGG
Mtw1-S3 for	GATATTGAAGAGCCTCAATTGGATTTACTTGATGATGTGTT ACGTACGCTGCAGGTCGAC
Mtw1-S2 rev	CATACATCATATCATAGCACATACTTTTTCCCACTTTATATT AATCGATGAATTCGAGCTCG
Ame1-S3 for	GATAAATAAAATTAATGAAAATCTTTCTAACGAATTACAAC CAAGTCTACGTACGCTGCAGGTCGAC
Ame1-S2 rev	CATATATATATATATATATATATATATACATCTTTTGAACC AATTCCCTAATCGATGAATTCGAGCTCG

2.2 Methods

2.2.1 FACS (Fluorescence associated cell scanning)

For FACS analysis, strains were grown in YPD at 23°C and shifted for five hours to 37°C. Samples of 0.1 OD were harvested in mid-exponential phase at both temperatures. After washing the samples with H_2O, cells were fixed in 500 µl of 70 % EtOH over night at room temperature. The cells were subsequently washed in 20x TE, resuspended in 100 µl of 20x TE with RNase A (10 µl of 10 mg/ml) for four hours at 37°C and washed again with PBS. Staining with propidium iodide (0.1 mg/ml) was performed in 50 µl PBS at 4°C

over night. The samples were diluted 1:10, sonicated briefly and analysed with the flow cytometer (Calibur, BD).

2.2.2 Plasmid loss assay

Plasmid loss was measured in a wildtype (AEY4) and a *cse4-R37A* strain (AEY4965) carrying a *CEN6-TRP5* plasmid containing either a functional centromere sequence (pRS414) or a centromere sequence without the CDEI element (pAE1771). First, yeast cells were grown in 2 ml selective YM-medium to stationary phase over night at 30°C, and cells were then used to inoculate 5 ml YPD medium supplemented with adenine, histidine, leucine, lysine, tryptophan and uracil. The cells were grown for at least 12 doublings at 30°C and 37°C over night. Before and after the incubation, equal amounts of cells were plated on YM medium with and without tryptophane. The plasmid loss rate (L) was determined by comparing the amount of cells containing the plasmid before (F_i) and after (F_f) the incubation in full medium as $1\text{-}10^x$ with $x= \log F_f - \log F_i$/number of doubling time (McNally and Rine 1991).

2.2.3 Chromosome loss assay

Generation of wild-type and mutant centromere-containing chromosome fragment was carried out as described in (Hegemann et al. 1988). In briefly, plasmid containing wildtype and mutant centromere sequence (pAE1769, 1768) were linearized with *NotI* to fuse the large, nonessential chromsome fragments to the left arm of chromosome III. The diploid strain used for this work was homozygous for the *ade2* mutation. The diploids were selected for *URA3* and restreaked on nonselective YPD plates for pink transformands. The loss of the SUP11 gene, which suppressed the *ade2* mutation, was monitored by red pigment formation and displayed the mitotic stability of the chromosome fragment.

2.2.4 Chromatin immunoprecipitation and quantitative real-time PCR

ChIP and quantititative real-time PCR was performed as previously described (Weber et al. 2008) with minor modifications. For immunoprecipitation of Cse4-3xHA, Ame1, Mtw1 and H4, 100 OD cells were harvested and crosslinked with 1 % formaldehyde for 30 min at room temperature. Cells were then sonicated for seven cycles (30 sec on and 60 sec off) at 4°C (Bioruptor, Diagenode). Per ChIP, 4-5 µl of antibody were used. After reverse cross-linking at 65°C, the sample was digested with RNase A for 1 hour followed by incubation with proteinase K for another hour. DNA extraction was performed with Qiaquick Gel Extraction Kit and ERC Buffer (Qiagen). The quantitative real-time PCR was performed in a Rotor Gene 3000 (Corbett Research) using the SYBR Green Real MasterMix (5 PRIME) according to the manufacturer's instructions. The PCR was carried out by an initial denaturation step for 2 min at 94°C followed by 45 cycles of 15 sec at 94°C, 30 sec at 56°C and 40 sec at 68°C. For the detection of the melt curve the samples were heated at 40°C for 2 min and stepwise heated from 50°C to 95°C every 5 sec. For the analysis, the C_t value of each reaction was determined and a standard curve of the input samples was generated. The amount of precipitated DNA was calculated for each ChIP experiment relative to this standard curve. Three technical replicates were performed for every ChIP. The standard deviations were calculated from three independent ChIPs, and significance levels were determined by student's t-test. Oligonucleotide sequences used for quantitative real-time PCR are given in Table 5.

Table 5: Oligonucleotides used for ChIP analysis

Primer	Primer sequence
Cen4 up	GCCAGAAATAGTAACTTTTGCCTAAATCAC
Cen4 down	GCTATGAAAGCCTCGGCATTTTGG
Pol1 (5´) fw	GCTGCAAGCCGCTCGAAATG
Pol1 (5´) rev	CCAGTGTCTTCATCACTTGAACTG

2.2.5 Genetic crosses, sporulation and tetrad dissection of *S. cerevisiae*

Two haploid strains of opposing mating types were mixed on a YPD plate and incubated over night at 30°C. Isolation of diploids was induced by streaking the mixture on a selective YM plate for two to three days. The diploids were then regenerated for eight hours on a YPD plate and subsequently incubated on sporulation medium (19 g/l KAc, 0.675 mM ZnAc, 20 g/l agar) for at least three days at 23°C or 30°C. For dissection of asci, a loop of sporulated cells was incubated for six to eight minutes with 10 µl zymolyase buffer (1 M Sorbitol, 0.1 M NaCitrate, 60 mM EDTA pH 8.0, 5 mg/ml zymolyase). The reaction was stopped by adding 100 µl H_2O. The dissection of the tetrads on a YPD plate was performed by using a micromanipulator (Narishige) connected to a Zeiss Axioscope FS microscope. The plates were incubated for two to three days at 23°C or 30°C. To determine the markers of the segregants, plates were replica plated on YM selective medium.

2.2.6 Yeast-two-hybrid analysis

The two-hybrid strain (AEY4217) was transfomed with the bait and prey vectors (pBTM117c and pACT2) for two-hybrid analysis. To this end, full length *CSE4* and different *cse4*-alleles (*cse4-R37A* and *cse4-K49R*) were introduced into the pACT2 vector. To analyse the interaction, the reporter strain contained two reporter genes, *HIS3* and a *lacZ* reporter. The activation of the lacZ reporter was analyzed by transferring the strains on a nitrocellulose membrane. The membrane was then frozen in liquid nitrogen and incubated with the buffer Z (60 mM Na_2HPO_4, 40 mM NaH_2PO_4, 10 mM KCl, 1 mM $MgSO_4$, pH 7.0 + freshly added 0.1% X-Gal) over night at 30°C to induce the colour reaction. The activation of the *lacZ* gene was indicated by blue stained yeast cells. The activation of the *HIS3* reporter gene was tested by incubating the strains on plates lacking histidine for three days at 30°C.

2.2.7 Protein extraction of *S. cerevisiae*

Yeast cells were grown in 5 ml liquid culture over night. After measuring the OD_{600}, 4-10 OD cells were harvested, washed once with TBS and resuspended in 100 µl cell lysis buffer (300 mM NaCl, 0.1% Nonidet P-40, 10 mM Tris pH 8, 1 mM EDTA in PBS containing protease inhibitor). The proteins were extracted by vortexing three times for 20 sec with acid-washed glass beads. 4x Lämmli buffer was added to each sample and samples were heated for 5 min at 95°C. Protein amounts equivalent to harvested OD units were loaded on the SDS-PAGE gels as indicated.

2.2.8 Acid extraction of yeast histones

The extraction of histones was performed as described in (Mullen et al. 1989). 100 ml of yeast cells were harvested at OD 2 and washed in 10 ml of sorbitol phophate buffer (1 M sorbitol in 50 mM KH_2PO_4 pH 7.5). The pellet was then resuspended in 5 ml sorbitol phosphate buffer (+ 20 µl β-Mercaptoethanol) and spheroblasts were made by adding 600 µl zymolyase (20 mg/ml H_2O) for 30 min at 30°C. The spheroblasts were washed with 5 ml sorbitol phosphate buffer and resuspended in 10 ml ice-cold NIB-buffer (0.25 M sucrose, 60 mM KCl, 15 mM NaCl, 5 mM $MgCl_2$, 1 mM $CaCl_2$, 15 mM Mes, 0.5 % Triton) with protease inhibitors for 30 min. The spheroblasts were then pelleted for 8 min (5500g). The NIB buffer incubation by pelleting was repeated twice. The crude nuclear pellet was resuspended in 10 ml cold 100 mM Tris pH 6.8, 0.4 M NaCl with protease inhibitors and incubated for 10 min on ice. After pelleting, the salt wash was repeated once with 5 min incubation on ice. Pelleted nuclei were resuspended in 1.35 ml cold H_2O with protease inhibitors. One-tenth volume of cold 4 N H_2SO_4 was added to the suspension while swirling and the histones were extracted over night on ice. After centrifugation for 10 min at 12000 g the supernatant was incubated with 13.5 ml cold acetone/HCl (acetone: 5 M HCl; 99:1) over night at -20°C. The histones were pelleted for 10 min at 10000 g and resuspended in 100 µl H_2O. The amount of histones was measured using Bradford reagent and the required amount of protein was applied on SDS-PAGE gel.

2.2.9 SDS-PAGE and immunoblotting

Protein samples were separated on 10, 12 or 15 % SDS Gels according to standard methods (Laemmli 1970). Transfer to nitrocellulose membrane (Amersham Hybond ECL, GE Healthcare) was accomplished by blotting with the BIO-RAD Tank Transfer System with 5.5 mA x h/cm^2. Transfer buffer with 39 mM Glycine, 48 mM Tris base, 0.037 % SDS and 20 % methanol was used (Sambrook et al. 1989). The membrane was subsequently blocked for 1 hour in 5 % milk/ TBST. For the blots against the Cse4 modifications, 1.5 % BA (ECL *Advance* blocking agent, GE Healthcare) in TBST was used for 30 min. The primary antibody was incubated in 5 % milk/TBST or, in the case of Cse4 modification antibody, in TBST over night at 4°C. The membrane was then washed with TBST for 10 min and incubated with the secondary antibody for 1 hour in 5 % milk/TBST or in 1.5 % BA/TBST at room temperature. The membrane was subsequently washed with TBST for 1 hour at room temperature, and the signals were detected with the Amersham ECL Western Blotting Analysis System (GE Healthcare) and Amersham Hyperfilm ECL chemiluminiscence films (GE Healthcare). The antibodies used for Western blotting are listed in Table 6.

2.2.10 Dot blot analysis

Different amounts of modified and unmodified peptides were spotted on nitrocellulose membrane (Amersham Hybond ECL, GE Healthcare), dried at room temperature and blocked for 1 hour in 5 % milk/TBST. The primary antibody was incubated 1:200 - 1:1000 as indicated in 5 % milk/TBST over night at 4°C. After washing the membrane, the secondary antibody was incubated for 1 hour at room temperature in 5 % milk/TBST.
Dot blot analysis was also used for the analysis of the HPLC fractions. For this purpose, 5 µl of every other fraction was spotted on a PVDF membrane (GE Healthcare). After drying, the membrane was blocked for 1 hour in 5 % milk/TBST at room temperature. The

primary antibody was incubated 1:1000 in 5 % milk/TBST over night at 4°C. The incubation of the second antibody and the detection of the signals were performed as described above. The antibodies used for dot blotting are listed in Table 6.

Table 6: Antibodies used in this study

Antibody	Company	Concentration
α-HA	covance; MMS101P	1:1000
α-myc	Sigma, M4439	1:1000
α-H4	abcam; ab31827	1:1000
α-H2B	active motif; 39237	1:3000
α-rabbit HRP	Sigma; A0545	1:5000
α-mouse HRP	Sigma; A9044	1:1000
α-Cse4-R37me	this study	1:1000 - 1:200
α-Cse4-R37me2a	this study	1:1000 - 1:200
α-Cse4-K49ac	this study	1:1000 - 1:200

2.2.11 Partial purification of Cse4

The partial purification of Cse4 was performed as described in (Waterborg 2000). In brief, Cse4 was purified from 6000 OD yeast cells. The crude histones were extracted in the presence of nuclear isolation buffer pH 7 (0.25 M sucrose, 10 mM $MgCl_2$, 2.5 mM spermidin, 0.5 mM spermin, 20 mM HEPES, 0.1% (w/v) Trition, 5 mM ß-Mercaptoethanol, 1 mM PMSF) with 100 mM butyrate. Each 500 OD pellet was resuspended in 3 ml nuclear isolation buffer and afterwards glass beads were added to the suspension until no free liquid remained. Each sample was vortexed for 2 min. Glass beads were added again and the samples were vortexed again for 2 min. Nuclear isolation buffer was added to the 30 ml mark of each falcon and the supernatants were filtrated with Poly-Prep Chromatorgraphy columns (BIO-RAD). The samples were washed again with 10 ml of nuclear isolation buffer and the supernatants were pooled. After centrifugation (30000 g, 10 min) and washing the pellet with 20 ml nuclear isolation buffer, the pellet was resuspended in 20 ml of 40 % guanidiumhydrochlorid in 0.1 M KP_i with 0.1 % ß-Mercapthoethanol. The suspension was homogenized by sonification on ice for 4 times 30 sec on, 60 sec off at 60-80 watts. The extract was clarified by centrifugation for 10 min at 30000 g. The DNA was precipitated with 0.4 N HCl for 30 min on ice and centrifugation for 30 min at 30000 g without brake. 0.1 M KP_i was added to the supernatant until the refractive index of 5 % guanidiumhydrochlorid was reached. The pH was adjusted to 6.8 and 5 mM ß-Mercaptoethanol was added. Afterwards 200 µl resin of the cation exchanger BioRex 70 per 10^{10} cells were added over night at room temperature. The resin was washed with 5 % guanidiumhydrochlorid in 0.1 M KP_i and 1.3 mM ß-Mercaptoethanol for 3 times. The crude histone extract was eluted with 10 column volumes of 40 % guanidiumhydrochlorid in 0.1 M KP_i and 1.3 mM ß-Mercaptoethanol. Afterwards the eluate was dialysed 3 times against 2.5 % acetic acid with 1 mM ß-Mercaptoethanol over night. After the ultrafiltration through Amicon Ultra 100K, the eluate was concentrate to 2 ml with Amicon Ultra 10K. The retentate was lyophilized and solved in 500 µl 8 M urea, 50 mM DTT, 1 M acetic acid and 50 mM NH_4OH. Afterwards the sample was fractionated for 94 min by reversed-phase HPLC on a Agilent Zorbax 300SB-C3 column between 35 and 53% acetonitrile (ACN; v/v) in 0.1 % trifluoroacetic acid at 1 ml/min. The 1 ml fractions were analysed by dot blot on a PVDF-membrane (GE Healthcare) and positive samples afterwards lyophilized. The samples were either used for colloidal Coomassie stained SDS-Gel or for Western blotting.

2.2.12 Antibody generation

Unmodified and modified Cse4 peptides used in this study to generate Cse4 modification-specific antibodies were synthesized by Biosynthan and listed in Table 7. The modified Cse4 peptides were used to generate Cse4 modification specific antibodies in rabbits. The immunizations of the rabbits by 10 mg modified peptides conjugated to KLH (Keyhole Limpet Hemacyanin) were performed by the companies Pineda and Biogenes. The specification of the immunsera against the modified peptides was tested by dot blot analysis. The antibodies were then affinity-purified and used for Western blot analysis.

Table 7: Peptides synthesized in this study

Cse4 peptide sequence	Modification
S I N D R A L S L G G C (33-41)	Monomethylation on Arginine
Q S I N D R A L S L G G C (32-41)	Asymmetrical dimethylation on Arginine
T R A T K N L F P G G C (45-53)	Acetylation on Lysine

2.2.13 Affinity purification of polyclonal antibodies

Modified and unmodified peptide columns were used to purify Cse4 specific antibodies. First 1 ml of sulfolink beads (Sigma) were equilibrate with 6 column volumes of reaction buffer (50 mM Tris, 5 mM EDTA-Na, pH 8.5). The beads were then incubated for 60 min on the wheel at room temperature with 1 mg of modified or unmodified peptide dissolved in 1 ml reaction buffer. The beads were washed with 3 column volumes of reaction buffer and incubated for 60 min with 1 column volume of 50 mM cysteine in reaction buffer to saturate the beads. After washing the beads with 16 column volumes each of 1 M NaCl and TBS/5 mM EDTA, 0.05 % NaN_3, the peptide columns were stored at 4°C in 1 column volume of TBS/5 mM EDTA, 0.05 % NaN_3.
For antibody purification, 5 mM EDTA was added to 5 ml serum and clarified by centrifugation (10000 g, 15-20 min, 4°C). The supernatant was then incubated with 125 µl beads coupled with the modified peptide for 2 h at 4°C on the wheel and washed three times with 10 ml TBS/5 mM EDTA. The antibody was eluted twice from the beads with 125 µl 0.1 M glycine pH 2.5 by incubation for 5 min at room temperature and centrifugation (2000 g, 30 sec). In the meantime, tubes were prepared on ice with 1 M Tris pH 9.5 to neutralize the antibody solution. The neutralization was followed with pH paper. The antibody solution was dialysed against PBS at 4°C and 0.05 % NaN_3 was added. Finally the antibody was stored at 4°C. The specificity was analyzed by dot blot. In the case of the R37me, R37me2a and K49ac antibodies used in this study, a second affinity purification was performed. For this purpose the antibody was incubated for 1 hour at room temperature on the wheel with 40 µl beads coupled with the unmodified peptide. After centrifugation (2000 g, 30 sec) the supernatant was again analyzed by dot blot and used for Western blot analysis.

2.2.14 Analysing the specificity of the Cse4 peptide antibodies

Peptide competition assay was performed to analyse the specific reactivity of the Cse4 modification antibodies. The R37me2a and K49ac antibody was pre-incubated with 100 pmol of modified or unmodified peptide for 30-60 min at 28°C. The R37me antibody was pre-incubated with 4000 pmol peptide under the same conditions. The dot blot and Western blot membrane was blocked with 1.5-3% BA/TBST (ECL Advance blocking

agent, GE Healthcare) for 30-60 min. The antibody was incubated in TBST or 1.5 % BA/TBST (1:200) over night at 4°C.

2.2.15 Mass spectrometry-analysis

The mass spectrometry analysis was carried out by Tiziana Bonaldi and Alessandro Cuomo, IFOM Milan, Italy.

Gel electrophoresis of Cse4 and in-gel digestion
Cse4 from partial histone purifications was separated by SDS-PAGE. The gel was stained with Coomassie Blue using Colloidal Blue Staining Kit (Sigma). The Cse4 band was excised and digested in-gel with trypsin (Promega) essentially as previously described (Shevchenko et al. 2006). Briefly, the gel band was washed four times with 50 mM ammonium bicarbonate/ 50 % ethanol and incubated with 10 mM DTT in 50 mM ammonium bicarbonate for 1 h at 56°C for protein reduction. An alkylation step was performed by incubating the sample with 55 mM iodoacetamide in 50 mM ammonium bicarbonate for 1 h at 25°C in the dark. Gel pieces were washed twice with 50 mM ammonium bicarbonate, 50 % ACN, dehydrated with 100 % ethanol and dried in a vacuum concentrator. Digestion was performed using 12.5 ng/ml trypsin in 50 mM ammonium bicarbonate for 16 h at 37ºC. The supernatant was transferred to a fresh tube, and the remaining peptides were extracted by incubating the gel pieces twice with 30 % ACN in 3 % trifluoroacetic acid (TFA), followed by dehydration with 100 % ACN. The extracts were combined, reduced in volume in a vacuum concentrator, desalted and concentrated using RP-C_{18} StageTip columns. The eluted peptides were used for subsequent mass spectrometric analysis (Rappsilber et al. 2007).

Mass spectrometry analysis (LC-MS/MS)
Peptide mixtures were separated by nano-LC/MSMS using an Agilent 1100 Series nanoflow LC system (Agilent Technologies), interfaced to a 7-Tesla LTQ-FT-Ultra mass spectrometer (ThermoFisher Scientific, Bremen, Germany). The nanoliter flow LC was operated in one column set-up with a 15 cm analytical column (75 µm inner diameter, 350 µm outer diameter) packed with C18 resin (ReproSil, Pur C18AQ 3 µm, Dr. Maisch, Germany). Solvent A was 0.1 % formic acid (FA) and 5 % ACN in ddH_2O and solvent B was 95 % ACN with 0.1 % FA. Samples were injected in an aqueous 0.1 % TFA solution at a flow rate of 500 nl/min. Peptides were separated with a gradient of 0-40 % solvent B over 90 min followed by a gradient of 40-60 % for 10 min and 60-80 % over 5 min at a flow rate of 250 nl/min. The mass spectrometer was operated in a data-dependent mode to automatically switch between MS and MS/MS acquisition. In the LTQ-FT full scan, MS spectra were acquired in a range of m/z 300 to 1350 by FTICR with resolution r = 100,000 at m/z 400 with a target value of 2,000,000. The five most intense ions were isolated for fragmentation in the linear ion trap using collision-induced dissociation at a target value of 5,000. Singly charged precursor ions were excluded. In the MS/MS method, a dynamic exclusion of 60 sec was applied, and the total cycle time was approximately 2 sec. The nanoelectrospray ion source (Proxeon, Odense, Denmark) was used with a spray voltage of 2.4 kV. No sheath and auxiliary gasses were used, and capillary temperature was set to 180ºC. Collision gas pressure was 1.3 millitorrs and normalized collision energy using wide band activation mode was 35 %. Ion selection threshold was 250 counts with an activation q = 0.25. The activation time of 30 msec was applied in MS2 acquisitions.

Data analysis and sequence assignment using MASCOT

The raw data from LTQ-FT Ultra were converted to mgf files using Raw2MSM software (Olsen et al. 2005). MS/MS peak lists were filtered to contain at most six peaks per 100 Dalton intervals and searched by Mascot Daemon (version 2.2.2, Matrix Science) against a concatenated forward and reversed version of the yeast ORF database (*Saccharomyces* Genome Database SGD at Stanford University -www.yeastgenome.org) (Elias et al. 2005); (Kall et al. 2008). This database was complemented with frequently observed contaminants (porcine trypsin, achromobacter lyticus lysyl endopeptidase and human keratins) as well as with their reversed sequences. Search parameters were: an initial MS tolerance of 7 ppm, a MS/MS mass tolerance at 0.5 Da and full trypsin cleavage specificity, allowing for up to two missed cleavages. Carbamidomethylation of cysteine was set as a fixed modification, and variable modifications included mono- and di-methylation on lysine and arginine residues, tri-methylation on lysines, oxidation on methionine and acetylation on the N-terminus of proteins. We accepted peptides and proteins with a false discovery rate (FDR) of less than 1%, estimated based on the number of accepted reverse hits (Elias et al. 2005). Filtered data were then manually confirmed using the Qual Browser version 2.0.7 (ThermoFisher Scientific). Extracted ion chromatograms (XIC) were constructed for precursor ions with mass tolerance of 10 ppm and mass precision up to 4 decimal places. Peak areas for both unmodified and modified peptide species were measured within the same retention time interval.

3. Results

3.1 Detection of PTMs on Cse4

Modifications on histones play an important role in the regulation of chromatin function. Foremost, the N-terminus of the histones is marked by modifications like acetylation, phosphorylation or methylation (Scharf and Imhof 2010). Next to canonical histones, the histone variants also have the potential of being modified, which consequently may alter the structure of the chromatin (Kamakaka and Biggins 2005). In this study, we asked whether the centromeric histone H3 variant in *S. cerevisiae* (Cse4) is posttranslationally modified, and we sought to gain insight into the functions of these potential modifications. Cse4 is exclusively localized to the centromere of the 16 chromosomes in budding yeast and is essential for chromosome segregation (Meluh et al. 1998). So far, no posttranslational modifications like acetylation or phosphorylation have been described for this variant in budding yeast. However, it was shown that proteolysis contributes to the centromeric localization through ubiquitination of Cse4 by the ubiquitin ligase Psh1 (Ranjitkar et al. 2010; Hewawasam et al. 2010; Collins et al. 2004). Furthermore, the human Cse4 homologue CENP-A is phosphorylated on serine 7 (Zeitlin et al. 2001; Kunitoku et al. 2003), and CenH3 in maize is phosphorylated on serine 50 (Zhang et al. 2005).

In the past, the identification of modified histones such as acetylation or phosphorylation was often performed by using TAU (Triton-Acetid acid-Urea) gels that separate different histone isoforms based on their charge and mass (Barratt et al. 1994). In recent years, many posttranslational modifications on the histones were identified by mass spectrometry or by homology to modifications identified on related histones. The identification of the phosphorylation on serine 7 of CENP-A was based on the homology to the phosphorylation on serine 10 of the canonical histone H3 (Zeitlin et al. 2001).

To study the posttranslational modifications on Cse4, a method had to be established to purify sufficient amounts of protein for mass spectrometry (MS) (Figure 7). For this purpose, a *cse4*Δ strain that carried a p*URA3*-*CSE4*-3xHA plasmid (AEY2781) was used, and partially purified histones were obtained (Waterborg 2000).

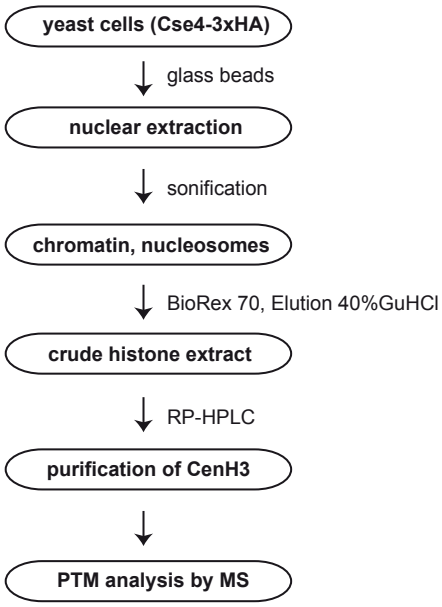

Figure 7: Overview of the procedure to purify the centromeric histone variant from *S. cerevisiae.* Purification of Cse4 was based on the method described in Waterborg 2000.

6000 OD of cells were harvested in order to obtain adequate amounts of Cse4 protein for MS analysis. After the extraction of the chromatin and the elution of the crude histone extract via the cation exchanger BioRex 70, the eluate was further fractionated with reverse-phase HPLC (High Performance Liquid Chromatography). The fractionation was performed on a Zorbax C3 column (Agilent, 4.6 x 250 mm) between 35 and 53 % acetonitrile in 0.1 % trifluoroacetic acid at 1 ml/min over 94 min. To test the different fractions after the HPLC, a dot blot against the HA-tagged Cse4 proteins was performed. Subsequently, Cse4-containing fractions were lyophilized, the proteins separated in a SDS-PAGE gel and stained with colloidal Coomassie. In a parallel gel, the fractions were analysed by Western blotting against Cse4-3xHA. We were thus able to identify the Cse4 band in the Coomassie-stained SDS gel (Figure 8).

It was evident that this method of Cse4 purification yielded enough partially purified Cse4. We previously also tried other methods, but none of them gave sufficient amounts of Cse4. For instance, the purification of TAP-tagged Cse4 (Puig et al. 2001) or histone purification using MNase digestion of the chromatin showed both a low solubility of the Cse4 protein during the purification and an insufficient amount of purified Cse4 protein.

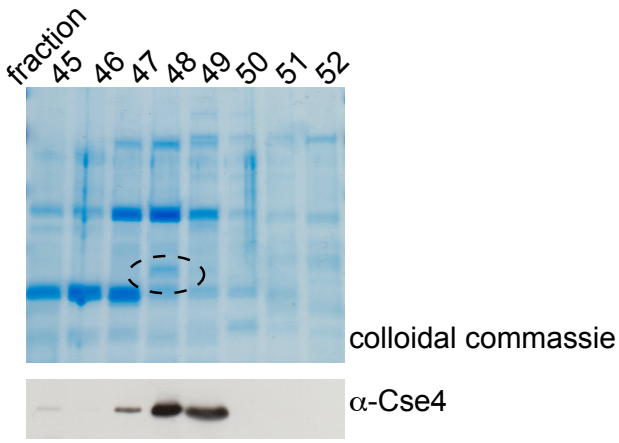

Figure 8: Partial purification of Cse4.
Colloidal Coomassie-stained SDS-PAGE gel (above) of HPLC fractions of partially purified Cse4-3xHA were used to excise the Cse4 band (dashed circle). Cse4-containing fractions were identified by Western blotting with α-HA antibody (below).

The Cse4 band after purification and separation on a SDS-PAGE gel was excised and analysed by mass spectrometry by Tiziana Bonaldi and Alessandro Cuomo from the European Institute of Oncology, Milano, Italy. The MS/MS analysis of the band confirmed the presence of the Cse4 protein with an average sequence coverage of 57 %. The analysis was based on peptides from a trypsin-digested protein, whose mass-to-charge ratio was measured. The peptide masses were compared to the *Saccharomyces* Genome database (www.yeastgenome.org). The identification of posttranslational modifications of the peptides was determined by mass-to-charge differences between unmodified and modified peptides (see Materials and Methods and Appendix, Figure 40).

In four independent experiments, we identified phosphorylation, methylation and acetylation in the N-terminus of Cse4 (Figure 9). All of the identified modifications in the N-terminus of Cse4 were located in the essential N-terminal domain, which encompasses amino acid sites 28-60 (Keith et al. 1999). These results showed for the first time that Cse4 was a target for posttranslational modifications. The phosphorylation on serine 33 (S33) was identified four independent times, whereas the mono-methylation on arginine 37 (R37) was identified twice. The acetylation on lysine 49 (K49) was determined once (Figure 9). It is very well possible that other modification sites on Cse4 exist, because this method covered only slightly more than half of the Cse4 protein. The following analyses will focus on the modified serine 33, arginine 37 and lysine 49. Taken together, this data showed that mass spectrometry was an excellent method to determine posttranslational modifications on Cse4.

Figure 9: Amino acid sequence of Cse4 with the identified modifications sites.
Identified peptides after trypsin-digestion of the protein are indicated in red. Cse4 was identified with a sequence coverage of 57 %. Modified amino-acids are illustrated according to their modification. Green-monomethylation, yellow-phosphorylation and blue-acetylation.

3.2 Methylation on arginine 37 of Cse4

The results above showed that Cse4 was a target for posttranslational modifications. Besides acetylation and phosphorylation of different amino acid sites, methylation on arginine 37 was determined. A quantification of the modification estimated that around 18 % of the analysed protein was monomethylated at this position (Appendix, Figure 40). Further analysis of this amino acid site in Cse4 showed a kinetochore-dependent function (see 3.3). For this reason, we generated specific antibodies against the methylated Cse4 to use them for further analysis of the role of Cse4 R37 methylation.

3.2.1 Generation and purification of antibodies against Cse4 R37 methylation

Specific peptide antibodies against modified histones can be used in order to gain insight into the function and role of the modification. Many such antibodies are utilised in cell biological approaches like Western blotting and fluorescence microscopy.

For the generation of specific antibodies against Cse4 R37 methylation, we synthesized peptides containing monomethylated and asymmetrically dimethylated arginine 37 and used these peptides for immunisation. Although the mass spectrometry identified monomethylation of arginine 37, but no dimethylation, we decided to additionally generate a specific antibody against asymmetrical dimethylation, because it was previously shown that arginine 2 of histone H3 is both mono- and asymmetrically dimethylated in yeast (Kirmizis et al. 2009). After the immunisation, the sera were tested against several dilutions of the modified and unmodified form of the Cse4 peptide on a dot blot (data not

shown). Surprisingly, different amounts of modified peptide were required to obtain a signal in the dot blot for the two antibodies. It showed that the concentration of the antibody against the monomethylation of arginine 37 (Cse4-R37me1) was 10 - 20 times lower than that of the antibody against the asymmetrical dimethylation of arginine 37 (Cse4-R37me2a) (data not shown, Figure 10). The likely reason for this could be that the peptide used for the generation of asymmetrical dimethylation of arginine 37 has an additional amino acid than the peptide used for the monomethylation of arginine 37. This could enhance the immunogenicity.

To increase the specificity of the antibodies against the modified Cse4 form, we purified the antibodies through columns containing covalently modified or unmodified peptide. Both antibodies, for the monomethylation as well as for the asymmetrical dimethylation of arginine 37, were specific after affinity purification against the modified Cse4 peptide (Figure 10). The antibodies against Cse4 R37 monomethylation as well as asymmetrical dimethylation distinguished between the Cse4 peptides containing monomethylated and asymmetrically dimethylated arginine 37 and the amounts of unspecific signals were very low. These results showed that the purified antibodies were specific to the modification they were raised against and could be used for the detection of mono- and asymmetrically dimethylated Cse4 *in vivo*.

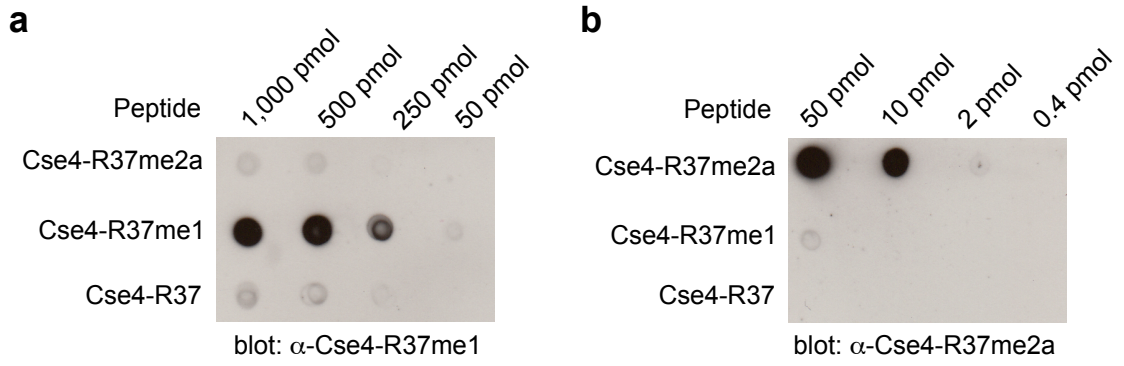

Figure 10: Specificity of Cse4-R37me1 and R37me2a antibodies.
a, Immuno-dot blot showing the specific reactivity of the Cse4-R37me1 antibody. The indicated amounts of modified and unmodified peptides were spotted on nitrocellulose membrane and probed against α-Cse4-R37me1 (1:200). **b,** Specificity of the Cse4-R37me2a antibody. Immuno-dot blot was performed as in **a** and probed against α-Cse4-R37me2a (1:200).

The specificity of the polyclonal anti-Cse4-peptide antibodies was further analysed using a peptide-competition assay. For this purpose, the antibody was first pre-incubated with different amounts of modified or unmodified competing peptides before the antibody was used for the dot blot. The results showed that both antibodies, when previously saturated

with their specific modified peptide, lost their ability to detect the peptide on the dot blot. The pre-incubation with the unmodified Cse4 peptide did not influence the ability of both antibodies to detect the specific modified Cse4 peptide on the dot blot (Figure 11). In the case of the antibody against the asymmetrical dimethylation of Cse4, it was also possible to saturate the antibody with the monomethylated peptide, and this had no influence of the ability of the antibody to detect the asymmetrically dimethylated Cse4 peptide on the dot blot.

Taken together, these results further corroborated the specificity of the polyclonal antibodies generated against the monomethylation and asymmetrical dimethylation of arginine 37 on Cse4.

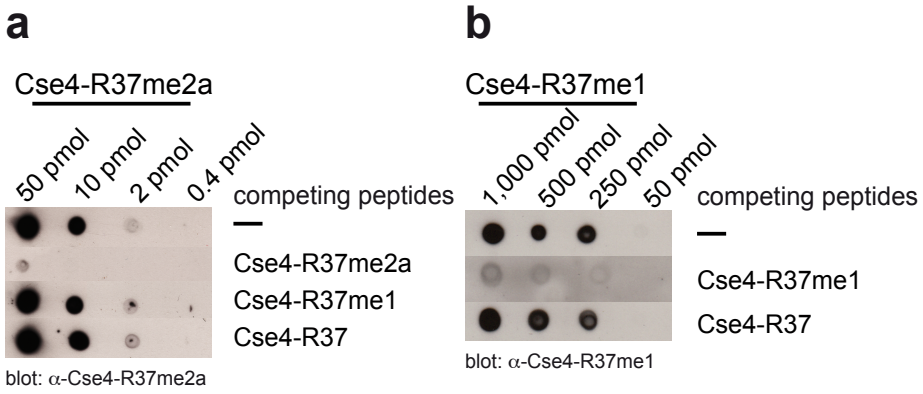

Figure 11: Peptide competition assay of the antibodies generated against Cse4-R37me1 and Cse4-R37me2a.
Indicated amounts of Cse4 peptide carrying R37me2a (**a**) and R37me1 (**b**) were spotted on the nitrocellulose membrane. Antibodies were pre-incubated with the competing peptides indicated to the right of the blot for 1 h for 28°C. Subsequently the antibodies were incubated on the membrane over night at 4°C.

3.2.2 Detection of Cse4 R37 methylation with antibodies in yeast

After the generation of specific antibodies against the monomethylated and asymmetrically dimethylated arginine 37 of Cse4, the antibodies were used in Western blots to detect the methylated Cse4 in wild-type cells. For this purpose, we compared the Cse4 methylation level in *cse4*Δ strains carrying plasmid-borne *CSE4*-3xHA or *cse4-R37A*-3xHA that carried a mutation in the methylation site (see for details on strain construction). We thus expected to obtain a decreased or a loss of the signal for the methylation of Cse4 in the strain carrying the *cse4-R37A* allele. Neither whole protein cell extracts from these strains nor histone extracts were sufficient to detect the methylated Cse4 by Western blotting (Figure 12), whereas Cse4 was readily detectable using an antibody against the HA tag.

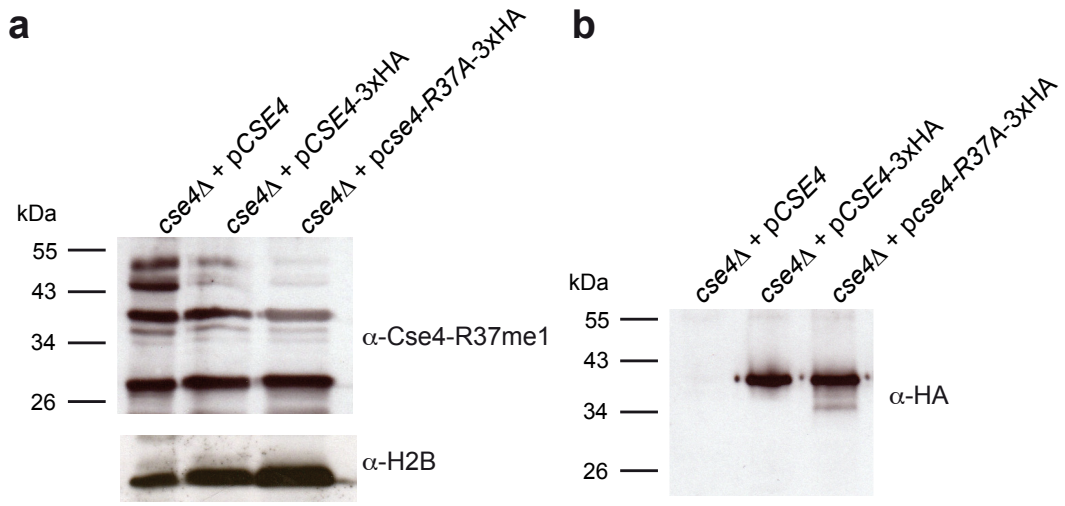

Figure 12: No specific signal for arginine methylation of Cse4 in conventional histone extractions.
a, Histone extractions were prepared from *cse4*Δ strain carrying either *CSE4* on a plasmid with or without HA-tag or HA-tagged *cse4-R37A*. 50 µg of histones from indicated strains were separated via SDS-PAGE and probed with α-Cse4-R37me1 antibody over night. **b,** Preparation as described in **a**. 5 µg of histones from each strain were separated via SDS-PAGE and probed with α-HA to detect Cse4-3xHA as control.

To increase the amount of Cse4 protein, we purified histones according to the method that we had previously used for the detection of the modifications via mass spectrometry (Waterborg 2000) from *cse4*Δ strains carrying plasmid-borne *CSE4*-3xHA or *cse4-R37A*-3xHA. After the separation of the histone extract of 6000 OD yeast cells via HPLC, equal amounts of Cse4 proteins were probed with α-Cse4-R37me1 and α-Cse4-R37me2a (Figure 13). The results of the Western blot against the asymmetrically dimethylated arginine 37 of Cse4 showed in both experiments a stronger signal in the sample with wild-type Cse4 in comparison to the strain containing the *cse4-R37A* allele. After stripping the blot and subsequent incubation with the antibody specific against the monomethylated arginine 37 of Cse4, the signal was also stronger in the wild-type strain. The signal in the *cse4-R37A* strain for both antibodies probably reflected a weak ability of the antibodies to recognize unmodified Cse4. The total Cse4 amount in the samples was detected using the HA-antibody as loading control. Altogether, this data demonstrated that Cse4 was monomethylated and asymmetrically dimethylated on arginine 37 *in vivo* and confirmed the methylation state on arginine 37 of Cse4 identified from the mass spectrometry.

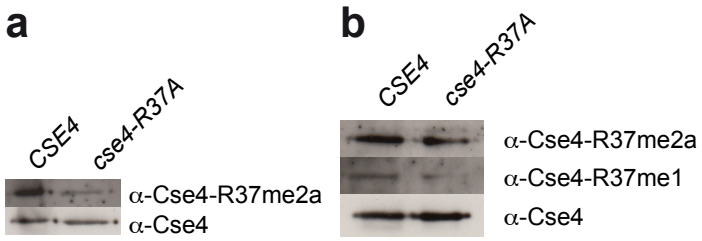

Figure 13: Cse4 was methylated on arginine 37 *in vivo*.
Histone extracts from wild-type (AEY2781) and *cse4-R37A* (AEY5040) cells were probed with α-Cse4-R37me1 (**b**) and α-Cse4-R37me2a (**a, b**) antibodies as well as with α-HA as loading control to detect Cse4-3xHA.

3.2.3 Increased methylated Cse4 in hydroxyurea-arrested cells

Due to the fact that the histone H3 variant Cse4 is located at the centromere and therefore involved in chromosome segregation, we asked whether the methylation on arginine 37 of Cse4 was cell cycle dependent. To this end, a *cse4*Δ strain carrying plasmid-borne *CSE4*-3xHA was arrested in S-phase using hydroxyurea and in G2/ M using nocodazole. The histones were extracted as above, and the methylation state of Cse4 was analysed using the Cse4-R37me1 and Cse4-R37me2a antibodies (Figure 14). The results showed that the amount of methylation on Cse4, for both monomethylation and asymmetrical dimethylation on arginine 37, was increased in the S-phase arrested cells in comparison to the asynchronous or G2/ M-phase arrested cells. This data demonstrated that the methylation on arginine 37 of Cse4 was cell-cycle dependent.

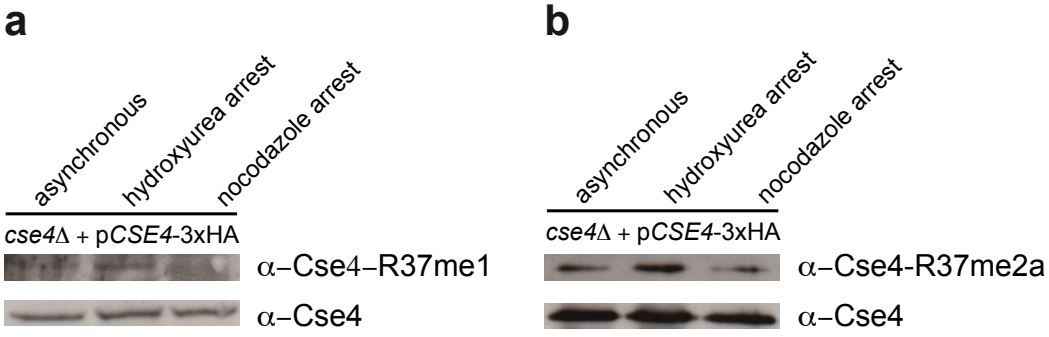

Figure 14: Cse4 R37 methylation was increased in S-phase arrested cells.
Histone extracts from asynchronous cultures of wild-type cells (AEY2781), or from cells arrested in S-phase with hydroxyurea and in G2/ M-phase with nocodazole were probed with α-Cse4-R37me1 (**a**) and α-Cse4-R37me2a (**b**) antibodies. The Cse4-R37me2a antibody was pre-incubated with unmodified competing peptide. Cse4-3xHA was detected with α-HA as loading control.

3.3 Functional analysis of Cse4 R37 methylation

3.3.1 Mutation of arginine 37 of Cse4 had no effect in wild-type cells

In order to analyse the function of the identified arginine 37 methylation on Cse4, the respective amino acid was mutated and the functional consequence of the mutation was tested. The amino acid was mutated to alanine (R37A) to prevent the modification of the site. The mutation of the amino acid to alanine was conducted on a plasmid encoding 3xHA-tagged Cse4 (pAE615). To test the function of the mutation in the yeast cells, the plasmid was transformed into a *cse4*Δ strain with an *URA3*-marked plasmid encoding wild-type Cse4, or as a control, with an empty vector. The transformants were then plated on 5-FOA (5-fluoro-orotic acid) medium to select against the *URA3*-marked *CSE4* plasmid. As expected, the negative control (vector) showed no growth on 5-FOA, because the deletion of *CSE4* is lethal (Stoler et al. 1995), and the cells are thus unable to survive in the absence of the *URA3*-marked *CSE4* plasmid (data not shown, Figure 16). In contrast, the strain carrying plasmid with *cse4-R37A* was able to survive on 5-FOA, showing that the mutation of Cse4 on arginine 37 was not lethal in wild-type cells. The strain containing the *cse4* allele was analysed for growth defects at different temperatures (Figure 15). The results showed that point mutation of arginine 37 in the N-terminus of Cse4 caused no growth defects at the analysed temperatures.

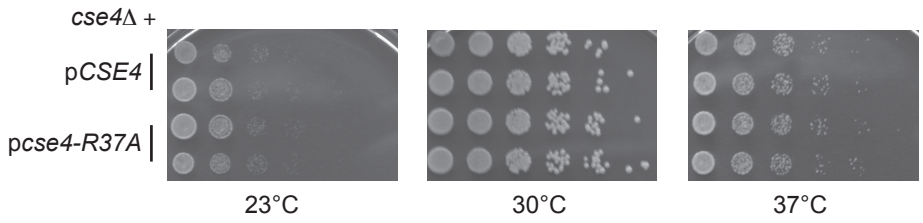

Figure 15: *Cse4-R37A* showed no temperature sensitivity in wild-type cells.
Plasmid-borne *cse4-R37A* and *CSE4* were introduced into a *cse4*Δ strain carrying an *URA3*-marked *CSE4*. After *URA3*-counterselection on 5-FOA, serial dilutions of the transformants were spotted on full medium and incubated for 2 days at the indicated temperature.

3.3.2 Mutation of arginine 37 of Cse4 showed a growth defect in cells lacking the kinetochore protein Cbf1

The kinetochore is a multiprotein complex consisting of more than 60 proteins that link the centromere to the microtubule to ensure the correct segregation of the chromosomes during meiosis and mitosis. This protein assembly can be subdivided into different protein layers, according to their function and distance to the centromeric DNA (Westermann et al. 2007).

We next asked whether a sensitization of the kinetochore by mutation of kinetochore components can cause defects of the *cse4* allele with a mutation in the identified modification site. For this purpose, we combined *cse4-R37A* with mutations in genes encoding kinetochore components. To this end, a *cse4*Δ strain containing a mutation in a gene encoding a kinetochore component and an *URA3*-marked plasmid encoding wild-type Cse4 was transformed with a plasmid carrying *cse4-R37A*, or as a control, with an empty vector. The transformants were then plated on 5-FOA to select against the *URA3*-marked *CSE4* plasmid. The negative control showed, as expected, no growth on 5-FOA. The strain containing *cse4-R37A* was able to survive on 5-FOA, showing that the mutation on arginine 37 of Cse4 was not lethal in the *cbf1*Δ cells (Figure 16a). The strain containing the *cse4-R37A* allele was then analysed for growth defects at different temperatures. Strikingly, the mutation of R37 to alanine caused a growth defect and temperature sensitivity in *cbf1*Δ cells (Figure 16b). Cbf1, the first kinetochore protein to be identified, is directly bound to the consensus sequence of the CDEI element of the centromeric region (RTCACRTG), but has no homologues in higher eukaryotes (Cai and Davis 1989; Baker et al. 1989). Next to its localization to the kinetochore, the Cbf1 protein functions as a transcription factor of methionine-biosynthesis genes (Cai and Davis 1990).

One might speculated that the observed growth defect of *cse4-R37A* in *cbf1*Δ cells was due to the size difference between arginine and alanine. To address this question, arginine 37 was also mutated to glutamine and lysine to prevent methylation of this site. Interestingly, the mutation of arginine 37 to glutamine showed inviability, a phenotype that was even stronger than that of *cse4-R37A*. The mutation of arginine 37 to lysine displayed no growth defects at the different temperatures in *cbf1*Δ cells (Figure 16a, b). Due to the fact that *cse4-R37A* and *cse4-R37Q* showed both a phenotype in *cbf1*Δ cells, we surmised that the phenotype was related to the absence of methylation rather than to the substituted amino acid.

The above results indicated that the *cse4-R37A* allele when encoded on a CEN-based plasmid, showed growth defects in *cbf1*Δ cells. We further tested whether a chromosomal integration of the *cse4* allele showed the same phenotypes. To this end, a *cse4-R37A* strain was constructed that contained this allele in the native *CSE4* chromosomal location, rather than on a plasmid, and crossed this strain to a *cbf1*Δ strain. After the dissection of the asci, the distribution of the unmarked *cse4-R37A* allele in the segregants was analysed using allele-specific PCR. Subsequently, the double mutants were tested for their growth defect and temperature sensitivity. Significantly, *cbf1*Δ *cse4-R37A* segregants showed a slow

growth at the permissive temperature and temperature sensitivity at 37°C, showing that the phenotype was not dependent on the expression source of Cse4-R37A (Figure 16c). Altogether, these data showed that the mutation of arginine 37 in Cse4 caused a synthetic growth defect in *cbf1*Δ cells.

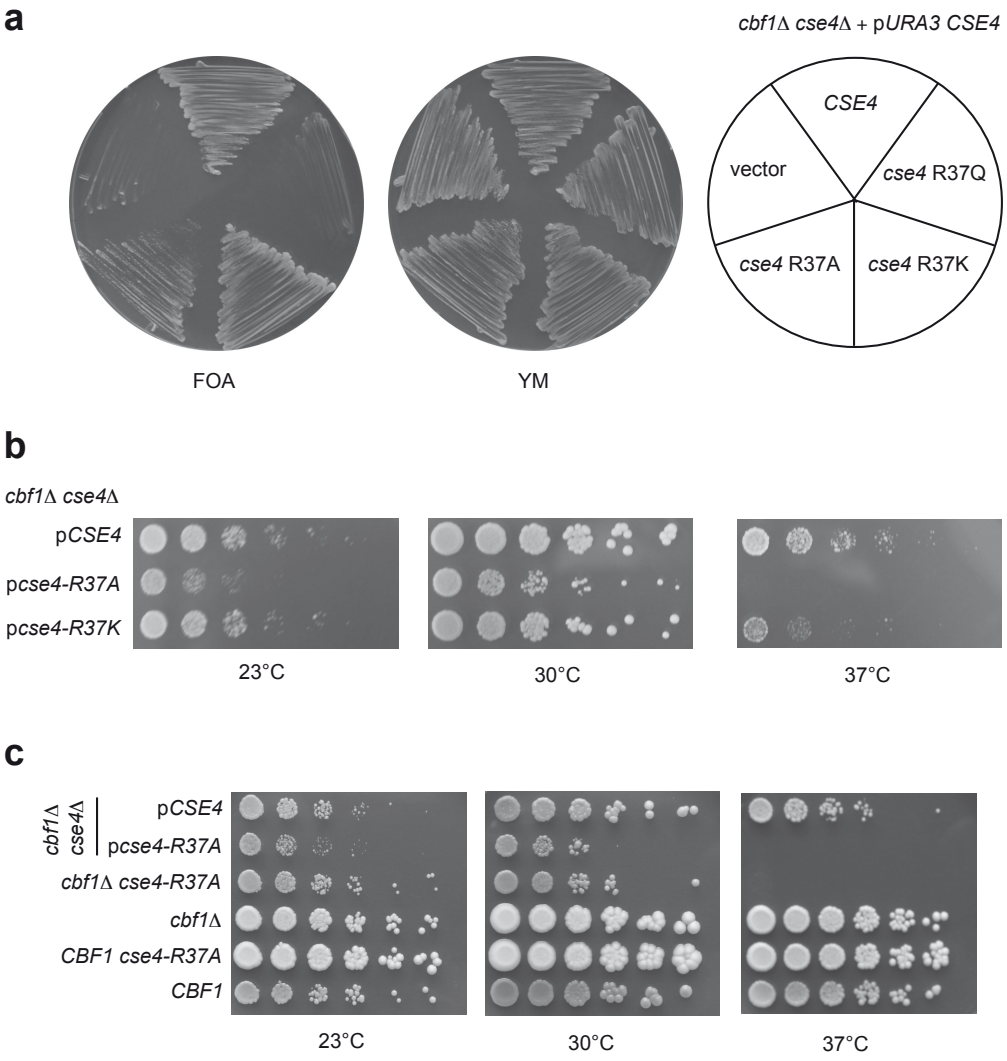

Figure 16: Mutation of arginine 37 of Cse4 caused growth defect in *cbf1*Δ cells.
a, Mutation of Cse4-R37 to alanine (*cse4-R37A*) or glutamine (*cse4-R37Q*) caused slow growth and inviability, whereas mutation of Cse4-R37 to lysine (*cse4-R37K*) showed no growth defects in *cbf1*Δ cells. Plasmid-borne *cse4-R37A*/ *-Q*/ *-K* was introduced into a *cbf1*Δ *cse4*Δ strain carrying a *URA3*-marked *CSE4* plasmid, and the ability of the cells to survive in the absence of *CSE4* was tested on *URA3*-counterselective medium containing 5-fluoro-orotic acid (FOA). **b**, Plasmid-borne *cse4-R37A/ -K* were introduced into a *cbf1*Δ *cse4*Δ strain and serial dilutions of these strains were spotted on YPD full medium. The incubation was performed for 3 days at indicated temperatures. **c**, *cse4-R37A* on a plasmid (second row) as well as chromosomally integrated (third row) caused slow growth at 30ºC and lethality at 37ºC in the *cbf1*Δ background. Rows 3 to 6 show a tetratype tetrad from a genetic cross of *cse4-R37A* with *cbf1*Δ.

3.3.3 Genetic interactions of *cse4-R37A* with mutations in genes encoding components of the Ctf19 complex

The presented results so far indicated that the absence of the methylation on arginine 37 of Cse4 showed strong synthetic growth defects with *cbf1*Δ. In the next step, we asked whether this effect was specific to the absence of Cbf1, or whether it extended to defects in the absence of other kinetochore components. To this end, different strains with mutations or deletions in genes encoding kinetochore components were used to analyse the different kinetochore protein complexes. The strain containing *cse4-R37A* was crossed to the kinetochore strains and the segregants were subsequently analysed at different temperatures. Interestingly, the absence of the Cse4 R37 methylation caused the most prominent effects with mutations in genes encoding components in the Ctf19 complex (Table 8). The Ctf19 complex belongs to the linker layer of the kinetochore, which connects the DNA-binding proteins of the inner kinetochore plate with the outer plate. One subcomplex of the Ctf19 complex is the four-protein complex COMA, which consists of Ctf19, Okp1, Mcm21 and Ame1 (Ortiz et al. 1999; Cheeseman et al. 2002). The *cse4-R37A* allele caused strong synthetic interactions like lethality or growth defects in all four strains that were deleted or mutated for the genes encoding components of the COMA complex (Figure 17a; Table 8). In detail, *cse4-R37A* showed synthetic lethality in combination with *ctf19Δ*, *mcm21Δ* and *ame1-4*. Furthermore, a severe growth defect was observed in *cse4-R37A okp1-5* cells.

Other components of the Ctf19 complex also displayed growth defects in combination with *cse4-R37A*, like Iml3, Ctf3 and Chl4 (Figure 17b, c; Table 8). The latter has been shown to be an important structural component for the interaction between Ctf19-Iml3 and Ctf19-Ctf3 in the kinetochore (Pot et al. 2003). This result illustrated that the mutations in genes encoding components of the Ctf19 complex showed strong synthetic interactions with the *cse4-R37A* allele.

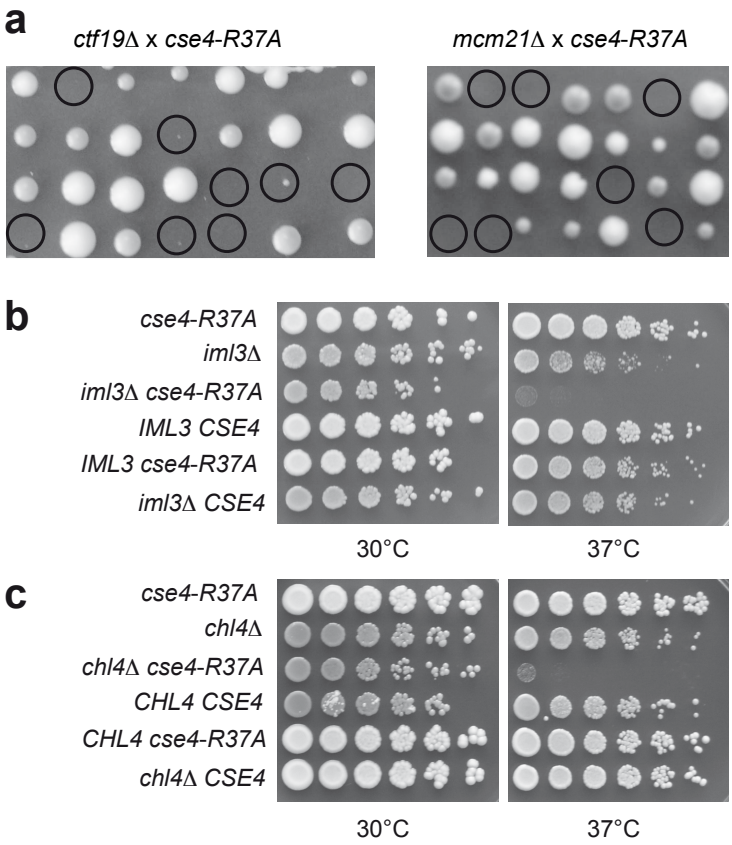

Figure 17: *cse4-R37A* caused synthetic lethality and growth defects in combination with mutations in genes encoding components of the Ctf19 complex.
a, Tetrad dissection of genetic crosses between *cse4-R37A* with *ctf19*Δ (left) and *mcm21*Δ (right). The dissection of the individual ascospores is aligned in vertical rows. The double mutants *ctf19*Δ *cse4-R37A* and *mcm21*Δ *cse4-R37A* are marked with circles. **b**, *cse4-R37A* caused synthetic growth defects in the absence of the Ctf19 component Iml3. Serial dilutions of the four segregants after the cross between *cse4-R37A* and *iml3*Δ were spotted on full medium and incubated for three days at the indicated temperatures. The top two rows represented the parental strains. **c**, *cse4-R37A* caused synthetic growth defects in combination with *chl4*Δ. Representation as in **b**.

Furthermore, we found that the *cse4-R37A* allele caused slight growth defects with *mtw1-11*, a component of the MIND complex and with *spc105-4* (Euskirchen 2002; Pagliuca et al. 2009). Synthetic lethality was furthermore observed in combination with the absence of the microtubule-associated kinesin Cin8. However, the *cse4-R37A* allele showed neither a strong defect in combination with mutations of the DNA binding complex CBF3 and Mif2, nor with mutations of the four-protein complex Ndc80 (Espelin et al. 1997, Brown et al. 1993; Wigge et al. 1998). Taken together, these data showed that the methylation on the arginine 37 of Cse4 became essential when kinetochore function was compromised by mutations of genes of the Ctf19 complex.

Table 8: Summary of the genetic interactions of *cse4-R37A* with mutations in genes encoding kinetochore components

Kinetochore component/complex	Allele	Synthetic phenotype with *cse4-R37A**
CENP-C	*mif2-3*	-
-	*cbf1Δ*	growth defect
CBF3 complex	*cep3-1, cep3-2*	-
	ndc10-1	slight growth defect
	ndc10-2	-
Ctf19 complex	*ctf19Δ*	lethality
	okp1-5	growth defect
	mcm21Δ	lethality
	ame1-4	lethality
	iml3Δ	growth defect
	chl4Δ	growth defect
	ctf3Δ	growth defect
Mtw1/MIND complex	*mtw1-11*	slight growth defect
Ndc80 complex	*ndc80-1*	-
	spc25-1	-
	spc24-1	-
Knl1 complex	*spc105-4*	slight growth defect
Kinesin motor protein	*cin8Δ*	lethality
Replication fork-associated factor	*csm3Δ*	-

* Additional phenotype caused by *cse4-R37A* in combination with the indicated allele of the gene encoding the respective kinetochore component. (-), no additional phenotype observed.

3.3.4 Methylation on arginine 37 of Cse4 affected centromere function

The centromeric sequence in *S. cerevisiae* encompasses ~125 bp of DNA and is subdivided into three elements (Furuyama and Biggins 2007). Changes in the sequence of the different elements affect centromere activity by causing aberrant chromosome segregation (Gaudet and Fitzgerald-Hayes 1987). Due to the fact that the kinetochore protein Cbf1 binds to the 8-bp CDEI sequence of the centromere (Cai and Davis 1990) and our observation that *cse4-R37A* caused a growth defect in *CBF1*-deleted cells, we hypothesized that the absence of the methylation of Cse4 affected the segregation of chromosomes lacking Cbf1 function. Therefore, we analysed the stability of a plasmid lacking the CDEI sequence of centromere 6 (Panzeri et al. 1985) in cells containing the *cse4-R37A* allele in comparison to wild-type cells. An intact centromeric plasmid served as a control. In wild-type cells, the plasmid lacking CDEI showed a reduced mitotic stability especially at 37°C, as it has been

previously reported (Panzeri et al. 1985) (Figure 18). However, a significant increase in plasmid instability of the CDEIΔ plasmid was observed in *cse4-R37A* cells in comparison to the wild-type cells both at 30°C and 37°C. This increase of plasmid instability was not observed with the intact centromeric plasmid in wild-type and *cse4-R37A* cells, not even at higher temperatures. This data showed that the *cse4-R37A* allele compromised the centromere stability in the absence of Cbf1 or deletion of the sequence domain of CDEI.

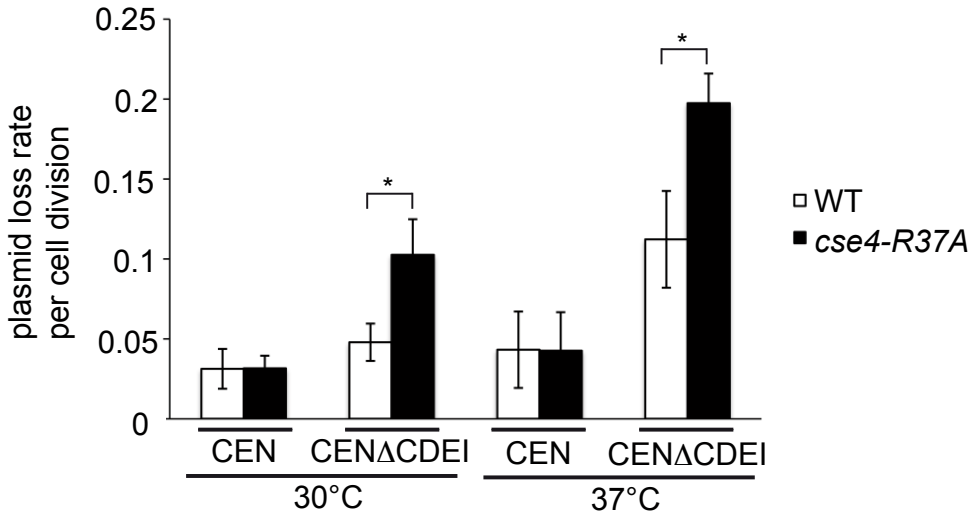

Figure 18: Mutation of arginine 37 of Cse4 caused a maintenance defect of plasmids lacking the CDEI sequence of CEN6.
Plasmid loss assay was perfomed of wt strain (AEY4) and *cse4-R37A* strain (AEY4965) containing a CEN6-*TRP5*-plasmid (pAE264) or a CEN6-CDEIΔ-*TRP5*-plasmid (pAE1771) at 30°C and 37°C. Error bars give standard deviation of three independent experiments. The asterisk indicates significant difference, *P* value < 0.05.

We next asked, whether this effect was only related to the loss of minichromosomes, or whether the segregation of a larger chromosome fragment was also affected by *cse4-R37A*. For this purpose, the stability of a linear, non essential chromosome fragment with a deletion in CDEI of CEN6 (Hegemann et al. 1988) and the equivalent wild-type fragment was analysed in wild-type and *cse4-R37A* cells. The transformed chromosome fragment was fused to the left arm of chromosome III and contained a *SUP11* gene, which suppresses the *ade2* mutation of the diploid cells. Loss of the *SUP11* gene can be monitored by red pigmentation of the analysed cells.

In agreement with the above observations, the cells containing the *cse4-R37A* showed an increased loss of the chromosome fragment with a deletion in the centromeric element I of CEN6 compared to wild-type cells, as measured by an increase of red colonies. As a control, a wild-type CEN6 was fused to chromosome III, and it showed no differences in the loss rate between wild-type and *cse4-R37A* cells (Figure 19). Taken together, this data

showed that the absence of methylation on arginine 37 of Cse4 disrupted centromere and chromosome segregation in the absence of CDEI, suggesting a role of Cse4 methylation in chromosome segregation.

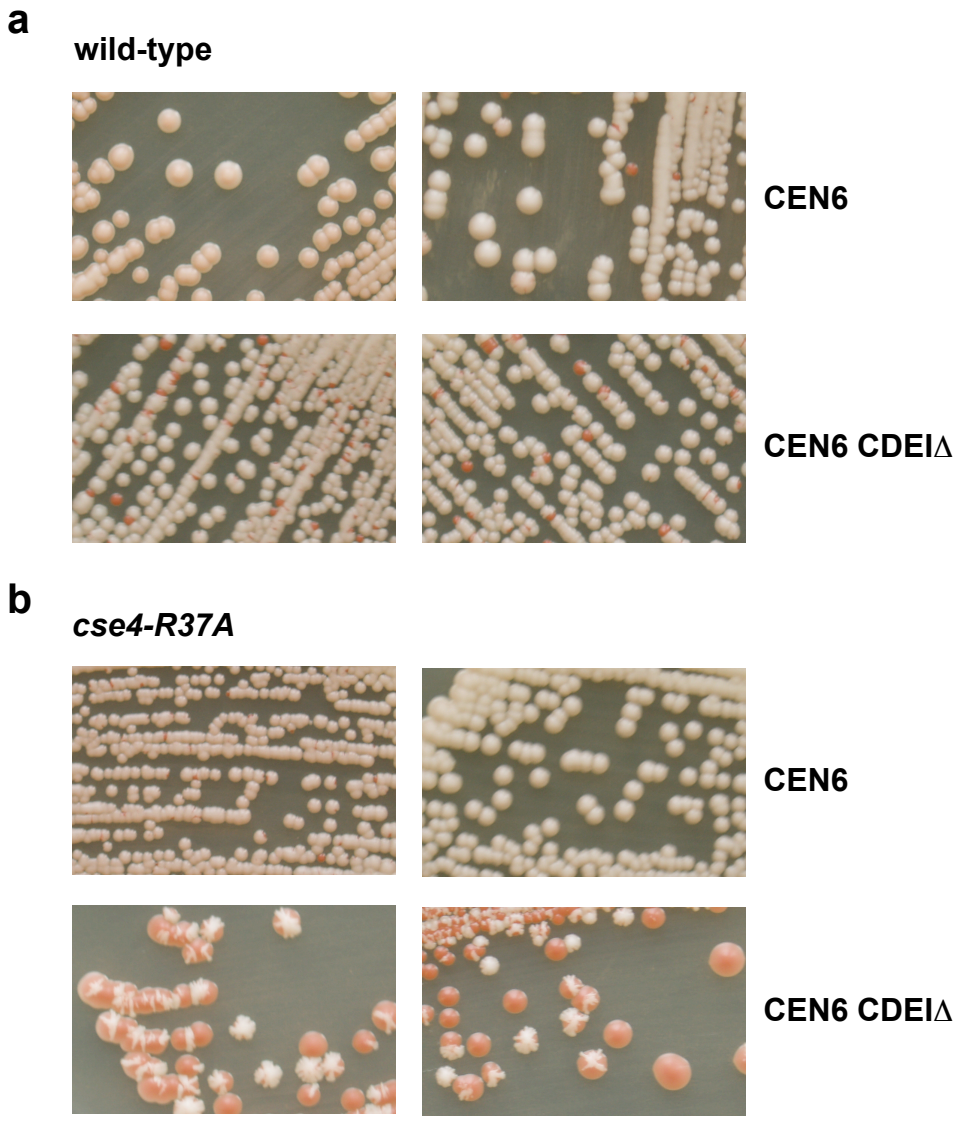

Figure 19: *cse4-R37A* caused increased loss of linear, non essential chromosome fragment with a deletion in CDEI of CEN6.
a, Transformation with linearized wt and deleted chromosome fragment in the *CSE4* diploid strain caused mitotically stable *SUP11*-marked chromosome fragment which suppressed the *ade2* mutation. The transformants showed a pink phenotype with minor red colonies. **b**, Analysis in *cse4-R37A* cells as described in **a**. Increased loss of CDEI deleted chromosome fragment in the *cse4-R37A* cells which was indicated by red colonies. Experimental procedure and picture courtesy of Prof. Ehrenhofer-Murray.

3.3.5 Absence of methylation of Cse4 caused a G2/ M arrest in *cbf1*Δ cells

The above experiments showed that the *cse4-R37A* allele in combination with a *cbf1*Δ strain caused a synthetic growth defect at 23°C and 30°C and a synthetic lethality at 37°C. To answer the question whether this observed phenotype is due to defects in the cell cycle,

the cells were analysed by flow cytometry (FACS). For this purpose, the cells were grown at 23°C, shifted for five hours to 37°C, and the DNA was stained with propidium iodide. Interestingly, the double mutant of *cbf1Δ* and *cse4-R37A* showed an accumulation of cells with 2n DNA content and a loss of cells with 1n DNA content at 23°C and particularly at 37°C in comparison to the wild-type and single mutants cells (Figure 20). The wild-type cells, the *cse4-R37A* cells as well as the *cbf1*Δ cells showed a distinct amount of cells containing 1n DNA content in comparison to the double mutant especially at the restrictive temperature. This result showed that the *cbf1*Δ *cse4-R37A* strain was characterized by a clear mitotic defect that was due to an arrest of the cells at the G2/ M boundary. This result was consistent with a defect of Cse4-R37A, and thus R37 methylation, in centromere function at the G2/ M boundary in the absence of Cbf1.

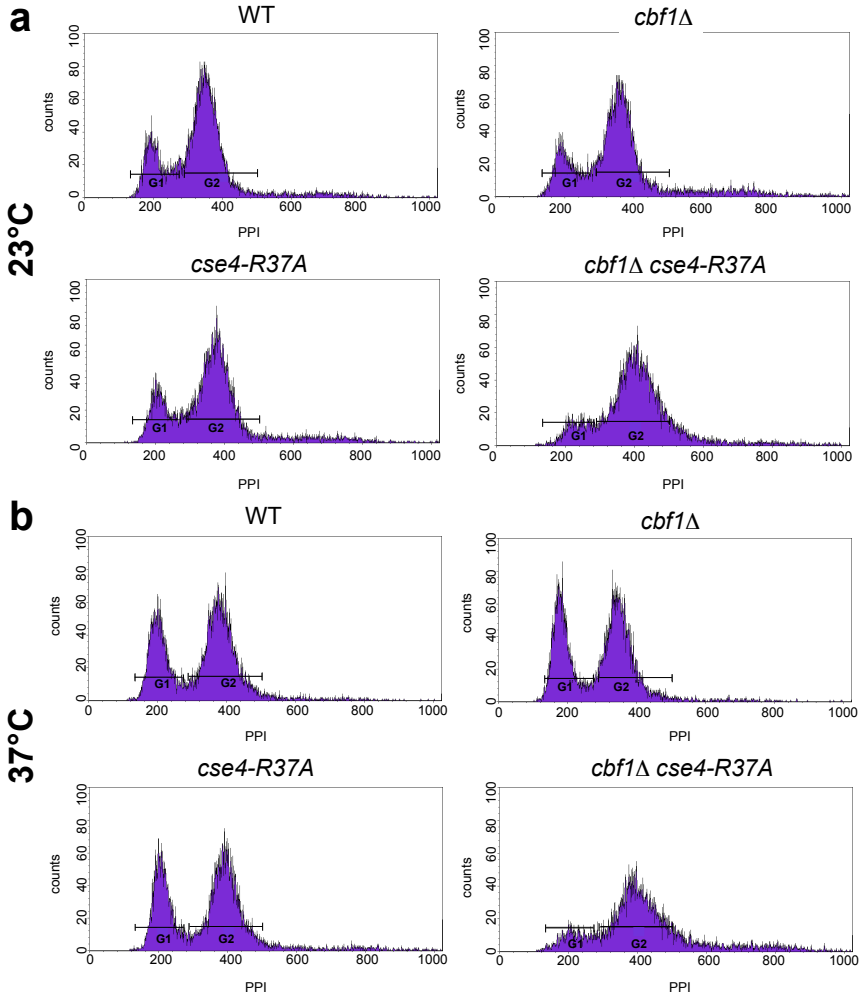

Figure 20: G2/ M arrest in *cbf1*Δ *cse4-R37A* cells at the permissive and restrictive temperature.
WT (AEY4), *cbf1*Δ (AEY4816), *cse4-R37A* (AEY4965) and *cbf1*Δ *cse4-R37A* (AEY4985) cells were grown to logarithmic phase at 23°C (**a**) and shifted to 37°C (**b**) for five hours. DNA was stained with propidium iodide (PPI) and analysed by FACS analysis.

The observation of a mitotic defect raised the question whether the double mutants of *cse4-R37A* and *cbf1*Δ showed sensitivity against the microtubule destabilization agent nocodazole. Nocodazole interferes with the polymerization of the microtubules, leading to a cell arrest in G2/ M. The absence of the formation of the metaphase spindles and the inability to segregate the chromosomes activates the spindle assembly checkpoint, forcing the cells to arrest in prometaphase. Interestingly, no significant sensitivity against the agent was observed of the double mutant *cbf1*Δ *cse4-R37A* on complete medium previously supplemented with different concentrations of nocodazole (Figure 21). This result showed that the microtubule attachment to the kinetochore was not affected in the double mutants at the selected nocodazole concentrations.

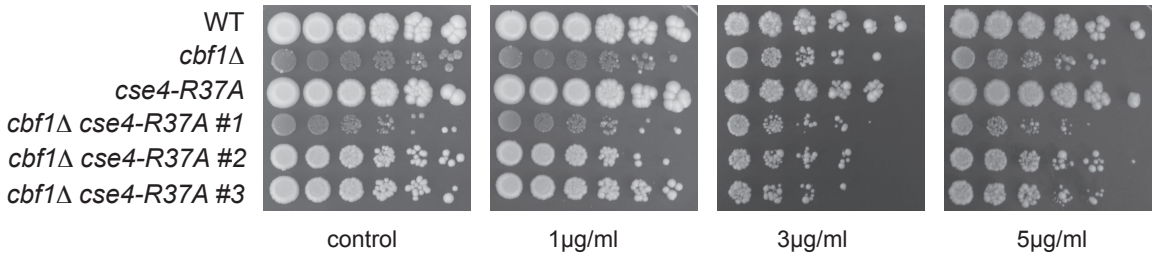

Figure 21: No significant sensitivity of *cbf1*Δ *cse4-R37A* cells to nocodazole.
Serial dilutions of WT (AEY4), *cbf1*Δ (AEY4816), *cse4-R37A* (AEY4965) and *cbf1*Δ *cse4-R37A* (AEY4984-4986) cells were spotted on full medium previously supplemented with different concentrations of nocodazole and incubated for three days at 30°C. Full medium supplemented with dimethylsulfoxide (DMSO) was used as negative control.

3.3.6 Cse4 deposition at the centromere was independent of Cse4 R37 methylation

The results above demonstrated that the *cse4-R37A* allele showed strong synthetic lethality in different mutants of genes encoding kinetochore components. Chromatin immunopreciptiation (ChIP) was performed to gain more insights into the mechanistic role and function of the methylation on arginine 37 of Cse4. One explanation of the growth defects and synthetic lethality of the *cse4-R37A* allele could be that there were decreased levels of Cse4 and thus R37 methylation at the centromeric region at the restrictive temperature. Consequently, the kinetochore would not be established properly. To analyse the amount of Cse4 at the centromeric region, we performed chromatin immunoprecipitation (ChIP) and Western blotting against HA-tagged wild-type Cse4 and Cse4-R37A in *cbf1*Δ cells at different temperatures. Importantly, equal Cse4 amounts were measured in the *cbf1*Δ as well as in the *cbf1*Δ *cse4-R37A* cells at 23°C by ChIP (Figure 22). At the restrictive temperature for *cbf1*Δ *cse4-R37A* cells, the Cse4 level was even

slightly increased, indicating that *cse4-R37A* did not compromise the presence of Cse4 at CEN4. The presence of histone H4 was not influenced by the additional mutation of arginine 37 of Cse4 in *cbf1*Δ cells or at the different temperatures. Measurement of total cellular levels of Cse4 by Western blotting showed that equal amount of Cse4 and Cse4-R37A were found also at the restrictive temperature in *cbf1*Δ *cse4-R37A* cells. This data showed that the mutation of arginine 37 in Cse4 did not affect the protein stability as well as the deposition of the protein at the centromeric region in *cbf1*Δ cells.

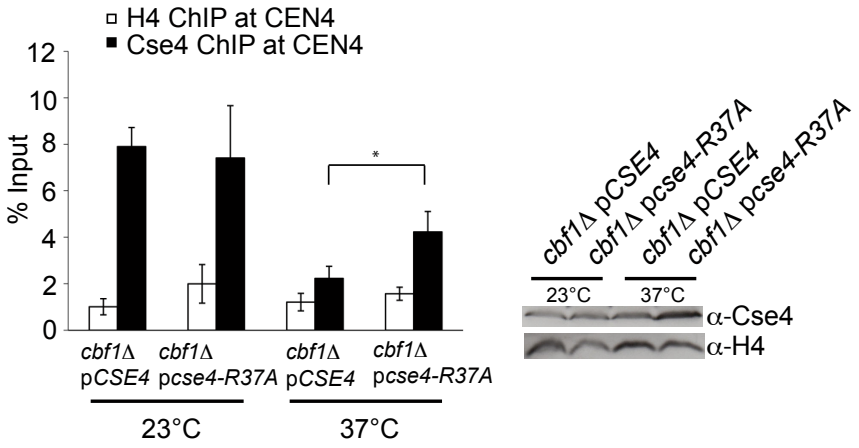

Figure 22: The association of Cse4 at CEN4 was not affected by Cse4 R37 methylation.
ChIP analysis was performed in *cbf1*Δ *cse4*Δ strains carrying either *CSE4* or *cse4-R37A* on a plasmid. The strains were grown to logarithmic phase at the permissive temperature (23°C) and shifted for four hours at the restrictive temperature (37°C). Samples were taken at both temperatures. ChIP was perfomed with α-HA (Cse4-3xHA) and, as a control, α-H4 antibody. Values give the enrichment relative to the input. Error bars give standard deviation of three independent ChIP experiments. The asterisk indicates significant difference, *P* value < 0.05. Right, western blot analysis of the amount of Cse4-3xHA and H4 in whole cell extract of the indicated strains at different temperatures.

Furthermore, we asked whether the observation that Cse4-R37A did not affect the deposition of the protein at the centromere in *cbf1*Δ cells could be confirmed by an independent method like fluorescence microscopy. For this purpose, we tagged Cse4 with GFP and crossed this strain with the *cbf1*Δ cells (Figure 23). However, after the dissection of the tetrads, a synthetic lethality between Cse4-GFP and *cbf1*Δ was observed, and a further analysis of the association of Cse4 at the centromeric region in the *cbf1*Δ cells by fluorescence microscopy was therefore not possible. This furthermore showed that the C-terminal GFP-tag comprised Cse4 function in *cbf1*Δ cells.

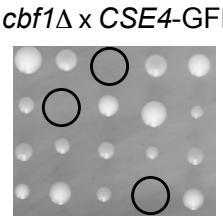

Figure 23: GFP-tagged *CSE4* was lethal in combination with *cbf1*Δ cells.
Tetrad dissection of genetic crosses between *cbf1*Δ with GFP-tagged Cse4 strain. The dissection of the individual ascospores is aligned in vertical rows. The double mutants *cbf1*Δ *CSE4*-GFP are marked with circles.

3.3.7 Cse4 R37 methylation regulated the recruitment of kinetochore components to the centromere

Another hypothesis to explain the growth defects and synthetic lethality with *cse4-R37A* in combination with mutants of kinetochore components was that the absence of methylation could cause defects in the assembly of the kinetochore. The presented results above show that the methylation of Cse4 contributed to centromere function and to chromosome segregation. In its absence, an interaction of Cse4 with kinetochore proteins could be disturbed, thus leading to a regulatory defect in kinetochore assembly. To test this hypothesis, the association of two kinetochore proteins, Mtw1 and Ame1, to CEN4 were measured in *cbf1*Δ and *cbf1*Δ *cse4-R37A* cells grown at 23°C and 37°C. Both kinetochore proteins are components of the central kinetochore layer, which connects the inner components with the microtubule-associated proteins. Mtw1 is a subcomponent of the MIND complex, and the COMA complex is represented by Ame1 (Euskirchen 2002; Ortiz et al. 1999). The association of the kinetochore proteins, Mtw1 as well as Ame1, was not affected at CEN4 in both strains at the permissive temperature. In contrast, significantly decreased levels of Mtw1 and Ame1 were measured at CEN4 in the *cbf1*Δ *cse4-R37A* cells in comparison to *cbf1*Δ cells at the restrictive temperature (37°C). The cellular protein levels of Mtw1 and Ame1 were unaffected in the indicated strains and temperatures (Figure 24). The decreased levels of both kinetochore proteins at the centromeric region in the *cbf1*Δ *cse4-R37A* cells at 37°C showed that the R37 methylation of Cse4 regulated the recruitment of the kinetochore components to the centromere.

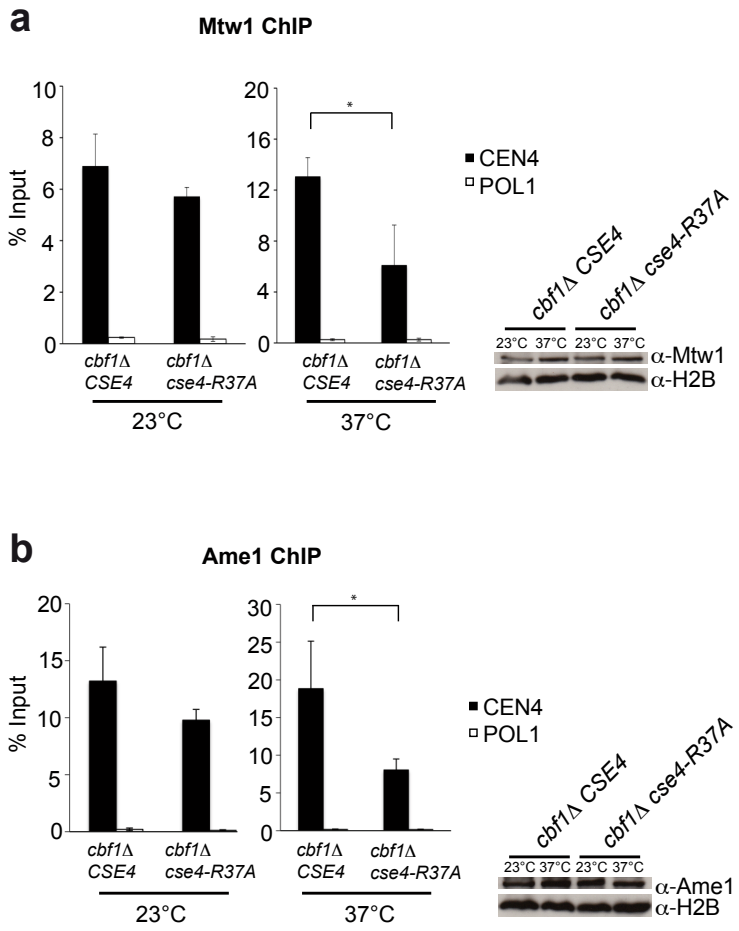

Figure 24: *Cse4-R37A* caused a defect in the recruitment of Mtw1/MIND and Ctf19/COMA complex components to the kinetochore in the absence of Cbf1.
a, Association of Mtw1 at CEN4 and *POL1* was measured by ChIP in *cbf1*Δ strains carrying either *CSE4* or *cse4-R37A*. Indicated strains were grown to early logarithmic phase at the permissive temperature (23°C) and shifted to the restrictive temperature (37°C) for four hours. ChIP analysis was performed with α-myc. Values give the enrichment relative to input. Error bars give standard deviation of three independent ChIP experiments. The asterisk indicates significant difference, *P* value < 0.05. Right, Western blot analysis of the amounts of Mtw1-9xmyc and H2B in whole cell extracts. **b,** ChIP of Ame1-9xmyc at CEN4 and *POL1*. ChIP-analysis and representation as in **a**.

3.3.8 Deletion of annotated arginine methyltransferases in *cbf1*Δ cells showed no synthetic genetic interaction with *cse4-R37A*

The R37 methylation of Cse4 was identified by mass spectrometry, and the phenotypic analysis of *cse4-R37A* allele suggested a role for this methylation in regulating kinetochore assembly and proper chromosome segregation. These observations raised the question which enzyme was involved in the methylation of Cse4. One might expect that the absence of the putative arginine methyltransferase would prevent the methylation of Cse4 on arginine 37, and an additional deletion of *CBF1* may therefore display the same phenotype as *cbf1*Δ *cse4-R37A* of growth defect and temperature sensitivity. Three genes for arginine methyltransferases are annotated in the *S. cerevisiae* genome - *HSL7*, *HMT1* and *RMT2*.

To test whether one of these enzymes was responsible for the arginine methylation on Cse4, we constructed mutants of the putative arginine methyltransferases in *cbf1*Δ cells. However, the absence of these arginine methyltransferases in *cbf1Δ* cells did not cause a growth defect at 23°C and 30°C or lethality at 37°C (Figure 25a). These results showed that the deletion of the analysed arginine methyltransferase in *cbf1Δ* cells did not display the expected phenotype. It cannot be rule out that a deletion of an arginine methyltransferase in *cbf1*Δ cells does not show the same phenotype as *cbf1*Δ *cse4-R37A,* or that a single arginine methyltransferase was not solely involved in the methylation of Cse4. Consequently, we asked whether a triple mutant of these arginine methyltransferases displayed the growth defect and synthetic lethality in combination with a deletion of *CBF1* (Figure 25b). However, the triple mutation of the arginine methyltransferases in *cbf1*Δ cells showed no growth defects and only a slight temperature sensitivity at 37°C, arguing that the analysed enzymes probably did not methylate Cse4 R37 alone or in combination.

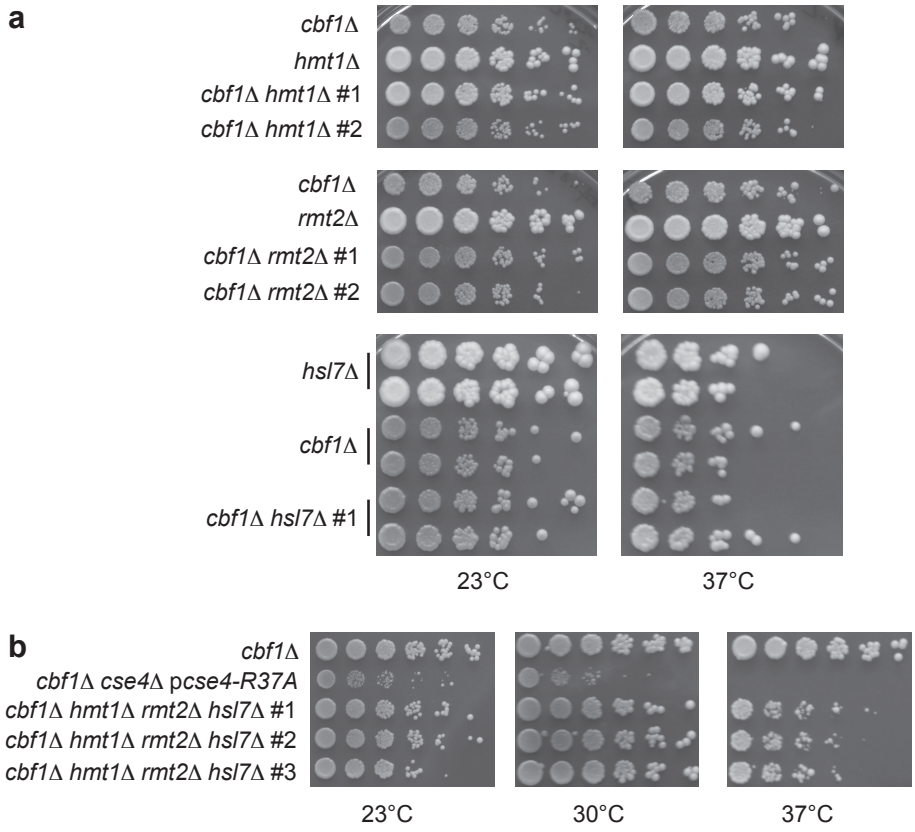

Figure 25: Single and triple deletion of the annotated arginine methyltransferases Hmt1, Rmt2 and Hsl7 did not cause growth defects and synthetic lethality in the absence of Cbf1.
a, Serial dilutions of segregants from crosses between *cbf1*Δ (AEY4816) and deletions of arginine methyltransferase *hmt1*Δ (AEY4818), *rmt2*Δ (AEY4820) and *hsl7*Δ (AEY4822) were spotted on full medium and incubated for five days at the indicated temperatures. The top rows show the parental strains. **b**, Serial dilutions of *cbf1*Δ (AEY4816), *cbf1*Δ *cse4*Δ p*cse4-R37A* (AEY4848) and three transformants of *cbf1*Δ *hmt1*Δ *rmt2*Δ *hsl7*Δ (AEY4931) were spotted on full medium and incubated for three days at indicated temperatures.

The mutation of R37 to alanine of Cse4 showed synthetic lethality in combination with a deletion of *CTF19*, and this presented a stronger phenotype than *cbf1*Δ *cse4-R37A*. We therefore asked whether this phenotype could be use to identify the methyltransferase and therefore crossed a *ctf19*Δ strain to strains deleted in genes encoding for the arginine methyltransferases (Figure 26). After dissection of the tetrads, we observed no synthetic lethality in the double mutants. Taken together, these results did not show the expected phenotype of the double mutants of arginine methyltransferases with Ctf19 and therefore did not give an indication as to the methyltransferase responsible for the Cse4 R37 methylation. However, also in this case, it cannot be rule out that a deletion of an arginine methyltransferase in *ctf19*Δ cells did not show the same phenotype as *ctf19*Δ *cse4-R37A* cells.

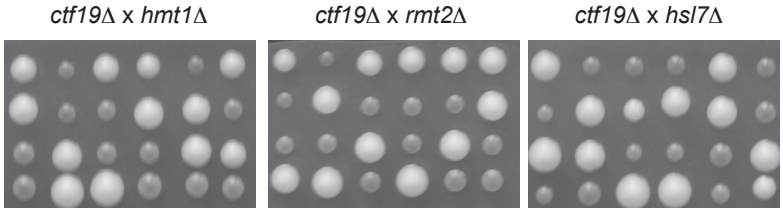

Figure 26: Deletion of annotated arginine methyltransferase in *ctf19*Δ cells revealed no synthetic lethality.
Tetrad dissection of genetic crosses between deletions of arginine methyltransferases Hmt1, Rmt2 and Hsl7 with *ctf19*Δ strain. The four spores from individual asci are aligned in vertical rows and were incubated at 30°C.

Furthermore, we asked whether the absence of the annotated arginine methyltransferases in wild-type cells caused a loss of methylation of Cse4 R37. To this end, *cse4*Δ strains carrying plasmid-borne *CSE4*-3xHA were constructed with deletion in genes encoding the arginine methyltransferases. The histones were extracted and the methylation state of Cse4 was analysed using Cse4-R37me2a antibodies (Figure 27). The results showed that the deletion of an arginine methyltransferase did not cause a loss or decrease of asymmetrical dimethylation of Cse4. This data demonstrated that probably none of the annotated arginine methyltransferases was responsible for the asymmetrical dimethylation on arginine 37 of Cse4.

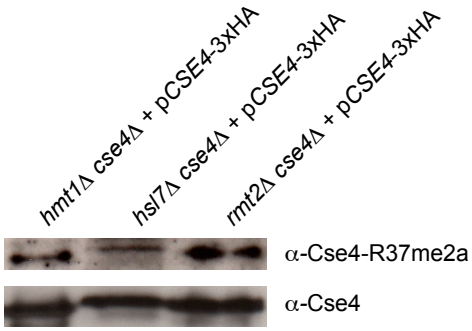

Figure 27: Deletion of genes encoding arginine methyltransferases did not cause a loss of asymmetrical dimethylation of Cse4 R37.
Histone extracts from *HMT1*, *HSL7* and *RMT2*- deleted cells were probed with α-Cse4-R37me2a antibody. Cse4-3xHA was detected with α-HA as loading control. The decrease of Cse4-R37me2a signal in the *HSL7*-deleted strain was due to the lower amount of total Cse4.

3.3.9 Deletion of putative S-adenosyl-L-methionine-dependent methyltransferases showed no synthetic lethality in *ctf19*Δ cells

The results above showed that a deletion of the arginine methyltransferases annotated in the *S. cerevisiae* genome did not display the same phenotype in *cbf1*Δ and *ctf19*Δ cells as the *cse4-R37A* allele. Therefore, we hypothesized that another S-adenosyl-L-methionine-dependent methyltransferase might be responsible for the modification on arginine 37 of Cse4. Most of the S-adenosyl-L-methionine-dependent methyltransferases are characterized by a seven-strand twisted β-sheet that acts as the binding motif for the cofactor S-adenosyl-L-methionine (Cheng and Roberts 2001). It was suggested that around 1 % of the open reading frames encode S-adenosyl-L-methionine-dependent methyltransferases (Katz et al. 2003). Based on the observed synthetic lethality of *cse4-R37A* in a *ctf19*Δ strain, a *ctf19*Δ strain was crossed with deletion strains of putative S-adenosyl-L-methionine-dependent methyltransferases (Appendix, Table 9) that were selected based on their annotation in the *S. cerevisiae* database. The deletion strains used in this screen were taken from the *S. cerevisiae* deletion library that encompasses around 5000 non-essential genes (Winzeler et al. 1999). To this end, 53 crosses between *ctf19*Δ strains and deletion strains of putative methyltransferases were performed. However, the results showed that none of the segregants revealed synthetic lethality between *ctf19*Δ cells and deletion of S-adenosyl-L-methionine-dependent methyltransferases. Taken together, the results did not provide evidence for the responsible methyltransferase of Cse4 R37. As above, it cannot be rule out that a deletion of a putative S-adenosyl-L-methionine-dependent methyltransferase in *ctf19*Δ cells did not show the same phenotype as *ctf19*Δ *cse4-R37A* cells.

3.4 Acetylation on lysine 49 of Cse4

The mass spectrometry analysis performed above identified acetylation on lysine 49 of Cse4 in addition to the methylation on arginine 37 of Cse4. Phenotypical analysis showed that this acetylation on lysine 49 displayed a kinetochore-dependent function in combination with the methylation on arginine 37 (see 3.5). Therefore, a specific antibody was generated against the acetylation of Cse4 K49 for use in further analyses.

3.4.1 Generation and purification of an antibody against Cse4 K49 acetylation

For the generation of a modification-specific antibody against the acetylation on lysine 49, a peptide was synthesized and used for immunization. As above for the anti-methylation antibodies, the specificity of the obtained sera was tested by dot blot against modified and unmodified peptide. To increase the specific reactivity against the modified peptide, the antibody was purified over a column coupled with modified peptide and subsequently incubated with the unmodified peptide. Afterwards, the specificity of the antibody against the modified peptide was tested by dot blot (Figure 28). The results showed that the antibody was specific for the modified Cse4-K49 peptide and displayed no signal for the unmodified Cse4-K49 peptide. The specificity of the antibody was also tested in a peptide competition assay. For this purpose, the antibody was pre-incubated with competing modified and unmodified Cse4-K49 peptides before the antibody was used in the dot blot. The results showed that the antibody that was pre-incubated with the competing modified peptide, lost the ability to detect the modified peptide on the dot blot membrane. Conversely, the pre-incubation with the unmodified peptide did not influence the ability of the antibody to detect the modified peptide. Altogether, these data showed that the polyclonal antibody generated against the acetylated Cse4 peptide was specific for the acetylation on lysine 49 of Cse4 and could distinguish between acetylated and non-acetylated Cse4-K49 peptides.

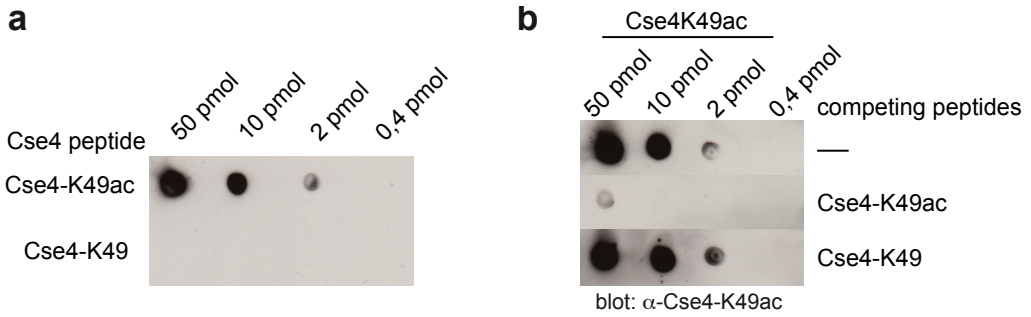

Figure 28: Specificity of Cse4-K49ac antibody.
Immuno-dot blots showing the specific reactivity of the Cse4-K49ac antibody. **a**, The indicated amounts of modified and unmodified peptides were spotted on nitrocellulose membrane and probed against α-Cse4-K49ac (1:200). **b,** Peptide competition assay of Cse4-K49ac antibody. Indicated amounts of Cse4 peptide carrying K49ac were spotted on the nitrocellulose membrane. Cse4-K49ac antibody was pre-incubated with the competing peptides indicated to the right of the blot for 1 h for 28°C. Afterwards the antibody was incubated on the membrane over night at 4°C.

3.4.2 Detection of Cse4 K49 acetylation with a modification-specific antibody

The results above showed that we had successfully generated a specific polyclonal antibody against Cse4 K49 acetylation. We asked whether the acetylation on lysine 49 could be detected using the specific antibody on Cse4 in yeast cells. To this end, we used different protein extractions to test the antibody in *cse4*Δ strains carrying the *CSE4* on a plasmid in comparison to strains carrying plasmid borne *cse4-K49R*. We expected to see a decreased signal in the *cse4-K49R* allele strain, because the mutation from lysine 49 to arginine should prevent recognition by the antibody. Using a conventional histone extraction from both strains, the antibody was unable to give rise to a specific signal in the *CSE4* containing strain for the acetylation of lysine 49 on Cse4 (Figure 29).

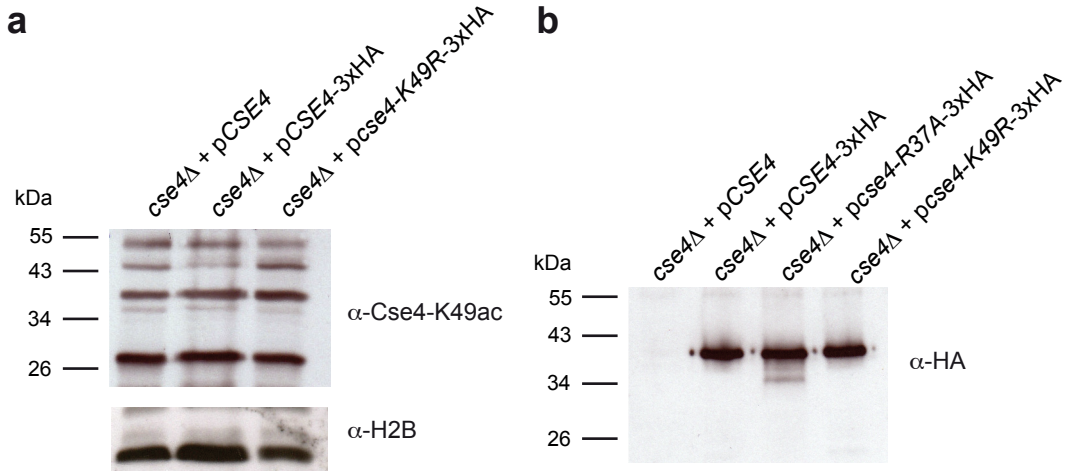

Figure 29: No specific signal for the acetylation on lysine 49 of Cse4 in histone extracts.
a, Histone extractions were prepared from *CSE4* deleted strain carrying either *CSE4* on a plasmid with or without HA-tag or HA-tagged *cse4-K49R*. 50 µg of histones from each strain were separated via SDS-PAGE and probed with α-K49ac antibody over night. **b,** Preparation as described in **a**. 5 µg of histones from indicated strains were separated via SDS-PAGE and probed with α-HA as control.

We therefore purified Cse4 from 6000 OD cells according to the same method that we had previously used for the mass spectrometric analysis. By using the specific antibody, we detected a signal for the acetylation on lysine 49 of Cse4 in the *CSE4* strain, and this signal was absent in the *cse4-K49R* strain (Figure 30a). In a second approach, the antibody was pre-incubated with the competing unmodified peptide before incubated on the membrane (Figure 30b). The result showed that the antibody previously saturated against the unmodified peptide detected a signal in the wild-type strain, which was absent in the *cse4-K49R* strain. The total amount of Cse4 was analysed by HA antibody to detect Cse4-3xHA as a loading control. To summarize, the results showed that the generated antibody detected specific the acetylation on lysine 49 *in vivo* and confirmed the acetylation state of Cse4 K49 identified by mass spectrometry.

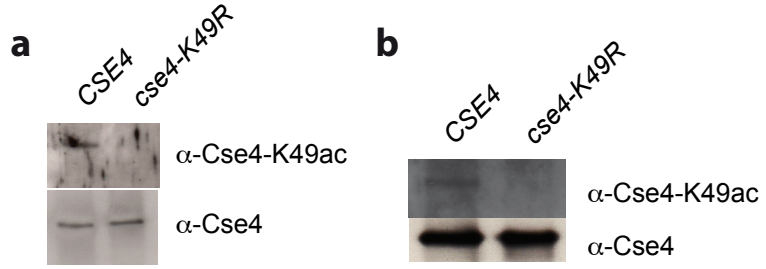

Figure 30: Cse4 was acetylated on lysine 49 *in vivo*.
a, Histone extracts from wild-type (AEY2781) and *cse4-K49R* (AEY2960) cells were probed with α-Cse4-K49ac antibody (1:200) and with α-HA as loading control to detect Cse4-3xHA. **b**, The α-Cse4-K49ac antibody was pre-incubated with unmodified peptide for 1 h at 28°C before the antibody was incubated on the membrane over night at 4°C. The representation is as described in **a**.

3.4.3 Increased acetylated Cse4 K49 in hydroxyurea-arrested cells

Since the methylation on arginine 37 of Cse4 fluctuated in the cell cycle, we asked whether the acetylation on lysine 49 on Cse4 was also cell-cycle dependent. For this purpose, a *cse4*Δ strain carrying plasmid-borne *CSE4*-3xHA was arrested in S-phase using hydroxyurea and in G2/ M with nocodazole. Subsequently, Cse4 was purified, and the amount of Cse4 K49 acetylation was analysed using the antibody specific against this modification (Figure 31). The result showed that the amount of acetylation on Cse4 K49 was increased in the S-phase arrested cells in comparison to the asynchronous or G2/ M-phase arrested cells. This data demonstrated that the acetylation on arginine 37 of Cse4, like the methylation of Cse4, was cell-cycle dependent.

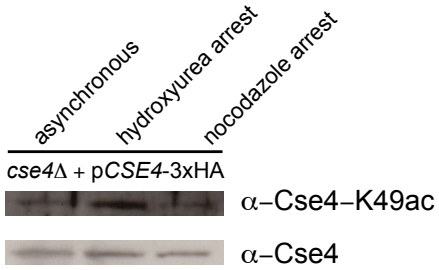

Figure 31: Cse4 K49 acetylation was increased in S-phase arrested cells.
Histone extracts from asynchronous cultures of wild-type cells (AEY2781), or from cells arrested in S-phase with hydroxyurea and in G2/ M-phase with nocodazole were probed with α-Cse4-K49ac. The K49ac antibody was pre-incubated with unmodified competing peptide. Cse4-3xHA was detected with α-HA as loading control.

3.5 Functional analysis of Cse4 K49 acetylation

3.5.1 Mutation of Cse4 modifications sites caused no growth defect in wild-type cells

Next to the methylation of arginine 37 on Cse4, the mass spectrometry identified as described above also phosphorylation of serine 33 and acetylation of lysine 49 in the N-terminus of Cse4. Analogous to the methylation of arginine 37, we mutated serine 33 of Cse4 to alanine and lysine 49 to arginine to imitate the unmodified state of the amino acid site in Cse4. At the same time, we also generated double mutants of these modifications sites. To test the function of the different mutations in the yeast cells, the plasmids encoding the mutated Cse4 were transformed into a *cse4Δ* strain containing an *URA3*-marked *CSE4* plasmid. Subsequently, the transformants were plated on 5-FOA to select against the *URA3*-marked *CSE4* plasmid. The strains carrying the *cse4-S33A* as well as *cse4-K49R* allele were able to survive on 5-FOA, and double mutants also survived, demonstrating that the mutation of these modification sites of Cse4 alone or in combination was not lethal. The strains carrying the mutations of the modifications sites were furthermore analysed for growth defects at 23°C, 30°C and 37°C (Figure 32). The results showed that none of the point mutations in the N-terminus of Cse4 alone or in combination with another mutation caused growth defects in the wild-type at the analysed temperatures.

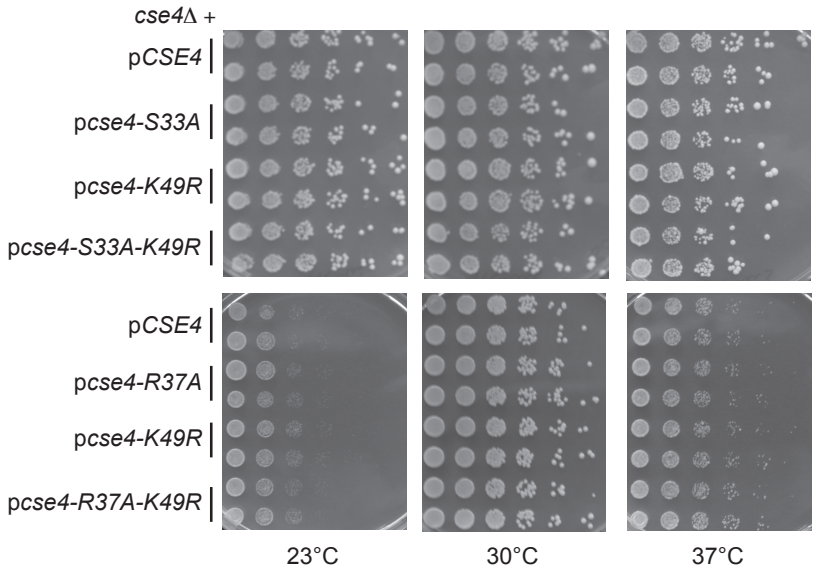

Figure 32: Analysed *cse4* alleles showed no temperature sensitivity.
Plasmid-borne point mutations of *CSE4* were introduced into a *cse4*Δ strain carrying an *URA3*-marked *CSE4*. After *URA3*-counterselection on 5-FOA, serial dilutions of the different transformants were spotted on full medium and incubated 5 days (upper panel) and 2 days (lower panel) at the indicated temperatures.

Additionally, the *cse4-S33A* as well as the *cse4-K49R* allele was combined with the temperature sensitive *cse4-103* allele. This allele is characterized by the mutation of two amino acids in the C-terminus of Cse4 (I156V, L193Q). It is assumed that the L193Q mutation in Cse4 disrupts the Cse4-H4 interface (Glowczewski et al. 2000). The results showed that neither the mutation of serine 33 to alanine nor the mutation of lysine 49 to arginine in Cse4 had a significantly influence on the temperature sensitivity of the *cse4-103* allele (data not shown).

3.5.2 Growth defect and synthetic lethality of *cse4-R37A* in cells lacking kinetochore components was suppressed by additional mutation of K49R

We have shown by mass spectrometry that several amino acid sites in the N-terminus of Cse4 are modified. All of them were located in the essential N-terminal domain (END), which encompasses amino acids 28-60 of Cse4 (Keith et al. 1999). The mutation of arginine 37 to alanine, which prevents the methylation of the amino acid site, displayed growth defects and synthetic lethality in mutants of kinetochore components. We further asked whether the phosphorylation on serine 33 and acetylation on lysine 49, which are in close proximity to arginine 37, also showed growth defects in the analysed kinetochore mutants. To this end, Cse4 mutants of serine 33 and lysine 49 were introduced into *cbf1*Δ cells. As already shown, the mutation of arginine 37 to alanine of Cse4 caused growth defects and synthetic lethality in a *cbf1*Δ strain. We observed that plasmid-borne *cse4-*

K49R as well as *cse4-S33A* showed no growth defects in this strain, nor did the *cse4-S33A-K49R* allele. Interestingly, the double mutation of arginine 37 and lysine 49 suppressed the growth defects of *cse4-R37A* in the *cbf1*Δ strain as well as the lethality at 37°C (Figure 33a, b). The same suppression was observed when *cse4-R37A-K49R* was chromosomally integrated in the *CSE4* locus (Figure 33c), showing that the suppression of *cse4-R37A* by *cse4-R37A-K49R* was not due to a different expression of the *cse4* allele on a plasmid in a *cbf1*Δ strain. Altogether, this data showed that the mutation of serine 33 to alanine of Cse4 caused no observably phenotype in *cbf1*Δ strain, but an additional mutation of lysine 49 to arginine of Cse4 suppressed the growth defect of a *cbf1*Δ *cse4-R37A* strain.

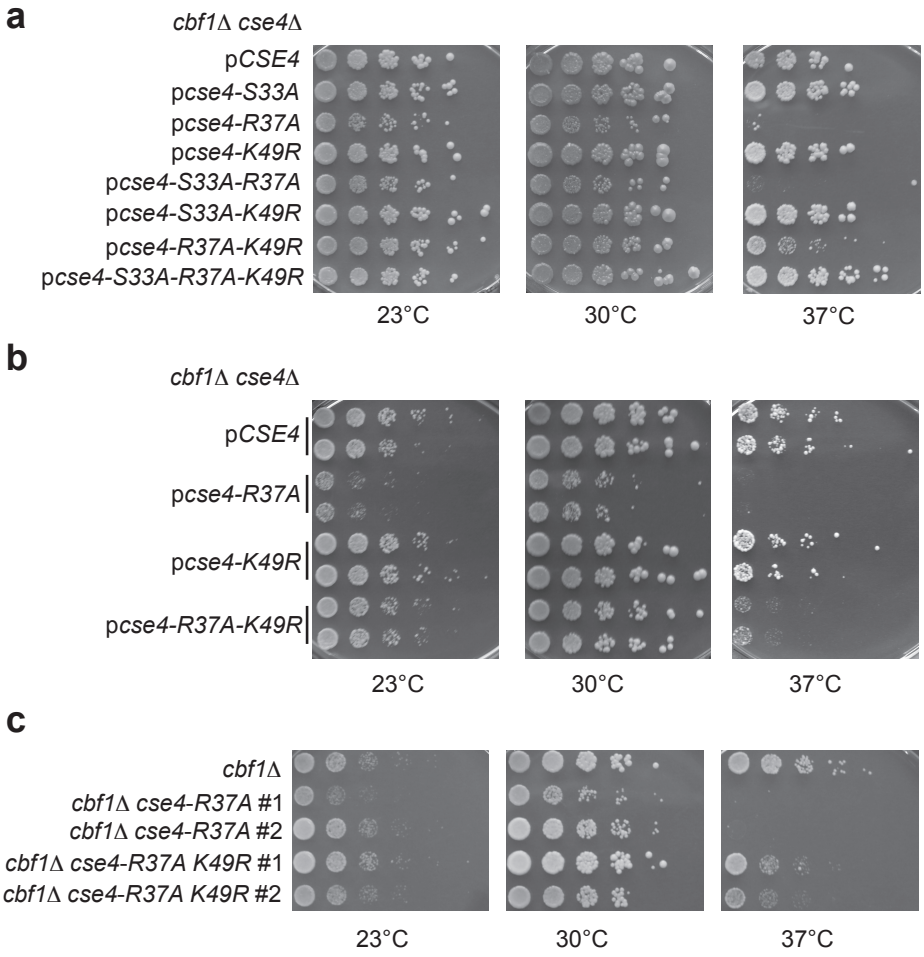

Figure 33: *Cse4-R37A* caused temperature sensitivity in combination with *cbf1*Δ and was suppressed by K49R.
a, Plasmid-borne point mutants of *CSE4* were introduced into a *cse4*Δ *cbf1*Δ strain carrying an *URA3*-marked *CSE4*. After *URA3*-counterselection on 5-FOA, serial dilutions of the different transformants were spotted on full medium and incubated for 5 days at the indicated temperature. **b**, Plasmid-borne *cse4-R37A* and *cse4-K49R* were introduced into a *cbf1*Δ *cse4*Δ strain carrying an *URA3*-marked *CSE4*. After *URA3*-counterselection on 5-FOA, serial dilutions of the different transformants were spotted on full medium and incubated at the indicated temperature. **c**, Serial dilutions of segregants from crosses between *cbf1*Δ and *cse4-R37A* as well as *cse4-R37A-K49R* were spotted on full medium and incubated at the indicated temperatures. The top row shows the *cbf1*Δ parental strain.

We furthermore asked whether the point mutations of Cse4 in the *cbf1*Δ cells caused sensitivity against nocodazole. As described above, the *cse4-R37A* showed no sensitivity against nocodazole in *cbf1*Δ cells. Also, none of the analysed point mutations of Cse4 showed sensitivity against nocodazole in the *cbf1*Δ cells (Figure 34). The observed growth defect of the Cse4-R37A mutant in *cbf1*Δ cells at different nocodazole concentrations was due to the immanent growth defect of Cse4-R37A in *cbf1*Δ cells and not due to the presence of nocodazole. These results suggested that the microtubule attachment was not affected by mutations in the Cse4 modification sites – serine 33, arginine 37 and lysine 49.

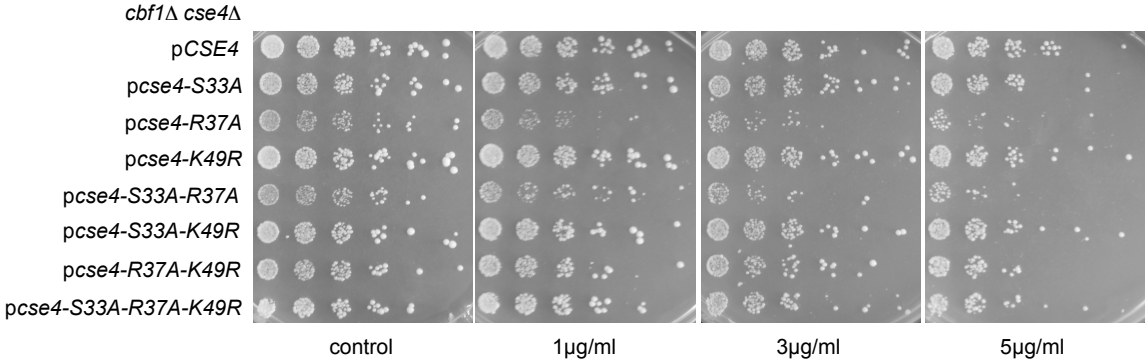

Figure 34: No sensitivity against nocodazole of *cse4* alleles in *cbf1*Δ strain.
Plasmid-borne point mutants of *CSE4* were introduced into a *cse4*Δ *cbf1*Δ strain carrying an *URA3*-marked *CSE4*. After *URA3*-counterselection on 5-FOA, serial dilutions of the different transformants were spotted on full medium containing indicated concentration of nocodazole and incubated three days at 30°C. Full medium supplemented with dimethylsulfoxide (DMSO) was used as negative control.

We further tested whether the suppressed growth defect by *cse4-R37A-K49R* in *cbf1*Δ cells was specific to Cbf1, or whether it also played a role in other mutants of kinetochore components. To this end, a *ctf19*Δ strain was transformed with plasmids encoding *cse4* alleles, and the transformants were then plated on 5-FOA medium to select against the *URA3*-marked *CSE4* plasmid. As negative control, an empty vector as well as a plasmid encoding the temperature sensitive *cse4-103* allele was used. As expected, the negative controls showed no growth on 5-FOA, indicating *cse4-103* and a deletion of *CSE4* is lethal in combination with *ctf19*Δ cells. Analogous to the results in the *cbf1*Δ cells, the *cse4-S33A* as well as the *cse4-K49R* allele showed no growth defect or lethality in a *ctf19*Δ strain. As described above, the *cse4-R37A* allele showed synthetic lethality in combination with *ctf19*Δ. Interestingly, we found that the additional mutation of lysine 49 to arginine rescued the synthetic lethality of *ctf19*Δ *cse4-R37A* cells (Figure 35). The double mutants *cse4-S33A-R37A*, *cse4-S33A-K49R* and *cse4-S33A-R37A-K49R* showed no additional phenotype due to the mutation of serine 33 on Cse4. Taken together, these results showed that an

additional mutation of lysine 49 to arginine suppressed the synthetic lethality of *ctf19*Δ *cse4-R37A* cells.

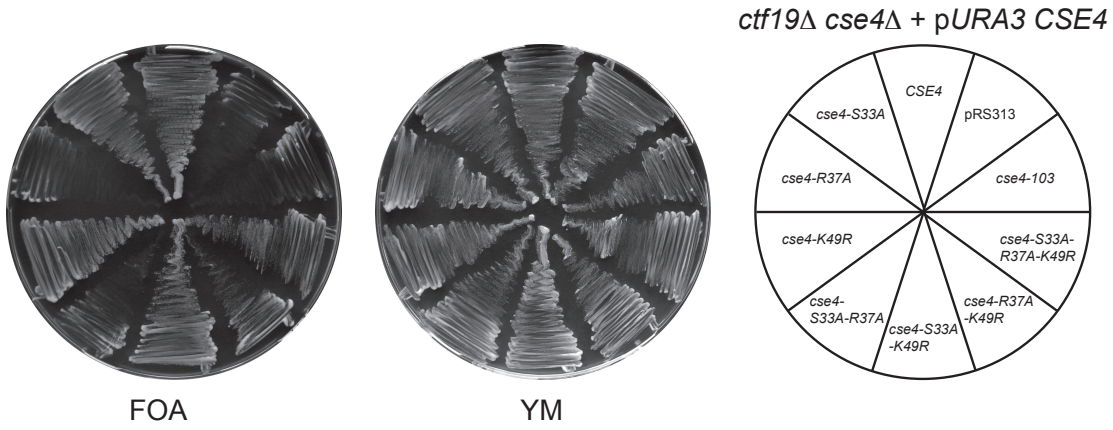

Figure 35: *Cse4-R37A* caused synthetic lethality in combination with *ctf19*Δ and was suppressed by K49R.
Indicated plasmid-borne point mutants of *CSE4* were introduced into a *ctf19*Δ *cse4*Δ strain carrying an *URA3*-marked *CSE4*. The ability of the cells to survive with the *cse4* alleles was tested on *URA3*-counterselective medium containing 5-fluoro-orotic acid (5-FOA, left). YM medium serves as control (middle). The plasmid encoding wild-type *CSE4* was used as positive control. The empty plasmid pRS313 and the *cse4-103* allele were transformed as negative control.

Furthermore, we tested whether the suppression of *ctf19*Δ *cse4-R37A* cells by additional mutation of lysine 49 was also observed in cells with chromosomally integrated *cse4-R37A-K49R.* For this purpose, a *ctf19*Δ strain was crossed to a *cse4-R37A-K49R* strain and the phenotype of the double mutants were analysed (Figure 36). The results showed that a chromosomally integrated *cse4-R37A-K49R* rescued the synthetic lethality of *cse4-R37A* in *ctf19*Δ cells and confirmed the results observed with plasmid-borne Cse4 mutants.

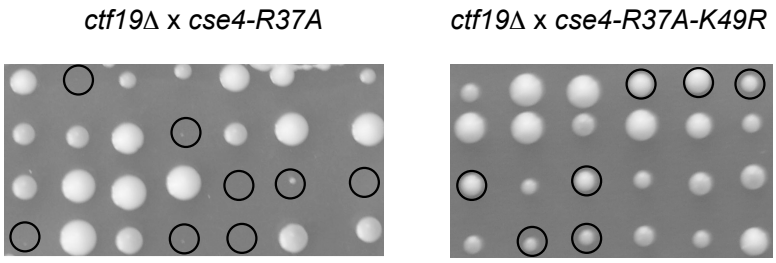

Figure 36: Additional mutation of K49R rescued the synthetic lethality of *ctf19*Δ *cse4-R37A* cells.
Tetrad dissection of genetic crosses between *ctf19*Δ and *cse4-R37A* (left) and *cse4-R37A-K49R* (right). The dissection of the individual ascospores is aligned in vertical rows. The tetrads were incubated at 30°C. The double mutants *ctf19*Δ *cse4-R37A* and *ctf19*Δ *cse4-R37A-K49R* are marked with circles.

Altogether, these data showed that the suppressed growth defect in *cbf1*Δ *cse4-R37A* cells by additional mutation of lysine 49 to arginine was not only limited to *cbf1*Δ cells, but was

also observed in *ctf19*Δ cells. Consequently, the results suggested that the acetylation on lysine 49 played a role in the kinetochore function and worked probably antagonistically to the methylation on arginine 37.

3.5.3 Growth defect and synthetic lethality of *cse4-R37A* in mutants of kinetochore components was dependent on the acetylation on lysine 49

The results above showed that the growth defect as well as the synthetic lethality of the *cse4-R37A* allele in cells lacking kinetochore components were rescued by the mutation of lysine 49 to arginine. In this context, the amino acid site arginine was chosen to imitate the unacetylated state of K49. To test whether the suppression was dependent on the mutation of K49 to arginine, we constructed a *cse4* allele that mimicked a hyperacetylation on lysine 49. To this end lysine 49 was mutated to glutamine. The plasmid borne *cse4-R37A-K49Q* allele was transformed in *cbf1*Δ *cse4*Δ, *ctf19*Δ *cse4*Δ and as control in *cse4*Δ cells containing an *URA3*-marked *CSE4* plasmid. After counterselection for the *URA3*-marked plasmid on 5-FOA, the *cse4-R37A-K49Q* allele showed no growth defect in wild-type cells but caused synthetic lethality in *cbf1*Δ as well as in *ctf19*Δ cells (Figure 37). In summary, the results showed that an additional mutation of lysine 49 to arginine in *ctf19*Δ *cse4-R37A* as well as *cbf1*Δ *cse4-R37A* cells caused a suppression of the growth defect or synthetic lethality. This suppression was reversed by mutation of *cse4-R37A-K49R* to *cse4-R37A-K49Q,* suggesting that the observed phenotype of *cse4-R37A* was dependent on the acetylation level of lysine 49 on Cse4.

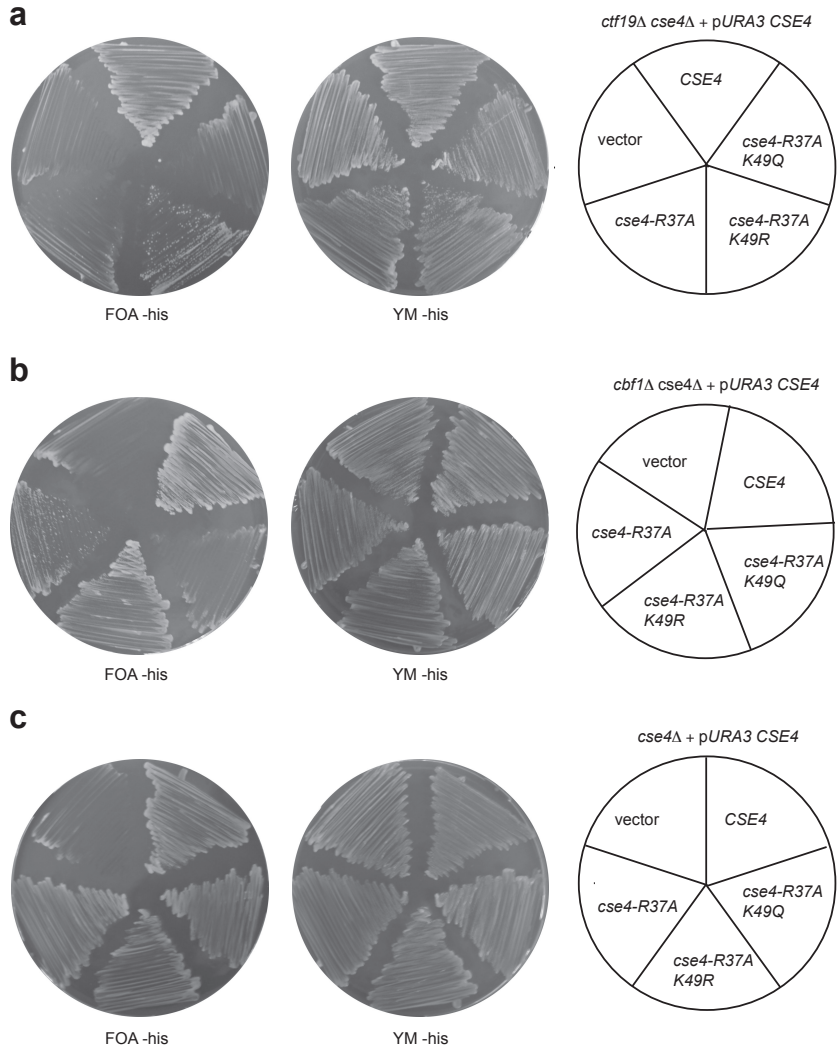

Figure 37: The *cse4-R37A-K49Q* allele caused synthetic lethality in mutants of kinetochore components.
a, Indicated plasmid-borne point mutants of *CSE4* were introduced into a *ctf19*Δ *cse4*Δ strain carrying an *URA3*-marked *CSE4*. The ability of the cells to survive with the Cse4 alleles was tested on *URA3*-counterselective medium containing 5-fluoro-orotic acid (5-FOA, left) and YM medium as control plate (middle). The plasmid encoding *CSE4* was used as positive control. The non-coding plasmid pRS313 was transformed as negative control. **b**, Cse4 mutants were transformed into *cbf1*Δ *cse4*Δ strain. Analysis and representation as described in **a**. **c**, Cse4 mutants were transformed as control into *cse4*Δ strain. Analysis and representation as described in **a**.

3.5.4 Deletion of *SAS2* did not suppress the phenotype of *cbf1*Δ *cse4-R37A* cells

The acetyltransferase Sas2 belongs to the MYST family of HATs and is a member of the SAS-I complex (Sterner and Berger 2000). The SAS-I complex consists of the catalytic Sas2 component and of the subunits, Sas4 and Sas5, which are essential for the SAS-I activity. It was shown that Sas2 acetylates H4K16 and to a lesser extent also H3K14 (Sutton et al. 2003; Kimura et al. 2002). Former experiments in the laboratory showed that Cse4 co-immunoprecipitated with Sas2 (Seitz 2004). Therefore, we asked whether the acetylation on lysine 49 of Cse4 was mediated by the histone acetyltransferase Sas2. We

hypothesized that the growth defect of the *cse4-R37A* allele in the *cbf1*Δ cells might be suppressed by additional deletion of *SAS2*, analogous to the phenotype observed in *cbf1*Δ *cse4-R37A-K49R* cells. To investigate this, *SAS2* was deleted in *cbf1*Δ cells containing different Cse4 mutants, and the cells were incubated at different temperatures (Figure 38). We observed no suppression of the growth defect of *cbf1*Δ *cse4-R37A* cells by additional deletion of *SAS2,* suggesting that lysine 49 of Cse4 was probably not a target for the histone acetyltransferase Sas2.

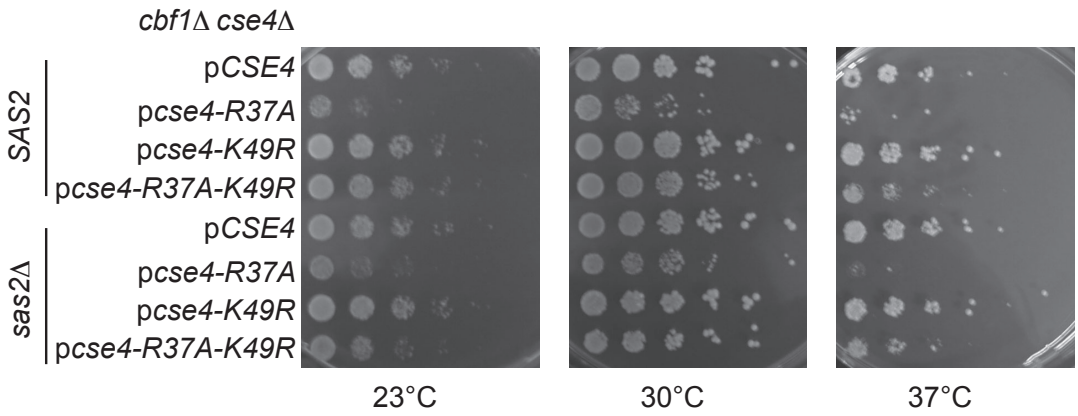

Figure 38: No suppression of *cbf1*Δ *cse4-R37A* by additional deletion of *SAS2*.
Plasmid-borne mutations of Cse4 were introduced into *cbf1*Δ *cse4*Δ cells with *SAS2* or *sas2*Δ and serial dilutions of these strains were spotted on YPD full medium. The incubation of the plates was performed at different temperatures for 3 days.

4. Discussion

Histones are predominantly modified at their N-terminus, which contributes to the dynamics of chromatin regulation in eukaryotic cells. In this study, we have investigated modifications on the centromeric histone H3 variant in *S. cerevisiae*, termed Cse4, and have characterized their function in the regulation of the centromeric region as well as in chromosome segregation.

Here we have shown for the first time both by mass spectrometry and by using specific antibodies that this histone H3 variant is posttranslationally modified at several amino acid sites. Within the long N-terminal extension of Cse4, we found sites that were phosphorylated, acetylated and methylated. Interestingly, we observed that the mutation of arginine 37, a target site for methylation, displayed lethality or growth defects in combination with mutations in genes encoding components of the kinetochore. Besides mitotic defects, we also observed defects in plasmid and chromosome segregation, which depended on the arginine methylation of Cse4. We measured reduced levels of kinetochore proteins at the centromeric region in the absence of Cse4 methylation, indicating that the methylation of Cse4 on arginine 37 regulates the recruitment of kinetochore proteins to the centromere.

Surprisingly, an additional mutation of the acetylated lysine 49 of Cse4 to arginine led to the suppression of the growth defects of the arginine 37 mutation. This indicates a potential antagonistic effect of the methylation and the acetylation in the N-terminus of Cse4. An integrated view of all these facts shows for the first time that the centromeric histone H3 variant, like canonical histones, is modified by methylation, acetylation and phosphorylation. A detailed analysis of these modifications showed that the methylation on arginine 37 of Cse4 contributed to full centromere and kinetochore function.

4.1 Cse4 - a target for posttranslational modifications

The centromeric histone H3 variant serves as an epigenetic mark at the centromeric region (Mendiburo et al. 2011). Here, we employed mass spectrometry to identify PTMs on Cse4. This technique is well establish and has previously been used to discover, determine, confirm or quantify posttranslational modification patterns of the histones as well as histone variants (Garcia et al. 2007). One of the first novel histone modification discovered by mass spectrometry was H4 monomethylation on arginine 3 (H4R3me1) by PRMT1

(Strahl et al. 2001). In our approach, we have idendified several amino acid sites that were modified by acetylation, phosphorylation and methylation. This result raises the question whether this is an exhaustive list of all Cse4 modifications. In this study, Cse4 was digested with the protease trypsin after separation via HPLC for bottum-up mass spectrometry to identify the posttranslational modifications. Trypsin cleaves the protein mainly at the carboxyl side of arginines and lysines. Consequently, the peptides are determined in their length by the cleavage, and not all peptides are detectable by mass spectrometry. Subsequently, the identified modifications of Cse4 in this study are limited to the analysed peptides. An other protease that could be utilize to identify modifications of histones is the endoproteinase Arg-C, which hydrolyzes peptides at the carboxyl side of the amino acid arginine (Masumoto et al. 2005; Cuomo et al. 2011). Another fact that has to be taken into consideration is that posttranslational modifications on histones can alter in the cell cycle dependent on their function, as it was shown for the phosphorylation on tyrosine 45 of histone H3 (Baker et al. 2010). By using asynchronous cells in this study, it is possible that some modifications on Cse4 were missed, because they were low in asynchronous cells and therefore below the detection level.

In this study, we could point out that the Cse4 protein is a target for posttranslational modifications, like phosphorylation, acetylation and methylation. Previous studies described that Cse4 is polyubiquitylated *in vivo* (Collins et al. 2004), and an *in vitro* ubiquitylation assay suggested that Cse4 is ubiquitylated at positions K4, K131, K155, K163 and K172 (Hewawasam et al. 2010). The ubiquitin molecule is a large protein of 76 amino acids and a molecular weight of 8,5 kDa, which affects the migration pattern of Cse4 in the SDS-PAGE gel. In our approach, no ubiquitination on a lysine residue of Cse4 was detectable. This could be explained by the fact that the amount of ubiquitinated Cse4 was to low in the exercised band for the detection by mass spectrometry.

A quantification of the methylation on Cse4 R37 estimated that around 18 % of the analysed protein was monomethylated. In comparison, other histone variants were also modified to a similar degree. It was shown that the histone H2A variant, Htz1 is acetylated to 38 % at lysine 14 and to 3 % at lysine 3 (Millar et al. 2006), arguing that the monomethylation on Cse4 R37 is probably abundant. In contrast, the asymmetrical dimethylation on Cse4 R37 could be not identified by mass spectrometry, probably due to a low abundance of this modification.

Another question regarding the identified modifications of Cse4 would be, whether homology to other well-known modifications on CenH3 molecules exists. Interestingly, only phosphorylation sites are described for CenH3 in other organisms. The centromeric

histone H3 homologue in human, CENP-A, is phosphorylated on serine 7 and plays a role in the final stage of cytokinesis (Zeitlin et al. 2001). A loss of this modification was shown to cause chromosome misalignment because of defects in microtubule attachment to the kinetochore (Kunitoku et al. 2003). The centromeric histone H3 variant in *Z. mays* is phosphorylated on serine 50 (Zhang et al. 2005). Nevertheless, the counterpart to the phosphorylation on serine 33 of Cse4 is absent in CENP-A as well as in the centromeric histone H3 variant from *Z. mays*. This is due to the long N-terminal extension of Cse4, which shows no homology to other histones.

4.2 Interaction between Cse4 R37 methylation and kinetochore proteins

In this study, growth defects as well as synthetic lethality were observed between mutants of genes encoding kinetochore components and the *cse4-R37A* allele. This result indicated an essential role of arginine 37 methylation on Cse4 when the kinetochore function was compromised by mutations of kinetochore components. A genetic interaction between Cse4 and kinetochore components has previously been reported in other studies. A screen for mutations synthetically lethal with a *cbf1* null allele yielded kinetochore components, like Cep3 or Ndc10, but also a *cse4* allele (Baker et al. 1998). Another test for genetic interactions between *cse4* mutations located in the END domain and genes encoding kinetochore subcomplexes found a synthetic lethality between *cse4-39* (D36A, R37A, R44A, R46A and K49A) with *ctf19*Δ, *mcm21*Δ as well as genes encoding subunits of the CBF3 complex (Chen et al. 2000), but single point mutations of this *cse4* allele were not analysed in more detail. These described synthetic interactions were in agreement with the results of this thesis, namely that mutations in the N-terminus of Cse4 caused synthetic interactions with mutations of genes encoding different kinetochore components.

Besides this genetic interaction, we also observed a decreased level of two kinetochore proteins at the centromeric region in *cbf1*Δ *cse4-R37A* cells, arguing that the methylation of Cse4 R37 contributes to the recruitment of kinetochore components to the centromere in *cbf1*Δ cells. These observations raised the hypothesis that this genetic interaction between the *cse4* allele and genes of kinetochore components reflects a direct biochemical interaction between Cse4 R37 methylation and other kinetochore proteins. Previous two-hybrid analyses showed that Cse4 interacts with the kinetochore protein Ctf19 (Ortiz et al. 1999) and Dam1 (Shang et al. 2003) as well as the kinetochore-associated protein Scm3 (Stoler et al. 2007). Another group found that the interaction between Ctf19 and Cse4 depended on the END domain of Cse4, because a deletion of amino acids 36-55 of Cse4

abolished the protein-protein interaction (Chen et al. 2000). Due to this earlier observation, we asked by two-hybrid analysis whether the interaction between Cse4 and Ctf19 required the methylation on arginine 37 or the acetylation on lysine 49 of Cse4 (Appendix, Figure 39). However, neither mutation of Cse4 R37 nor of Cse4 K49 abrogated the interaction. This result was in agreement with the observation that a yeast two-hybrid interaction still exists between Ctf19 and the *cse4-559* allele, where the essential minimal END domain of Cse4 is directly attached to the histone fold domain (Chen et al. 2000). However, this two-hybrid test has several caveats. For instance, effects on the protein folding can interfere with protein interactions due to the tag used in this method. It is also easily possible that Cse4 in the context of the yeast two-hybrid construct is not a target for posttranslational modifications, or that the yeast two-hybrid interaction with Ctf19 is independent of the methylation on arginine 37 as well as the acetylation on lysine 49. Also, the mutation of arginine to alanine or the mutation of lysine to arginine may not structurally reflect the unmodified form of these amino acids. Another method to measure the dependence of protein-protein interactions on posttranslational modifications would be to fuse the bait protein with the modifying enzyme to ensure constitutive modification of the bait protein via the physical linkage between the protein and its modifying enzyme (Guo et al. 2004). However, this would require knowledge of the modifying enzyme. In order to further characterize the interaction between Cse4 and Ctf19, it would be interesting to determine whether the yeast two-hybrid interaction is dependent on the activity of an acetyltransferase or a methyltransferase.

One might also speculate that the interaction partner of Cse4 R37 methylation could be a kinetochore-associated protein other than Ctf19, which caused the observed defect in kinetochore assembly by a loss of methylation on Cse4 R37. Other kinetochore proteins that are candidates for such a "reader" for the methylation on Cse4 R37, are for example components of the Ctf19 complex or Mif2. The latter was shown to copurify with H2A, H2B, H4 and Cse4, arguing that there is an interaction between the centromeric nucleosome and Mif2 (Westermann et al. 2003). The identity of such a methyl-arginine-binding protein could be revealed by isolating a suppressor mutant of the *cbf1*Δ *cse4-R37A* defect. In this approach, the growth defect would be suppressed by another mutation, arguing that this mutation could be a compensatory mutation in a potential interaction partner of Cse4 R37 methylation. This method was already been used for other *cse4* mutants. Thereby, it was shown that the histone fold domain mutant, *cse4-1*, was suppressed by *SCM3* (Chen et al. 2000). Further analysis showed that Cse4 co-immunoprecipitated and interacted with Scm3 (Stoler et al. 2007; Camahort et al. 2007;

Mizuguchi et al. 2007; Pidoux et al. 2009; Williams et al. 2009). Consequently, the Scm3 protein could also be a potential interaction partner of methylated Cse4 R37. Another way to determine the interactor of Cse4 R37 methylation could also involve a biochemical approach using specific binding to the modified Cse4 R37 peptide, or co-immunoprecipitation of association partner of methylated Cse4 by using the modification-specific antibodies.

One might also speculate that the Cse4 R37 methylation has an effect on the modification of other kinetochore proteins. This phenomenon was previously described for the ubiquitination of lysine 124 on H2B, which is required for methylation of lysine 233 on the kinetochore protein Dam1. This observation suggests an *in trans* regulatory association between a histone modification and a modification of a non-histone protein (Latham et al. 2011). Consequently, it would be interesting to see whether the loss of Cse4 R37 methylation affects the modification on another kinetochore protein.

In summary, our results showed a genetic interaction between *cse4* alleles and genes encoding kinetochore components. It will be interesting to determine a biochemical interaction between the methylation on Cse4 R37 and components of the kinetochore.

4.3 Role of Cse4 R37 methylation in the absence of Cbf1

In this study, we showed that the absence of Cse4 R37 methylation displayed no phenotype in wild-type cells. This observation is in agreement with former experiments, which described temperature and chromosome sensitivity only for the quintuple Cse4 mutant (D36A, R37A, R44A, R46A and K49A) (Chen et al. 2000). In addition, it was also shown that most histone modifications do not display a phenotype in a wild-type background under standard conditions (Edwards et al. 2011; Gardner et al. 2011). This observation raised the question, why the methylation of Cse4 only shows an effect in the absence of the CDEI binding kinetochore protein, Cbf1? A recent study discussed the possibility that the Cbf1 protein, which is bound to the CDEI sequence of the centromeric DNA, together with the CDEIII-tethered CBF3 complex perfectly fixes the centromeric nucleosome to the AT-rich CDEII sequence (Cole et al. 2011). Another group showed that in *cbf1*Δ cells the protection of the centromeric region is decreased and shifted more towards the CDEIII region (Krassovsky et al. 2012). One might also speculate that the kinetochore, which is associated with the centromeric nucleosome and the centromeric region, is affected in the absence of Cbf1. An additional loss of the Cse4 R37 methylation could then impair the formation of the kinetochore and disrupt chromosome segregation. In this context it is

imaginable that the monomethylation and asymmetrical dimethylation of Cse4 R37 have different functions in the recruitment of the kinetochore, as it was shown for the methylation on H3R2 in yeast (Kirmizis et al. 2007; Kirmizis et al. 2009). Taken together, we suggest that during S-phase, when the kinetochore is disassembled from replicating chromatin, the methylation is preferentially transferred to the N-terminus of Cse4. One might speculate that in this phase the accessibility for the methylation of the Cse4 N-terminus is increased. After replication fork passage, Cse4 is integrated into the centromere (Xiao et al. 2011) and the kinetochore is subsequently reassembled on the centromeric DNA to link the chromatids to the microtubules. At that time, the methylation on arginine 37 of Cse4 contributes to this recruitment of the kinetochore components to the centromeric region. This indicates that the methylation of Cse4 R37 is regulated during the cell cycle and associated with replication.

4.4 Approaches to identify the enzyme responsible for Cse4 R37 methylation

A further aspect raised by the identified modifications on Cse4 is the question of the identity of the responsible enzymes. In the genome of *S. cerevisiae*, there are three annotated arginine methyltransferases. The methyltransferase Hsl7 was found in a screen to identify factors that genetically interact with the N-terminus of histone H3 and H4 (Ma et al. 1996). Rmt2 methylates the ribosomal protein L12 (Chern et al. 2002), and the nuclear ribonucleoprotein Npl3 is a substrate for the arginine methyltransferase Hmt1 (Wong et al. 2010). All of them use S-adenosyl-L-methionine as co-factor to methylate arginine of their target protein. However, neither single mutants nor the triple mutation of *HSL7*, *RMT2* and *HMT1* displayed growth defects or temperature sensitivity in combination with *cbf1*Δ, arguing that these enzymes are not involved in Cse4 R37 methylation. One explanation of this result is that the mutation of arginine 37 to alanine does not correspond to the chemical structure of an unmethylated arginine. This assumption could also explain the observed differences in the phenotype of *cbf1*Δ *cse4-R37A* and *cbf1*Δ *cse4-R37K* cells. However, in addition an analysis of the amount of Cse4 R37 methylation signal showed no differences in the strains deleted in genes encoding the arginine methyltransferases Hsl7, Hmt1 and Rmt2 with the antibody against Cse4-R37me2a, arguing that these enzymes were probably not responsible for the asymmetrical dimethylation on arginine 37 of Cse4.

These observations led to the notion that another S-adenosyl-L-methionine dependent methyltransferase might be responsible for the methylation of Cse4 R37. To investigate this, we crossed deletion strains of putative S-adenosyl-L-methionine dependent methyltransferases with cells lacking Ctf19. This screen was limited in the number of analysed methyltransferases because of the fact that the deletion of genes like *NOP1*, *DIM1* is not viable, or other deletions are sterile and therefore could not mate with a *ctf19*Δ strain, like *STE14*. Thus, the screen was limited to 53 putative S-adenosyl-L-methionine dependent methyltransferases. However, the responsible enzyme for the methylation on arginine 37 of Cse4 could not be identified with this approach.

In general, identification of the enzyme of a newly identified histone modification poses a challenge. The responsible methyltransferases for methylation on arginine 2 of H3 (Kirmizis et al. 2009) as well as the enzyme catalysing the methylation on H4K20 (Edwards et al. 2011) or dimethylation on lysine 37 of H2B (Gardner et al. 2011) are still unknown in *S. cerevisiae*. In this context, neither a deletion nor an overexpression of the analysed enzymes affected the amount of the modification on the histone. With respect to these results, one possibility to search for the enzyme responsible for the methylation on Cse4 R37 is to perform Western blotting of strains deleted for or overexpressing genes encoding putative S-adenosyl-L-methionine dependent methyltransferases. Furthermore, an aspect that has to be taken into consideration is that the methylation of Cse4 R37 could be catalyzed by a still uncharacterized enzyme, which shows no homology to methyltransferases. A method to identify this Cse4 specific enzyme would be to fractionate a nuclear extract and analyse the different fractions for methyltransferase activity on recombinant Cse4 protein or a Cse4 peptide. A similar approach was used for the identification of the H4 specific methyltransferase, PRMT1 (Wang et al. 2001). Nevertheless, this method is very laborious, because it has to be ensured that the different fractions maintain their enzymatic activity during the purification. Another possibility is that more than one enzyme is responsible for the methylation on Cse4 R37. Taken together, the responsible enzyme for the methylation of Cse4 R37 remains to be identified.

4.5 A putative crosstalk between arginine 37 methylation and lysine 49 acetylation in the N-terminus of Cse4

In this study, a compensation of *cse4-R37A* phenotypes was observed by the additional mutation of Cse4 K49 to arginine. This result suggests that the methylation on arginine 37 acts antagonistically to the acetylation on lysine 49 of Cse4. Several histone modifications

have been identified to affect each other *in trans* as well *in cis*. An example for an *in cis* interaction between posttranslational modifications was observed on the N-terminus of the H3. It was shown that an H3 peptide phosphorylated at serine 10 could not be further methylated at lysine 9 by the H3 specific methyltransferase SUV39H1 (Rea et al. 2000), which was caused by a direct electrostatic inhibition between these modifications. An *in cis* interplay between an arginine methylation and lysine acetylation, as suggested in this study, has been described for the N-terminus of H4. The methylation of arginine 3 of H4 facilitates the acetylation of different lysine residues in the H4 tail (Wang et al. 2001). However, the hyperacetylation of H4 inhibits further methylation of H4 R3 by PRMT1 (Wang et al. 2001).

Nevertheless, the question remains what the mechanism of this observed antagonistical effect in the N-terminus of Cse4 is? For the answer of this question, it would be interesting to analyse whether the absence of acetylation on lysine 49 suppresses the kinetochore recruitment effect. This could be verified by chromatin immunoprecipitation of kinetochore components in *cbf1*Δ *cse4-R37A-K49R* cells. Subsequently, in comparison to the effect of the methylation of Cse4 R37, one might hypothesize that the acetylation of lysine 49 attracts a negative or inhibits a positive regulator of the kinetochore assembly. One possibility is that the acetylation on lysine 49 inhibits the binding of a kinetochore protein, leading to defects in the assembly of the kinetochore. This might suggest that the level of lysine 49 acetylation is low at the centromeric region in a wild-type. Another possibility is that both N-termini of two Cse4 molecules within a nucleosome interact with each other, suggesting that these two modifications are distributed to two Cse4 molecules and probably influence the stability of the centromeric nucleosome. A two-hybrid analysis of the N-terminal tail of Cse4 with itself could be employed to test this hypothesis. One might also suggest that the acetylation on lysine 49 can influence the interaction of Cse4 R37 methylation to another protein. A similar observation was shown for the phosphorylation on H3S10, which inhibits the interaction between the methylation on H3K9 and the heterochromatin protein HP1 (Fischle et al. 2005). In this context, it would be interesting to determine the differences in the amount of lysine 49 acetylation in a strain encoding the *cse4-R37A* allele in contrast to a wild-type strain. Another approach to gain more insights into the crosstalk between these two modifications would be to determine, whether it is possible to acetylate a methylated Cse4 peptide. However, this would require knowledge of the responsible acetyltransferase of lysine 49.

Taken together, our observations led us to suggest that an *in cis* interaction between the methylation on arginine 37 and the acetylation on lysine 49 in the N-terminus of Cse4 exists.

4.6 Putative kinases for the phosphorylation on serine 33 of Cse4

In this study, it was shown that the mutation of serine 33 to alanine in the N-terminus of Cse4 displayed no growth defect in wild-type cells as well as in strains with deletions in strains encoding kinetochore proteins. Consequently the function of the phosphorylation on serine 33 in the N-terminus of Cse4 remains unknown until this point of study. However, one might speculate which enzyme could be responsible for the phosphorylation on Cse4 S33. In the genome of *S. cerevisiae,* over 100 proteins are annotated as putative serine/threonine kinases. Computational analysis of protein phosphorylation in yeast identified no potential protein kinase for phosphorylation on Cse4 (Ptacek et al. 2005). Nevertheless, a putative kinase for the phosphorylation of serine 33 could be the Aurora B kinase Ipl1. In previous studies, it was shown that Ipl1 phosphorylates kinetochore components like Dam1, Ndc80 and Mif2 in yeast (Cheeseman et al. 2002; Akiyoshi et al. 2009; Westermann et al. 2003) and the human Ipl1 homologues phosphorylate CENP-A on serine 7 in human cells (Zeitlin et al. 2001; Kunitoku et al. 2003). Another putative serine/threonine kinase is Ksp1 or the Polo-like kinase Cdc5 that were identified by immunoprecipitation of a Cse4 mutant (Ranjitkar et al. 2010). One might also speculate that the dephosphorylation of serine 33 could be mediated through the phosphatase Glc7, which was shown to dephosphorylate Ipl1 targets (Pinsky et al. 2006; Francisco and Chan 1994).

4.7 An acetyltransferase for the acetylation of Cse4 K49

Former experiments showed that Cse4 co-immunoprecipitated with the acetyltransferase Sas2 (Seitz 2004). This suggests that Sas2 could catalyze the acetylation on Cse4, perhaps also on lysine 49. However, our results speak against this possibility, although it is again possible that the mutation of lysine 49 to arginine did not adequately reflect the unacetylated state of this amino acid. Previously, it was shown that the target of Sas2, H4K16, is hypoacetylated at the centromeric region in wild-type cells, and that the overexpression of *SAS2* only effects *cse4* alleles that contain mutations in the histone fold domain and not in the N-terminus (Choy et al. 2011). This leads to the conclusion that the

lysine 49 of Cse4 is probably not a target of Sas2. Another histone acetyltransferase that could be responsible for the acetylation on lysine 49 is Gcn5. It has been suggested that this histone acetyltransferase is involved in cell-cycle progression, and genetic interactions are described for the *cse4-1* allele with a deletion of *GCN5* (Vernarecci et al. 2008). For the identification of the responsible enzyme, the amount of Cse4 K49 acetylation has to be analysed in strains with deletions of the putative acetyltransferase.

4.8 Summary

In this study, it was shown that the centromeric histone H3 variant, Cse4 is posttranslationally modified by phosphorylation, methylation and acetylation. For the methylation of Cse4 R37 we reveal a mechanism in the regulation of the centromeric chromatin. It was shown, that the methylation of Cse4 R37 regulates the recruitment of kinetochore components to the centromere and its absence causes defects in chromosome segregation. With this study, the view of Cse4 and its function within the kinetochore has expanded. This mechanism contributes to the understanding of the function of the centromere and highlights the epigenetic features of centromere identity. Due to the fact that the histone H3 variant is conserved in eukaryotes, it is conceivable that a similar mechanism exists in larger eukaryotes to ensure genome stability.

5. References

Ahmad, K. and Henikoff, S. 2002. The histone variant H3.3 marks active chromatin by replication-independent nucleosome assembly. *Mol Cell* **9**(6): 1191-1200.

Akiyoshi, B., Nelson, C.R., Ranish, J.A., and Biggins, S. 2009. Analysis of Ipl1-mediated phosphorylation of the Ndc80 kinetochore protein in Saccharomyces cerevisiae. *Genetics* **183**(4): 1591-1595.

Albert, I., Mavrich, T.N., Tomsho, L.P., Qi, J., Zanton, S.J., Schuster, S.C., and Pugh, B.F. 2007. Translational and rotational settings of H2A.Z nucleosomes across the Saccharomyces cerevisiae genome. *Nature* **446**(7135): 572-576.

Albright, S.C., Nelson, P.P., and Garrard, W.T. 1979. Histone molar ratios among different electrophoretic forms of mono- and dinucleosomes. *J Biol Chem* **254**(4): 1065-1073.

Allshire, R.C. and Karpen, G.H. 2008. Epigenetic regulation of centromeric chromatin: old dogs, new tricks? *Nat Rev Genet* **9**(12): 923-937.

Altaf, M., Auger, A., Monnet-Saksouk, J., Brodeur, J., Piquet, S., Cramet, M., Bouchard, N., Lacoste, N., Utley, R.T., Gaudreau, L. et al. 2010. NuA4-dependent acetylation of nucleosomal histones H4 and H2A directly stimulates incorporation of H2A.Z by the SWR1 complex. *J Biol Chem* **285**(21): 15966-15977.

Annunziato, A.T. and Hansen, J.C. 2000. Role of histone acetylation in the assembly and modulation of chromatin structures. *Gene Expr* **9**(1-2): 37-61.

Archambault, V. and Glover, D.M. 2009. Polo-like kinases: conservation and divergence in their functions and regulation. *Nat Rev Mol Cell Biol* **10**(4): 265-275.

Arents, G. and Moudrianakis, E.N. 1995. The histone fold: a ubiquitous architectural motif utilized in DNA compaction and protein dimerization. *Proc Natl Acad Sci U S A* **92**(24): 11170-11174.

Baker, R.E., Fitzgerald-Hayes, M., and O'Brien, T.C. 1989. Purification of the yeast centromere binding protein CP1 and a mutational analysis of its binding site. *J Biol Chem* **264**(18): 10843-10850.

Baker, R.E., Harris, K., and Zhang, K. 1998. Mutations synthetically lethal with cep1 target S. cerevisiae kinetochore components. *Genetics* **149**(1): 73-85.

Baker, S.P., Phillips, J., Anderson, S., Qiu, Q., Shabanowitz, J., Smith, M.M., Yates, J.R., 3rd, Hunt, D.F., and Grant, P.A. 2010. Histone H3 Thr 45 phosphorylation is a replication-associated post-translational modification in S. cerevisiae. *Nat Cell Biol* **12**(3): 294-298.

Bannister, A.J. and Kouzarides, T. 2011. Regulation of chromatin by histone modifications. *Cell Res* **21**(3): 381-395.

Bansal, P.K., Abdulle, R., and Kitagawa, K. 2004. Sgt1 associates with Hsp90: an initial step of assembly of the core kinetochore complex. *Mol Cell Biol* **24**(18): 8069-8079.

Barratt, M.J., Hazzalin, C.A., Cano, E., and Mahadevan, L.C. 1994. Mitogen-stimulated phosphorylation of histone H3 is targeted to a small hyperacetylation-sensitive fraction. *Proc Natl Acad Sci U S A* **91**(11): 4781-4785.

Barth, T.K. and Imhof, A. 2010. Fast signals and slow marks: the dynamics of histone modifications. *Trends Biochem Sci* **35**(11): 618-626.

Biggins, S., Severin, F.F., Bhalla, N., Sassoon, I., Hyman, A.A., and Murray, A.W. 1999. The conserved protein kinase Ipl1 regulates microtubule binding to kinetochores in budding yeast. *Genes Dev* **13**(5): 532-544.

Black, B.E., Foltz, D.R., Chakravarthy, S., Luger, K., Woods, V.L., Jr., and Cleveland, D.W. 2004. Structural determinants for generating centromeric chromatin. *Nature* **430**(6999): 578-582.

Black, B.E., Jansen, L.E., Maddox, P.S., Foltz, D.R., Desai, A.B., Shah, J.V., and Cleveland, D.W. 2007. Centromere identity maintained by nucleosomes assembled with histone H3 containing the CENP-A targeting domain. *Mol Cell* **25**(2): 309-322.

Blower, M.D. and Karpen, G.H. 2001. The role of Drosophila CID in kinetochore formation, cell-cycle progression and heterochromatin interactions. *Nat Cell Biol* **3**(8): 730-739.

Blower, M.D., Sullivan, B.A., and Karpen, G.H. 2002. Conserved organization of centromeric chromatin in flies and humans. *Dev Cell* **2**(3): 319-330.

Boyarchuk, E., Montes de Oca, R., and Almouzni, G. 2011. Cell cycle dynamics of histone variants at the centromere, a model for chromosomal landmarks. *Curr Opin Cell Biol* **23**(3): 266-276.

Brown, C.J., Ballabio, A., Rupert, J.L., Lafreniere, R.G., Grompe, M., Tonlorenzi, R., and Willard, H.F. 1991. A gene from the region of the human X inactivation centre is expressed exclusively from the inactive X chromosome. *Nature* **349**(6304): 38-44.

Brown, M.T., Goetsch, L., and Hartwell, L.H. 1993. MIF2 is required for mitotic spindle integrity during anaphase spindle elongation in Saccharomyces cerevisiae. *J Cell Biol* **123**(2): 387-403.

Brownell, J.E., Zhou, J., Ranalli, T., Kobayashi, R., Edmondson, D.G., Roth, S.Y., and Allis, C.D. 1996. Tetrahymena histone acetyltransferase A: a homolog to yeast Gcn5p linking histone acetylation to gene activation. *Cell* **84**(6): 843-851.

Bruno, M., Flaus, A., Stockdale, C., Rencurel, C., Ferreira, H., and Owen-Hughes, T. 2003. Histone H2A/H2B dimer exchange by ATP-dependent chromatin remodeling activities. *Mol Cell* **12**(6): 1599-1606.

Bungard, D., Fuerth, B.J., Zeng, P.Y., Faubert, B., Maas, N.L., Viollet, B., Carling, D., Thompson, C.B., Jones, R.G., and Berger, S.L. 2010. Signaling kinase AMPK activates stress-promoted transcription via histone H2B phosphorylation. *Science* **329**(5996): 1201-1205.

Cai, M. and Davis, R.W. 1990. Yeast centromere binding protein CBF1, of the helix-loop-helix protein family, is required for chromosome stability and methionine prototrophy. *Cell* **61**(3): 437-446.

Cai, M.J. and Davis, R.W. 1989. Purification of a yeast centromere-binding protein that is able to distinguish single base-pair mutations in its recognition site. *Mol Cell Biol* **9**(6): 2544-2550.

Camahort, R., Li, B., Florens, L., Swanson, S.K., Washburn, M.P., and Gerton, J.L. 2007. Scm3 is essential to recruit the histone h3 variant cse4 to centromeres and to maintain a functional kinetochore. *Mol Cell* **26**(6): 853-865.

Camahort, R., Shivaraju, M., Mattingly, M., Li, B., Nakanishi, S., Zhu, D., Shilatifard, A., Workman, J.L., and Gerton, J.L. 2009. Cse4 is part of an octameric nucleosome in budding yeast. *Mol Cell* **35**(6): 794-805.

Carrozza, M.J., Utley, R.T., Workman, J.L., and Cote, J. 2003. The diverse functions of histone acetyltransferase complexes. *Trends Genet* **19**(6): 321-329.

Caterino, T.L. and Hayes, J.J. 2011. Structure of the H1 C-terminal domain and function in chromatin condensation. *Biochem Cell Biol* **89**(1): 35-44.

Cheeseman, I.M., Anderson, S., Jwa, M., Green, E.M., Kang, J., Yates, J.R., 3rd, Chan, C.S., Drubin, D.G., and Barnes, G. 2002. Phospho-regulation of kinetochore-microtubule attachments by the Aurora kinase Ipl1p. *Cell* **111**(2): 163-172.

Cheeseman, I.M., Chappie, J.S., Wilson-Kubalek, E.M., and Desai, A. 2006. The conserved KMN network constitutes the core microtubule-binding site of the kinetochore. *Cell* **127**(5): 983-997.

Cheeseman, I.M., Enquist-Newman, M., Muller-Reichert, T., Drubin, D.G., and Barnes, G. 2001. Mitotic spindle integrity and kinetochore function linked by the Duo1p/Dam1p complex. *J Cell Biol* **152**(1): 197-212.

Chen, Y., Baker, R.E., Keith, K.C., Harris, K., Stoler, S., and Fitzgerald-Hayes, M. 2000. The N terminus of the centromere H3-like protein Cse4p performs an essential function distinct from that of the histone fold domain. *Mol Cell Biol* **20**(18): 7037-7048.

Cheng, X. and Roberts, R.J. 2001. AdoMet-dependent methylation, DNA methyltransferases and base flipping. *Nucleic Acids Res* **29**(18): 3784-3795.

Chern, M.K., Chang, K.N., Liu, L.F., Tam, T.C., Liu, Y.C., Liang, Y.L., and Tam, M.F. 2002. Yeast ribosomal protein L12 is a substrate of protein-arginine methyltransferase 2. *J Biol Chem* **277**(18): 15345-15353.

Chestier, A. and Yaniv, M. 1979. Rapid turnover of acetyl groups in the four core histones of simian virus 40 minichromosomes. *Proc Natl Acad Sci U S A* **76**(1): 46-50.

Cheung, W.L., Ajiro, K., Samejima, K., Kloc, M., Cheung, P., Mizzen, C.A., Beeser, A., Etkin, L.D., Chernoff, J., Earnshaw, W.C. et al. 2003. Apoptotic phosphorylation of histone H2B is mediated by mammalian sterile twenty kinase. *Cell* **113**(4): 507-517.

Choo, K.H., Vissel, B., Nagy, A., Earle, E., and Kalitsis, P. 1991. A survey of the genomic distribution of alpha satellite DNA on all the human chromosomes, and derivation of a new consensus sequence. *Nucleic Acids Res* **19**(6): 1179-1182.

Choy, J.S., Acuna, R., Au, W.C., and Basrai, M.A. 2011. A role for histone H4K16 hypoacetylation in Saccharomyces cerevisiae kinetochore function. *Genetics* **189**(1): 11-21.

Clarke, L. and Carbon, J. 1985. The structure and function of yeast centromeres. *Annu Rev Genet* **19**: 29-55.

Clements, A., Poux, A.N., Lo, W.S., Pillus, L., Berger, S.L., and Marmorstein, R. 2003. Structural basis for histone and phosphohistone binding by the GCN5 histone acetyltransferase. *Mol Cell* **12**(2): 461-473.

Cohen, R.L., Espelin, C.W., De Wulf, P., Sorger, P.K., Harrison, S.C., and Simons, K.T. 2008. Structural and functional dissection of Mif2p, a conserved DNA-binding kinetochore protein. *Mol Biol Cell* **19**(10): 4480-4491.

Cole, H.A., Howard, B.H., and Clark, D.J. 2011. The centromeric nucleosome of budding yeast is perfectly positioned and covers the entire centromere. *Proc Natl Acad Sci U S A* **108**(31): 12687-12692.

Collins, K.A., Furuyama, S., and Biggins, S. 2004. Proteolysis contributes to the exclusive centromere localization of the yeast Cse4/CENP-A histone H3 variant. *Curr Biol* **14**(21): 1968-1972.

Costanzi, C. and Pehrson, J.R. 1998. Histone macroH2A1 is concentrated in the inactive X chromosome of female mammals. *Nature* **393**(6685): 599-601.

Crosio, C., Fimia, G.M., Loury, R., Kimura, M., Okano, Y., Zhou, H., Sen, S., Allis, C.D., and Sassone-Corsi, P. 2002. Mitotic phosphorylation of histone H3: spatio-temporal regulation by mammalian Aurora kinases. *Mol Cell Biol* **22**(3): 874-885.

Cuomo, A., Moretti, S., Minucci, S., and Bonaldi, T. 2011. SILAC-based proteomic analysis to dissect the "histone modification signature" of human breast cancer cells. *Amino Acids* **41**(2): 387-399.

Cuthbert, G.L., Daujat, S., Snowden, A.W., Erdjument-Bromage, H., Hagiwara, T., Yamada, M., Schneider, R., Gregory, P.D., Tempst, P., Bannister, A.J. et al. 2004. Histone deimination antagonizes arginine methylation. *Cell* **118**(5): 545-553.

Dalal, Y., Wang, H., Lindsay, S., and Henikoff, S. 2007. Tetrameric structure of centromeric nucleosomes in interphase Drosophila cells. *PLoS Biol* **5**(8): e218.

Dawson, M.A., Bannister, A.J., Gottgens, B., Foster, S.D., Bartke, T., Green, A.R., and Kouzarides, T. 2009. JAK2 phosphorylates histone H3Y41 and excludes HP1alpha from chromatin. *Nature* **461**(7265): 819-822.

Desai, A. and Mitchison, T.J. 1997. Microtubule polymerization dynamics. *Annu Rev Cell Dev Biol* **13**: 83-117.

Deuring, R., Fanti, L., Armstrong, J.A., Sarte, M., Papoulas, O., Prestel, M., Daubresse, G., Verardo, M., Moseley, S.L., Berloco, M. et al. 2000. The ISWI chromatin-remodeling protein is required for gene expression and the maintenance of higher order chromatin structure in vivo. *Mol Cell* **5**(2): 355-365.

Di Lorenzo, A. and Bedford, M.T. 2011. Histone arginine methylation. *FEBS Lett* **585**(13): 2024-2031.

Dlakic, M. 2001. Chromatin silencing protein and pachytene checkpoint regulator Dot1p has a methyltransferase fold. *Trends Biochem Sci* **26**(7): 405-407.

Dunleavy, E.M., Almouzni, G., and Karpen, G.H. 2011. H3.3 is deposited at centromeres in S phase as a placeholder for newly assembled CENP-A in G phase. *Nucleus* **2**(2): 146-157.

Dunleavy, E.M., Roche, D., Tagami, H., Lacoste, N., Ray-Gallet, D., Nakamura, Y., Daigo, Y., Nakatani, Y., and Almouzni-Pettinotti, G. 2009. HJURP is a cell-cycle-dependent maintenance and deposition factor of CENP-A at centromeres. *Cell* **137**(3): 485-497.

Earnshaw, W.C. and Rothfield, N. 1985. Identification of a family of human centromere proteins using autoimmune sera from patients with scleroderma. *Chromosoma* **91**(3-4): 313-321.

Edwards, C.R., Dang, W., and Berger, S.L. 2011. Histone H4 lysine 20 of Saccharomyces cerevisiae is monomethylated and functions in subtelomeric silencing. *Biochemistry* **50**(48): 10473-10483.

Elias, J.E., Haas, W., Faherty, B.K., and Gygi, S.P. 2005. Comparative evaluation of mass spectrometry platforms used in large-scale proteomics investigations. *Nat Methods* **2**(9): 667-675.

Espelin, C.W., Kaplan, K.B., and Sorger, P.K. 1997. Probing the architecture of a simple kinetochore using DNA-protein crosslinking. *J Cell Biol* **139**(6): 1383-1396.

Espelin, C.W., Simons, K.T., Harrison, S.C., and Sorger, P.K. 2003. Binding of the essential Saccharomyces cerevisiae kinetochore protein Ndc10p to CDEII. *Mol Biol Cell* **14**(11): 4557-4568.

Euskirchen, G.M. 2002. Nnf1p, Dsn1p, Mtw1p, and Nsl1p: a new group of proteins important for chromosome segregation in Saccharomyces cerevisiae. *Eukaryot Cell* **1**(2): 229-240.

Finch, J.T. and Klug, A. 1976. Solenoidal model for superstructure in chromatin. *Proc Natl Acad Sci U S A* **73**(6): 1897-1901.

Fischle, W., Tseng, B.S., Dormann, H.L., Ueberheide, B.M., Garcia, B.A., Shabanowitz, J., Hunt, D.F., Funabiki, H., and Allis, C.D. 2005. Regulation of HP1-chromatin binding by histone H3 methylation and phosphorylation. *Nature* **438**(7071): 1116-1122.

Foltz, D.R., Jansen, L.E., Bailey, A.O., Yates, J.R., 3rd, Bassett, E.A., Wood, S., Black, B.E., and Cleveland, D.W. 2009. Centromere-specific assembly of CENP-a nucleosomes is mediated by HJURP. *Cell* **137**(3): 472-484.

Francisco, L. and Chan, C.S. 1994. Regulation of yeast chromosome segregation by Ipl1 protein kinase and type 1 protein phosphatase. *Cell Mol Biol Res* **40**(3): 207-213.

Freidkin, I. and Katcoff, D.J. 2001. Specific distribution of the Saccharomyces cerevisiae linker histone homolog HHO1p in the chromatin. *Nucleic Acids Res* **29**(19): 4043-4051.

Furuyama, S. and Biggins, S. 2007. Centromere identity is specified by a single centromeric nucleosome in budding yeast. *Proc Natl Acad Sci U S A* **104**(37): 14706-14711.

Furuyama, T., Dalal, Y., and Henikoff, S. 2006. Chaperone-mediated assembly of centromeric chromatin in vitro. *Proc Natl Acad Sci U S A* **103**(16): 6172-6177.

Garcia, B.A., Shabanowitz, J., and Hunt, D.F. 2007. Characterization of histones and their post-translational modifications by mass spectrometry. *Curr Opin Chem Biol* **11**(1): 66-73.

Gardner, K.E., Zhou, L., Parra, M.A., Chen, X., and Strahl, B.D. 2011. Identification of lysine 37 of histone H2B as a novel site of methylation. *PLoS One* **6**(1): e16244.

Gaudet, A. and Fitzgerald-Hayes, M. 1987. Alterations in the adenine-plus-thymine-rich region of CEN3 affect centromere function in Saccharomyces cerevisiae. *Mol Cell Biol* **7**(1): 68-75.

Gkikopoulos, T., Singh, V., Tsui, K., Awad, S., Renshaw, M.J., Scholfield, P., Barton, G.J., Nislow, C., Tanaka, T.U., and Owen-Hughes, T. 2011. The SWI/SNF complex acts to constrain distribution of the centromeric histone variant Cse4. *EMBO J* **30**(10): 1919-1927.

Glowczewski, L., Yang, P., Kalashnikova, T., Santisteban, M.S., and Smith, M.M. 2000. Histone-histone interactions and centromere function. *Mol Cell Biol* **20**(15): 5700-5711.

Grant, P.A., Duggan, L., Cote, J., Roberts, S.M., Brownell, J.E., Candau, R., Ohba, R., Owen-Hughes, T., Allis, C.D., Winston, F. et al. 1997. Yeast Gcn5 functions in two multisubunit complexes to acetylate nucleosomal histones: characterization of an Ada complex and the SAGA (Spt/Ada) complex. *Genes Dev* **11**(13): 1640-1650.

Grant, P.A., Eberharter, A., John, S., Cook, R.G., Turner, B.M., and Workman, J.L. 1999. Expanded lysine acetylation specificity of Gcn5 in native complexes. *J Biol Chem* **274**(9): 5895-5900.

Greaves, I.K., Rangasamy, D., Ridgway, P., and Tremethick, D.J. 2007. H2A.Z contributes to the unique 3D structure of the centromere. *Proc Natl Acad Sci U S A* **104**(2): 525-530.

Grewal, S.I. and Jia, S. 2007. Heterochromatin revisited. *Nat Rev Genet* **8**(1): 35-46.

Grune, T., Brzeski, J., Eberharter, A., Clapier, C.R., Corona, D.F., Becker, P.B., and Muller, C.W. 2003. Crystal structure and functional analysis of a nucleosome recognition module of the remodeling factor ISWI. *Mol Cell* **12**(2): 449-460.

Guo, D., Hazbun, T.R., Xu, X.J., Ng, S.L., Fields, S., and Kuo, M.H. 2004. A tethered catalysis, two-hybrid system to identify protein-protein interactions requiring post-translational modifications. *Nat Biotechnol* **22**(7): 888-892.

Hake, S.B. and Allis, C.D. 2006. Histone H3 variants and their potential role in indexing mammalian genomes: the "H3 barcode hypothesis". *Proc Natl Acad Sci U S A* **103**(17): 6428-6435.

Hansen, J.C., Ausio, J., Stanik, V.H., and van Holde, K.E. 1989. Homogeneous reconstituted oligonucleosomes, evidence for salt-dependent folding in the absence of histone H1. *Biochemistry* **28**(23): 9129-9136.

Hassan, A.H., Prochasson, P., Neely, K.E., Galasinski, S.C., Chandy, M., Carrozza, M.J., and Workman, J.L. 2002. Function and selectivity of bromodomains in anchoring chromatin-modifying complexes to promoter nucleosomes. *Cell* **111**(3): 369-379.

Hayashi, T., Fujita, Y., Iwasaki, O., Adachi, Y., Takahashi, K., and Yanagida, M. 2004. Mis16 and Mis18 are required for CENP-A loading and histone deacetylation at centromeres. *Cell* **118**(6): 715-729.

Haynes, S.R., Dollard, C., Winston, F., Beck, S., Trowsdale, J., and Dawid, I.B. 1992. The bromodomain: a conserved sequence found in human, Drosophila and yeast proteins. *Nucleic Acids Res* **20**(10): 2603.

Heard, E. 2005. Delving into the diversity of facultative heterochromatin: the epigenetics of the inactive X chromosome. *Curr Opin Genet Dev* **15**(5): 482-489.

Hegemann, J.H., Shero, J.H., Cottarel, G., Philippsen, P., and Hieter, P. 1988. Mutational analysis of centromere DNA from chromosome VI of Saccharomyces cerevisiae. *Mol Cell Biol* **8**(6): 2523-2535.

Heitz, E. 1928. Das Heterochromatin der Moose. *1 Jahrb wiss Bot* **69**: 762-818.

Heun, P., Erhardt, S., Blower, M.D., Weiss, S., Skora, A.D., and Karpen, G.H. 2006. Mislocalization of the Drosophila centromere-specific histone CID promotes formation of functional ectopic kinetochores. *Dev Cell* **10**(3): 303-315.

Hewawasam, G., Shivaraju, M., Mattingly, M., Venkatesh, S., Martin-Brown, S., Florens, L., Workman, J.L., and Gerton, J.L. 2010. Psh1 is an E3 ubiquitin ligase that targets the centromeric histone variant Cse4. *Mol Cell* **40**(3): 444-454.

Hizume, K., Yoshimura, S.H., and Takeyasu, K. 2005. Linker histone H1 per se can induce three-dimensional folding of chromatin fiber. *Biochemistry* **44**(39): 12978-12989.

Holstege, F.C., Jennings, E.G., Wyrick, J.J., Lee, T.I., Hengartner, C.J., Green, M.R., Golub, T.R., Lander, E.S., and Young, R.A. 1998. Dissecting the regulatory circuitry of a eukaryotic genome. *Cell* **95**(5): 717-728.

Hornung, P., Maier, M., Alushin, G.M., Lander, G.C., Nogales, E., and Westermann, S. 2011. Molecular architecture and connectivity of the budding yeast Mtw1 kinetochore complex. *J Mol Biol* **405**(2): 548-559.

Howman, E.V., Fowler, K.J., Newson, A.J., Redward, S., MacDonald, A.C., Kalitsis, P., and Choo, K.H. 2000. Early disruption of centromeric chromatin organization in centromere protein A (Cenpa) null mice. *Proc Natl Acad Sci U S A* **97**(3): 1148-1153.

Hoyt, M.A., He, L., Loo, K.K., and Saunders, W.S. 1992. Two Saccharomyces cerevisiae kinesin-related gene products required for mitotic spindle assembly. *J Cell Biol* **118**(1): 109-120.

Hsu, J.Y., Sun, Z.W., Li, X., Reuben, M., Tatchell, K., Bishop, D.K., Grushcow, J.M., Brame, C.J., Caldwell, J.A., Hunt, D.F. et al. 2000. Mitotic phosphorylation of histone H3 is governed by Ipl1/aurora kinase and Glc7/PP1 phosphatase in budding yeast and nematodes. *Cell* **102**(3): 279-291.

Jansen, L.E., Black, B.E., Foltz, D.R., and Cleveland, D.W. 2007. Propagation of centromeric chromatin requires exit from mitosis. *J Cell Biol* **176**(6): 795-805.

Jedrusik, M.A. and Schulze, E. 2007. Linker histone HIS-24 (H1.1) cytoplasmic retention promotes germ line development and influences histone H3 methylation in Caenorhabditis elegans. *Mol Cell Biol* **27**(6): 2229-2239.

Jenuwein, T. and Allis, C.D. 2001. Translating the histone code. *Science* **293**(5532): 1074-1080.

Jones, M.H., He, X., Giddings, T.H., and Winey, M. 2001. Yeast Dam1p has a role at the kinetochore in assembly of the mitotic spindle. *Proc Natl Acad Sci U S A* **98**(24): 13675-13680.

Kall, L., Storey, J.D., MacCoss, M.J., and Noble, W.S. 2008. Assigning significance to peptides identified by tandem mass spectrometry using decoy databases. *J Proteome Res* **7**(1): 29-34.

Kamakaka, R.T. and Biggins, S. 2005. Histone variants: deviants? *Genes Dev* **19**(3): 295-310.

Katz, J.E., Dlakic, M., and Clarke, S. 2003. Automated identification of putative methyltransferases from genomic open reading frames. *Mol Cell Proteomics* **2**(8): 525-540.

Keith, K.C., Baker, R.E., Chen, Y., Harris, K., Stoler, S., and Fitzgerald-Hayes, M. 1999. Analysis of primary structural determinants that distinguish the centromere-specific function of histone variant Cse4p from histone H3. *Mol Cell Biol* **19**(9): 6130-6139.

Kimura, A., Umehara, T., and Horikoshi, M. 2002. Chromosomal gradient of histone acetylation established by Sas2p and Sir2p functions as a shield against gene silencing. *Nat Genet* **32**(3): 370-377.

Kirmizis, A., Santos-Rosa, H., Penkett, C.J., Singer, M.A., Green, R.D., and Kouzarides, T. 2009. Distinct transcriptional outputs associated with mono- and dimethylated histone H3 arginine 2. *Nat Struct Mol Biol* **16**(4): 449-451.

Kirmizis, A., Santos-Rosa, H., Penkett, C.J., Singer, M.A., Vermeulen, M., Mann, M., Bahler, J., Green, R.D., and Kouzarides, T. 2007. Arginine methylation at histone H3R2 controls deposition of H3K4 trimethylation. *Nature* **449**(7164): 928-932.

Kitagawa, K., Skowyra, D., Elledge, S.J., Harper, J.W., and Hieter, P. 1999. SGT1 encodes an essential component of the yeast kinetochore assembly pathway and a novel subunit of the SCF ubiquitin ligase complex. *Mol Cell* **4**(1): 21-33.

Klose, R.J. and Zhang, Y. 2007. Regulation of histone methylation by demethylimination and demethylation. *Nat Rev Mol Cell Biol* **8**(4): 307-318.

Kornberg, R.D. 1974. Chromatin structure: a repeating unit of histones and DNA. *Science* **184**(139): 868-871.

Krassovsky, K., Henikoff, J.G., and Henikoff, S. 2012. Tripartite organization of centromeric chromatin in budding yeast. *Proc Natl Acad Sci U S A* **109**(1): 243-248.

Krogan, N.J., Kim, M., Tong, A., Golshani, A., Cagney, G., Canadien, V., Richards, D.P., Beattie, B.K., Emili, A., Boone, C. et al. 2003. Methylation of histone H3 by Set2 in Saccharomyces cerevisiae is linked to transcriptional elongation by RNA polymerase II. *Mol Cell Biol* **23**(12): 4207-4218.

Kunitoku, N., Sasayama, T., Marumoto, T., Zhang, D., Honda, S., Kobayashi, O., Hatakeyama, K., Ushio, Y., Saya, H., and Hirota, T. 2003. CENP-A phosphorylation by Aurora-A in prophase is required for enrichment of Aurora-B at inner centromeres and for kinetochore function. *Dev Cell* **5**(6): 853-864.

Lachner, M., O'Carroll, D., Rea, S., Mechtler, K., and Jenuwein, T. 2001. Methylation of histone H3 lysine 9 creates a binding site for HP1 proteins. *Nature* **410**(6824): 116-120.

Laemmli, U.K. 1970. Cleavage of structural proteins during the assembly of the head of bacteriophage T4. *Nature* **227**(5259): 680-685.

Latham, J.A., Chosed, R.J., Wang, S., and Dent, S.Y. 2011. Chromatin signaling to kinetochores: transregulation of Dam1 methylation by histone H2B ubiquitination. *Cell* **146**(5): 709-719.

Lefrancois, P., Euskirchen, G.M., Auerbach, R.K., Rozowsky, J., Gibson, T., Yellman, C.M., Gerstein, M., and Snyder, M. 2009. Efficient yeast ChIP-Seq using multiplex short-read DNA sequencing. *BMC Genomics* **10**: 37.

Li, Y., Danzer, J.R., Alvarez, P., Belmont, A.S., and Wallrath, L.L. 2003. Effects of tethering HP1 to euchromatic regions of the Drosophila genome. *Development* **130**(9): 1817-1824.

Luger, K., Mader, A.W., Richmond, R.K., Sargent, D.F., and Richmond, T.J. 1997. Crystal structure of the nucleosome core particle at 2.8 A resolution. *Nature* **389**(6648): 251-260.

Ma, X.J., Lu, Q., and Grunstein, M. 1996. A search for proteins that interact genetically with histone H3 and H4 amino termini uncovers novel regulators of the Swe1 kinase in Saccharomyces cerevisiae. *Genes Dev* **10**(11): 1327-1340.

Martin, C. and Zhang, Y. 2007. Mechanisms of epigenetic inheritance. *Curr Opin Cell Biol* **19**(3): 266-272.

Maskell, D.P., Hu, X.W., and Singleton, M.R. 2010. Molecular architecture and assembly of the yeast kinetochore MIND complex. *J Cell Biol* **190**(5): 823-834.

Masumoto, H., Hawke, D., Kobayashi, R., and Verreault, A. 2005. A role for cell-cycle-regulated histone H3 lysine 56 acetylation in the DNA damage response. *Nature* **436**(7048): 294-298.

McNally, F.J. and Rine, J. 1991. A synthetic silencer mediates SIR-dependent functions in Saccharomyces cerevisiae. *Mol Cell Biol* **11**(11): 5648-5659.

Meluh, P.B., Yang, P., Glowczewski, L., Koshland, D., and Smith, M.M. 1998. Cse4p is a component of the core centromere of Saccharomyces cerevisiae. *Cell* **94**(5): 607-613.

Mendiburo, M.J., Padeken, J., Fulop, S., Schepers, A., and Heun, P. 2011. Drosophila CENH3 is sufficient for centromere formation. *Science* **334**(6056): 686-690.

Meneghini, M.D., Wu, M., and Madhani, H.D. 2003. Conserved histone variant H2A.Z protects euchromatin from the ectopic spread of silent heterochromatin. *Cell* **112**(5): 725-736.

Millar, C.B., Xu, F., Zhang, K., and Grunstein, M. 2006. Acetylation of H2AZ Lys 14 is associated with genome-wide gene activity in yeast. *Genes Dev* **20**(6): 711-722.

Mizuguchi, G., Xiao, H., Wisniewski, J., Smith, M.M., and Wu, C. 2007. Nonhistone Scm3 and histones CenH3-H4 assemble the core of centromere-specific nucleosomes. *Cell* **129**(6): 1153-1164.

Mullen, J.R., Kayne, P.S., Moerschell, R.P., Tsunasawa, S., Gribskov, M., Colavito-Shepanski, M., Grunstein, M., Sherman, F., and Sternglanz, R. 1989. Identification and characterization of genes and mutants for an N-terminal acetyltransferase from yeast. *EMBO J* **8**(7): 2067-2075.

Muller, H.J. 1930. Types of visible variations induced by X-rays in Drosophila. *Journal of Genetics* **22**: 299-335.

Nakayama, J., Rice, J.C., Strahl, B.D., Allis, C.D., and Grewal, S.I. 2001. Role of histone H3 lysine 9 methylation in epigenetic control of heterochromatin assembly. *Science* **292**(5514): 110-113.

Nowak, S.J. and Corces, V.G. 2004. Phosphorylation of histone H3: a balancing act between chromosome condensation and transcriptional activation. *Trends Genet* **20**(4): 214-220.

Okada, M., Okawa, K., Isobe, T., and Fukagawa, T. 2009. CENP-H-containing complex facilitates centromere deposition of CENP-A in cooperation with FACT and CHD1. *Mol Biol Cell* **20**(18): 3986-3995.

Olsen, J.V., de Godoy, L.M., Li, G., Macek, B., Mortensen, P., Pesch, R., Makarov, A., Lange, O., Horning, S., and Mann, M. 2005. Parts per million mass accuracy on an Orbitrap mass spectrometer via lock mass injection into a C-trap. *Mol Cell Proteomics* **4**(12): 2010-2021.

Ortiz, J., Stemmann, O., Rank, S., and Lechner, J. 1999. A putative protein complex consisting of Ctf19, Mcm21, and Okp1 represents a missing link in the budding yeast kinetochore. *Genes Dev* **13**(9): 1140-1155.

Pagliuca, C., Draviam, V.M., Marco, E., Sorger, P.K., and De Wulf, P. 2009. Roles for the conserved spc105p/kre28p complex in kinetochore-microtubule binding and the spindle assembly checkpoint. *PLoS One* **4**(10): e7640.

Palmer, D.K., O'Day, K., Wener, M.H., Andrews, B.S., and Margolis, R.L. 1987. A 17-kD centromere protein (CENP-A) copurifies with nucleosome core particles and with histones. *J Cell Biol* **104**(4): 805-815.

Panzeri, L., Landonio, L., Stotz, A., and Philippsen, P. 1985. Role of conserved sequence elements in yeast centromere DNA. *EMBO J* **4**(7): 1867-1874.

Perche, P.Y., Vourc'h, C., Konecny, L., Souchier, C., Robert-Nicoud, M., Dimitrov, S., and Khochbin, S. 2000. Higher concentrations of histone macroH2A in the Barr body are correlated with higher nucleosome density. *Curr Biol* **10**(23): 1531-1534.

Perpelescu, M., Nozaki, N., Obuse, C., Yang, H., and Yoda, K. 2009. Active establishment of centromeric CENP-A chromatin by RSF complex. *J Cell Biol* **185**(3): 397-407.

Pidoux, A.L. and Allshire, R.C. 2004. Kinetochore and heterochromatin domains of the fission yeast centromere. *Chromosome Res* **12**(6): 521-534.

Pidoux, A.L., Choi, E.S., Abbott, J.K., Liu, X., Kagansky, A., Castillo, A.G., Hamilton, G.L., Richardson, W., Rappsilber, J., He, X. et al. 2009. Fission yeast Scm3: A CENP-A receptor required for integrity of subkinetochore chromatin. *Mol Cell* **33**(3): 299-311.

Pinsky, B.A., Kotwaliwale, C.V., Tatsutani, S.Y., Breed, C.A., and Biggins, S. 2006. Glc7/protein phosphatase 1 regulatory subunits can oppose the Ipl1/aurora protein kinase by redistributing Glc7. *Mol Cell Biol* **26**(7): 2648-2660.

Pot, I., Measday, V., Snydsman, B., Cagney, G., Fields, S., Davis, T.N., Muller, E.G., and Hieter, P. 2003. Chl4p and iml3p are two new members of the budding yeast outer kinetochore. *Mol Biol Cell* **14**(2): 460-476.

Prunell, A. and Kornberg, R.D. 1982. Variable center to center distance of nucleosomes in chromatin. *J Mol Biol* **154**(3): 515-523.

Ptacek, J., Devgan, G., Michaud, G., Zhu, H., Zhu, X., Fasolo, J., Guo, H., Jona, G., Breitkreutz, A., Sopko, R. et al. 2005. Global analysis of protein phosphorylation in yeast. *Nature* **438**(7068): 679-684.

Puig, O., Caspary, F., Rigaut, G., Rutz, B., Bouveret, E., Bragado-Nilsson, E., Wilm, M., and Seraphin, B. 2001. The tandem affinity purification (TAP) method: a general procedure of protein complex purification. *Methods* **24**(3): 218-229.

Qian, J., Lesage, B., Beullens, M., Van Eynde, A., and Bollen, M. 2011. PP1/Repo-man dephosphorylates mitotic histone H3 at T3 and regulates chromosomal aurora B targeting. *Curr Biol* **21**(9): 766-773.

Ramey, V.H., Wang, H.W., Nakajima, Y., Wong, A., Liu, J., Drubin, D., Barnes, G., and Nogales, E. 2011. The Dam1 ring binds to the E-hook of tubulin and diffuses along the microtubule. *Mol Biol Cell* **22**(4): 457-466.

Ranjitkar, P., Press, M.O., Yi, X., Baker, R., MacCoss, M.J., and Biggins, S. 2010. An E3 ubiquitin ligase prevents ectopic localization of the centromeric histone H3 variant via the centromere targeting domain. *Mol Cell* **40**(3): 455-464.

Rappsilber, J., Mann, M., and Ishihama, Y. 2007. Protocol for micro-purification, enrichment, pre-fractionation and storage of peptides for proteomics using StageTips. *Nat Protoc* **2**(8): 1896-1906.

Rea, S., Eisenhaber, F., O'Carroll, D., Strahl, B.D., Sun, Z.W., Schmid, M., Opravil, S., Mechtler, K., Ponting, C.P., Allis, C.D. et al. 2000. Regulation of chromatin structure by site-specific histone H3 methyltransferases. *Nature* **406**(6796): 593-599.

Richmond, T.J. and Davey, C.A. 2003. The structure of DNA in the nucleosome core. *Nature* **423**(6936): 145-150.

Rosenberg, J.S., Cross, F.R., and Funabiki, H. 2011. KNL1/Spc105 recruits PP1 to silence the spindle assembly checkpoint. *Curr Biol* **21**(11): 942-947.

Saha, A., Wittmeyer, J., and Cairns, B.R. 2006. Chromatin remodelling: the industrial revolution of DNA around histones. *Nat Rev Mol Cell Biol* **7**(6): 437-447.

Sambrook, J., Fritsch, E.F., and Maniatis, T. 1989. Molecular Cloning: A Laboratory Manual. *Cold spring Harbor Laboratory Press*.

Santaguida, S. and Musacchio, A. 2009. The life and miracles of kinetochores. *EMBO J* **28**(17): 2511-2531.

Schalch, T., Duda, S., Sargent, D.F., and Richmond, T.J. 2005. X-ray structure of a tetranucleosome and its implications for the chromatin fibre. *Nature* **436**(7047): 138-141.

Scharf, A.N. and Imhof, A. 2010. Every methyl counts--epigenetic calculus. *FEBS Lett* **585**(13): 2001-2007.

Scharfenberger, M., Ortiz, J., Grau, N., Janke, C., Schiebel, E., and Lechner, J. 2003. Nsl1p is essential for the establishment of bipolarity and the localization of the Dam-Duo complex. *EMBO J* **22**(24): 6584-6597.

Seitz, S. 2004. Connecting the histone acetyltransferase complex SAS-I to the centromere in S. cerevisiae. *Dissertation, Mathematisch-Naturwissenschaftliche Fakultät I der Humboldt-Universität zu Berlin*.

Shang, C., Hazbun, T.R., Cheeseman, I.M., Aranda, J., Fields, S., Drubin, D.G., and Barnes, G. 2003. Kinetochore protein interactions and their regulation by the Aurora kinase Ipl1p. *Mol Biol Cell* **14**(8): 3342-3355.

Sherman, F. 1991. Getting started with yeast. *Methods Enzymol* **194**: 3-21.

Shevchenko, A., Tomas, H., Havlis, J., Olsen, J.V., and Mann, M. 2006. In-gel digestion for mass spectrometric characterization of proteins and proteomes. *Nat Protoc* **1**(6): 2856-2860.

Shogren-Knaak, M., Ishii, H., Sun, J.M., Pazin, M.J., Davie, J.R., and Peterson, C.L. 2006. Histone H4-K16 acetylation controls chromatin structure and protein interactions. *Science* **311**(5762): 844-847.

Slack, J.M. 2002. Conrad Hal Waddington: the last Renaissance biologist? *Nat Rev Genet* **3**(11): 889-895.

Smith, M.M., Yang, P., Santisteban, M.S., Boone, P.W., Goldstein, A.T., and Megee, P.C. 1996. A novel histone H4 mutant defective in nuclear division and mitotic chromosome transmission. *Mol Cell Biol* **16**(3): 1017-1026.

Stemmann, O., Neidig, A., Kocher, T., Wilm, M., and Lechner, J. 2002. Hsp90 enables Ctf13p/Skp1p to nucleate the budding yeast kinetochore. *Proc Natl Acad Sci U S A* **99**(13): 8585-8590.

Sterner, D.E. and Berger, S.L. 2000. Acetylation of histones and transcription-related factors. *Microbiol Mol Biol Rev* **64**(2): 435-459.

Stoler, S., Keith, K.C., Curnick, K.E., and Fitzgerald-Hayes, M. 1995. A mutation in CSE4, an essential gene encoding a novel chromatin-associated protein in yeast, causes chromosome nondisjunction and cell cycle arrest at mitosis. *Genes Dev* **9**(5): 573-586.

Stoler, S., Rogers, K., Weitze, S., Morey, L., Fitzgerald-Hayes, M., and Baker, R.E. 2007. Scm3, an essential Saccharomyces cerevisiae centromere protein required for G2/M progression and Cse4 localization. *Proc Natl Acad Sci U S A* **104**(25): 10571-10576.

Strahl, B.D. and Allis, C.D. 2000. The language of covalent histone modifications. *Nature* **403**(6765): 41-45.

Strahl, B.D., Briggs, S.D., Brame, C.J., Caldwell, J.A., Koh, S.S., Ma, H., Cook, R.G., Shabanowitz, J., Hunt, D.F., Stallcup, M.R. et al. 2001. Methylation of histone H4 at arginine 3 occurs in vivo and is mediated by the nuclear receptor coactivator PRMT1. *Curr Biol* **11**(12): 996-1000.

Suka, N., Luo, K., and Grunstein, M. 2002. Sir2p and Sas2p opposingly regulate acetylation of yeast histone H4 lysine16 and spreading of heterochromatin. *Nat Genet* **32**(3): 378-383.

Sullivan, B.A. and Karpen, G.H. 2004. Centromeric chromatin exhibits a histone modification pattern that is distinct from both euchromatin and heterochromatin. *Nat Struct Mol Biol* **11**(11): 1076-1083.

Sun, Z.W. and Allis, C.D. 2002. Ubiquitination of histone H2B regulates H3 methylation and gene silencing in yeast. *Nature* **418**(6893): 104-108.

Sutton, A., Shia, W.J., Band, D., Kaufman, P.D., Osada, S., Workman, J.L., and Sternglanz, R. 2003. Sas4 and Sas5 are required for the histone acetyltransferase activity of Sas2 in the SAS complex. *J Biol Chem* **278**(19): 16887-16892.

Tachiwana, H., Kagawa, W., Shiga, T., Osakabe, A., Miya, Y., Saito, K., Hayashi-Takanaka, Y., Oda, T., Sato, M., Park, S.Y. et al. 2011. Crystal structure of the human centromeric nucleosome containing CENP-A. *Nature* **476**(7359): 232-235.

Tanaka, T.U., Rachidi, N., Janke, C., Pereira, G., Galova, M., Schiebel, E., Stark, M.J., and Nasmyth, K. 2002. Evidence that the Ipl1-Sli15 (Aurora kinase-INCENP) complex promotes chromosome bi-orientation by altering kinetochore-spindle pole connections. *Cell* **108**(3): 317-329.

Thoma, F., Koller, T., and Klug, A. 1979. Involvement of histone H1 in the organization of the nucleosome and of the salt-dependent superstructures of chromatin. *J Cell Biol* **83**(2 Pt 1): 403-427.

Trojer, P. and Reinberg, D. 2007. Facultative heterochromatin: is there a distinctive molecular signature? *Mol Cell* **28**(1): 1-13.

Tsukada, Y., Fang, J., Erdjument-Bromage, H., Warren, M.E., Borchers, C.H., Tempst, P., and Zhang, Y. 2006. Histone demethylation by a family of JmjC domain-containing proteins. *Nature* **439**(7078): 811-816.

Vagnarelli, P., Ribeiro, S.A., and Earnshaw, W.C. 2008. Centromeres: old tales and new tools. *FEBS Lett* **582**(14): 1950-1959.

Vakoc, C.R., Mandat, S.A., Olenchock, B.A., and Blobel, G.A. 2005. Histone H3 lysine 9 methylation and HP1gamma are associated with transcription elongation through mammalian chromatin. *Mol Cell* **19**(3): 381-391.

van Leeuwen, F., Gafken, P.R., and Gottschling, D.E. 2002. Dot1p modulates silencing in yeast by methylation of the nucleosome core. *Cell* **109**(6): 745-756.

Vernarecci, S., Ornaghi, P., Bagu, A., Cundari, E., Ballario, P., and Filetici, P. 2008. Gcn5p plays an important role in centromere kinetochore function in budding yeast. *Mol Cell Biol* **28**(3): 988-996.

Waddington, C.H. 1942. The epigenotype. *Endeavour* **1**: 18-20.

Waddington, C.H. 1957. The strategy of the genes: a discussion of some aspects of theoretical biology. *Allen & Unwin*.

Walfridsson, J., Bjerling, P., Thalen, M., Yoo, E.J., Park, S.D., and Ekwall, K. 2005. The CHD remodeling factor Hrp1 stimulates CENP-A loading to centromeres. *Nucleic Acids Res* **33**(9): 2868-2879.

Wang, H., Huang, Z.Q., Xia, L., Feng, Q., Erdjument-Bromage, H., Strahl, B.D., Briggs, S.D., Allis, C.D., Wong, J., Tempst, P. et al. 2001. Methylation of histone H4 at arginine 3 facilitating transcriptional activation by nuclear hormone receptor. *Science* **293**(5531): 853-857.

Waterborg, J.H. 2000. Steady-state levels of histone acetylation in Saccharomyces cerevisiae. *J Biol Chem* **275**(17): 13007-13011.

Watson, J.D. and Crick, F.H. 1953. The structure of DNA. *Cold Spring Harb Symp Quant Biol* **18**: 123-131.

Weber, J.M., Irlbacher, H., and Ehrenhofer-Murray, A.E. 2008. Control of replication initiation by the Sum1/Rfm1/Hst1 histone deacetylase. *BMC Mol Biol* **9**: 100.

Westermann, S., Cheeseman, I.M., Anderson, S., Yates, J.R., 3rd, Drubin, D.G., and Barnes, G. 2003. Architecture of the budding yeast kinetochore reveals a conserved molecular core. *J Cell Biol* **163**(2): 215-222.

Westermann, S., Drubin, D.G., and Barnes, G. 2007. Structures and functions of yeast kinetochore complexes. *Annu Rev Biochem* **76**: 563-591.

Westermann, S., Wang, H.W., Avila-Sakar, A., Drubin, D.G., Nogales, E., and Barnes, G. 2006. The Dam1 kinetochore ring complex moves processively on depolymerizing microtubule ends. *Nature* **440**(7083): 565-569.

Widom, J. 1992. A relationship between the helical twist of DNA and the ordered positioning of nucleosomes in all eukaryotic cells. *Proc Natl Acad Sci U S A* **89**(3): 1095-1099.

Wieland, G., Orthaus, S., Ohndorf, S., Diekmann, S., and Hemmerich, P. 2004. Functional complementation of human centromere protein A (CENP-A) by Cse4p from Saccharomyces cerevisiae. *Mol Cell Biol* **24**(15): 6620-6630.

Wigge, P.A., Jensen, O.N., Holmes, S., Soues, S., Mann, M., and Kilmartin, J.V. 1998. Analysis of the Saccharomyces spindle pole by matrix-assisted laser desorption/ionization (MALDI) mass spectrometry. *J Cell Biol* **141**(4): 967-977.

Wigge, P.A. and Kilmartin, J.V. 2001. The Ndc80p complex from Saccharomyces cerevisiae contains conserved centromere components and has a function in chromosome segregation. *J Cell Biol* **152**(2): 349-360.

Williams, J.S., Hayashi, T., Yanagida, M., and Russell, P. 2009. Fission yeast Scm3 mediates stable assembly of Cnp1/CENP-A into centromeric chromatin. *Mol Cell* **33**(3): 287-298.

Williams, S.K., Truong, D., and Tyler, J.K. 2008. Acetylation in the globular core of histone H3 on lysine-56 promotes chromatin disassembly during transcriptional activation. *Proc Natl Acad Sci U S A* **105**(26): 9000-9005.

Winzeler, E.A., Shoemaker, D.D., Astromoff, A., Liang, H., Anderson, K., Andre, B., Bangham, R., Benito, R., Boeke, J.D., Bussey, H. et al. 1999. Functional characterization of the S. cerevisiae genome by gene deletion and parallel analysis. *Science* **285**(5429): 901-906.

Wong, C.M., Tang, H.M., Kong, K.Y., Wong, G.W., Qiu, H., Jin, D.Y., and Hinnebusch, A.G. 2010. Yeast arginine methyltransferase Hmt1p regulates transcription elongation and termination by methylating Npl3p. *Nucleic Acids Res* **38**(7): 2217-2228.

Wysocka, J., Allis, C.D., and Coonrod, S. 2006. Histone arginine methylation and its dynamic regulation. *Front Biosci* **11**: 344-355.

Xiao, H., Mizuguchi, G., Wisniewski, J., Huang, Y., Wei, D., and Wu, C. 2011. Nonhistone Scm3 binds to AT-rich DNA to organize atypical centromeric nucleosome of budding yeast. *Mol Cell* **43**(3): 369-380.

Zeitlin, S.G., Barber, C.M., Allis, C.D., and Sullivan, K.F. 2001. Differential regulation of CENP-A and histone H3 phosphorylation in G2/M. *J Cell Sci* **114**(Pt 4): 653-661.

Zhang, X., Li, X., Marshall, J.B., Zhong, C.X., and Dawe, R.K. 2005. Phosphoserines on maize CENTROMERIC HISTONE H3 and histone H3 demarcate the centromere and pericentromere during chromosome segregation. Plant Cell 17(2): 572-583.

6. Appendix

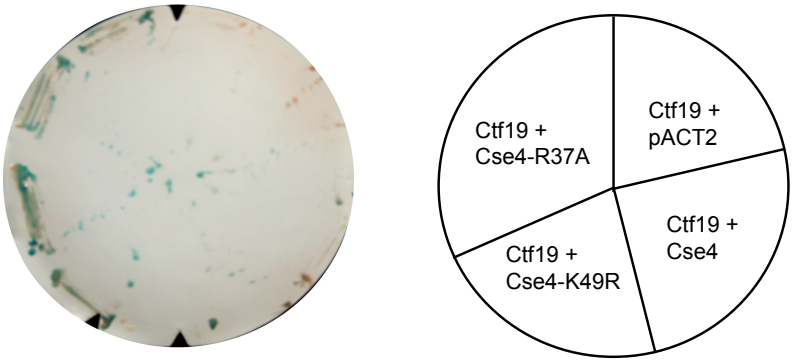

Figure 39: Additional mutation of R37 and K49 did not disturbed interaction between Cse4 and Ctf19. Y2H transformands were plated on YM medium and stamped on a nitrocellulose membrane. Interaction was analyzed by β-galactosidase filter assay and confirmed by blue stained colonies after incubation at 30°C. Experimental procedure and picture courtesy of Edisa Osmic.

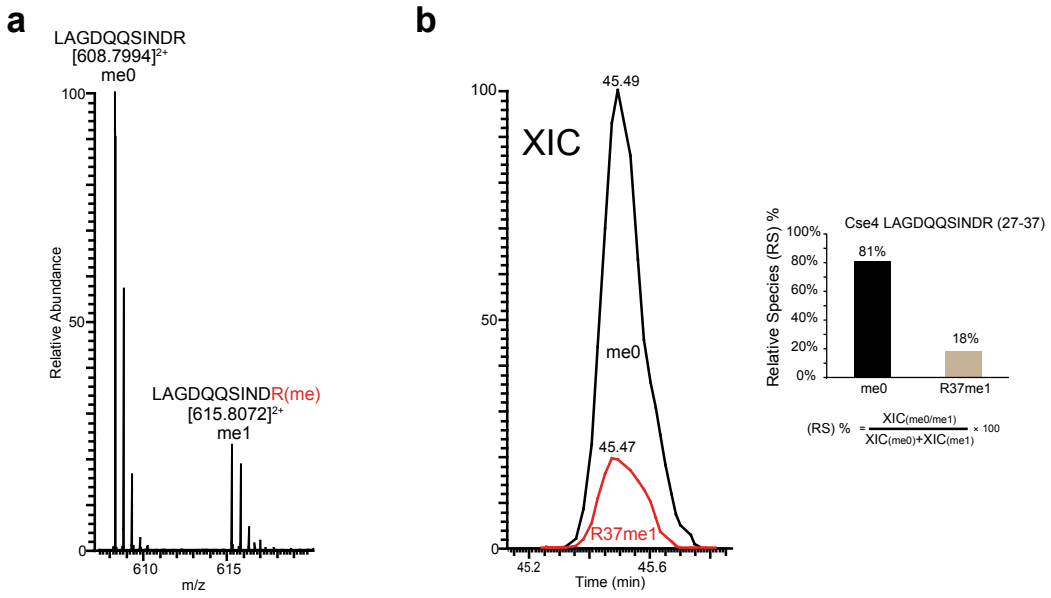

Figure 40: Identification and estimation of relative abundance of modified Cse4 species.
a, Zoomed mass spectrum of precursor ions at m/z $[608.7994]^{2+}$and $[615.8072]^{2+}$ corresponding to the unmodified (me0) and mono-methylated (me1) 27-L.AGDQQSIND.R-37 peptide. **b**, Extract ion chromatograms (XIC) relative to both me0 and me1 species were used to estimate the relative abundance of the two species, as reported in the formula (right panel). Experimental procedure was performed by Tiziana Bonaldi and Alessandro Cuomo.

Table 9: Overview of putative S-adenosyl-L-methionine-dependent methyltransferases in *S. cerevisiae*.

Class*	Gene*	Systematic name*
Protein MTF	*PPM1*	YDR435C
	MTQ1	YNL063W
	SET1	YHR119W
	SET2	YJL168C
	SET3	YKR029C
	MTQ2	YDR140W
	SEE1	YIL064W
	DOT1	YDR440W
	HPM1	YIL110W
	RKM4	YDR257C
tRNA MTF	*PPM2*	YOL141W
	TRM1	YDR120C
	TRM2	YKR056W
	TRM3	YDL112W
	TRM4	YBL024W
	TRM7	YBR061C
	TRM8	YDL201W
	TRM9	YML014W
	TRM10	YOL093W
	TRM11	YOL124C
	TRM12	YML005W
rRNA/mRNA MTF	*MRM2*	YGL136C
	TGS1	YPL157W
	MTF1	YMR228W
	PET56	YOR201C
	BUD23	YCR047C
other MTF	*MET1*	YKR069W
	ERG6	YML008C
	TMT1	YER175C
	COQ1	YBR003W
	COQ3	YOL096C
	COQ5	YML110C
	CTM1	YHR109W
	DPH5	YLR172C
	PEM1	YGR157W
	OPI3	YJR073C
	SAM4	YPL273W
	CRG1	YHR209W
	YNL092W	YNL092W
	ABP140	YOR239W
	RSM22	YKL155C
	YBR271W	YBR271W
	IRC15	YPL017C
	OMS1	YDR316W
	YBR141C	YBR141C
	YJR129C	YJR129C
	YLR063W	YLR063W
	YLR137W	YLR137W
	YMR209C	YMR209C
	YNL024C	YNL024C
	SET4	YJL105W
	SET5	YHR207C
	SET6	YPL165C

*- Standard gene names are given as annotated in the *Saccharomyces* Genome database to the corresponding ORF. Classification of the genes was performed according to their biological function.

Danksagung

Ich möchte mich bei Ann Ehrenhofer-Murray bedanken für die Bereitstellung und Betreuung dieser Arbeit, sowie dem großen Interesse an deren Entwicklung und die ständige Diskussions- und Gesprächsbereitschaft.

Bei Tiziana Bonaldi und Alessandro Cuomo bedanke ich mich für die Analyse der posttranslationalen Modifikationen an Cse4. Ebenso gilt mein besonderer Dank Robert Schneider und Ulrike Zeissler für die Möglichkeit der Antikörperaufreinigung am MPI in Freiburg. Zudem bedanke ich mich bei allen wissenschaftlichen Leitern anderer Labore, die Hefestämme und Plasmide für diese Arbeit zur Verfügung gestellt haben.

Den ehemaligen und derzeitigen Mitarbeitern der Abteilung für Genetik der Universität Duisburg-Essen, insbesondere Karolin, Rita, Jan, Tanja, Gesine, Maria, Martin, Jessica, Christian, Juliane, Christiane, Louisa, Martina, Anđa gilt mein besonderer Dank für die gute Zusammenarbeit, die allzeit mögliche Diskussionsbereitschaft und das angenehme Arbeitsklima. Ein besonderes Dankeschön geht an Stefan für die fortwährende Diskussionsbereitschaft bei auftretenden Fragen hinsichtlich der Epigenetik.

Weitherhin möchte im mich bei allen ehemaligen und derzeitigen Mitgliedern des Graduiertenkollegs „Transcription, chromatin structure and DNA repair in development and differentiation“ für die anregenden Diskussionen, die mir während meiner Doktorarbeit sehr geholfen haben, bedanken.

Abschließend möchte ich mich bei meinen Eltern, meiner Familie und Jens herzlichst für die moralische Unterstützung sowie für die aufmunternden Worte und den ständigen Rückhalt in jeglichen Lebenslagen bedanken.

Lebenslauf

Der Lebenslauf ist in der Online-Version aus Gründen des Datenschutzes nicht enthalten.

Erklärung:

Hiermit erkläre ich, gemäß § 6 Abs. (2) f) der Promotionsordnung der Fakultäten für Biologie, Chemie und Mathematik zur Erlangung des Dr. rer. nat., dass ich das Arbeitsgebiet, dem das Thema „Identification and characterization of posttranslational modifications on CenH3 in *Saccharomyces cerevisiae*“ zuzuordnen ist, in Forschung und Lehre vertrete und den Antrag von Anke Samel befürworte und die Betreuung auch im Falle eines Weggangs, wenn nicht wichtige Gründe dem entgegenstehen, weiterführen werde.

Essen, den _____ _____

Erklärung:

Hiermit erkläre ich, gemäß § 7 Abs. (2) c) + e) der Promotionsordnung der Fakultäten für Biologie, Chemie und Mathematik zur Erlangung des Dr. rer. nat., dass ich die vorliegende Dissertation selbstständig verfasst und mich keiner anderen als der angegebenen Hilfsmittel bedient habe.

Essen, den _____ _____

Erklärung:

Hiermit erkläre ich, gemäß § 7 Abs. (2) d) + f) der Promotionsordnung der Fakultäten für Biologie, Chemie und Mathematik zur Erlangung des Dr. rer. nat., dass ich keine anderen Promotionen bzw. Promotionsversuche in der Vergangenheit durchgeführt habe und dass diese Arbeit von keiner anderen Fakultät/Fachbereich abgelehnt worden ist.

Essen, den _____ _____